universität wien

DIPLOMARBEIT

Time Resolved Transepithelial Impedance Spectroscopy Of Caco 2 Monolayers Relying on Lithographically Patterned Basolateral Electrode Cell Arrays

angestrebter akademischer Grad

Magistra der Naturwissenschaften (Mag. rer.nat.)

Verfasserin / Verfasser:	Maria Hufnagl
Matrikel-Nummer:	0107574
Studienrichtung (lt. Studienblatt):	A 411 Diplomstudium Physik UniStG
Betreuerin / Betreuer:	Univ. Prof. Dr. Emmerich Bertagnolli

Wien, im November 2010

Acknowledgments

Contents

Chapter 1

Abstract

1.1 Kurzfassung

Pharmazeutische Transportstudien werden immer wichtiger um vielversprechende Arzneien zu überprüfen und bekannte Medikamente zu testen. Diese Studien verwenden adhärente Zellkulturen, die auf Membranen aufgewachsen wurden, um den Transport von pharmazeutischen Substanzen zwischen apikalem und basolateralem Kompartment zu messen. Eine der adhärenten Zellkulturen, die für diese Studien verwendet wird, ist die Caco-2 Ziellinie aus dem menschlichen Grimmdarm. Die ist wegen ihrer Fähigkeit zur funktionellen Differentiation ein anerkanntes Modell für den menschlichen Dünndarm [Press 08], [Weissenboeck 04]. Mit Hilfe von Caco-2 Zellkulturen kann die Aufnahme und Absorption von pharmazeutischen Substanzen im Dünndarm effizient überprüft werden. Caco-2 Zellkulturen teilen sich so lange bis sie eine dichte Monolage von ausdifferenzierten Epithelzellen bilden. Pharmazeutische Transportstudien benötigen eine konfluente und sehr dichte Epithelschicht.

Um sowohl die Konfluenz als auch die Zelldichte zu überprüfen wird üblicherweise der Parameter 'TEER' (transepithelial electrical resistance) verwendet. Der TEER Wert gibt Auskunft über die transepitheliale spezifische Impedanz einer Zellschicht. TEER wird in $\Omega\mathrm{cm}^2$ während einer einzigen Impedanzmessung bei einer Messfrequenz von 12.5 Hz bestimmt. Da die Zellkultur für die Messung aus ihrer gewohnten Umgebung entfernt werden müssen ist diese Messung als invasiv zu betrachten.

Um ein ungestörtes Wachstum zu ermöglichen wurde ein an die Wachstumsbedingungen angepasster Messaufbau entwickelt, mit dem das Konzept des transepithelialen Widerstandes bis zu Frequenzen von 100 kHz erweitert wurde, um die elektrischen Eigenschaften von Caco-2 Zellschichten genauer zu untersuchen. Die Caco-2 Epithelzellen erzeugen selbst kein elektrisches Signal. Im Gegensatz zu neuronalen Zelllinien können sie als elektrisch passive Zellen betrachtet werden. Trotzdem beeinflussen deren biologische Strukturen und Verhalten die Umgebung der Zellen im Hinblick auf elektrische Parameter. Diese Einflüsse können mit

Hilfe von Imedanzmessungen erfasst werden [Coster 96]. Die Zellschicht selbst kann als eine passive elektrische Schaltung mit variablen Widerständen und Kapazitäten betrachtet werden. Um diese komplexen Schaltungen zu untersuchen wurde die Methode der Impedanzspektroskopie an der erwähnten Zelllinie verwendet. Diese Methode ermöglicht es, Informationen über resistive, kapazitive, induktive und diffusive Charakteristika des untersuchen Systems zu bestimmen. Angewandt auf Caco-2 Zellkulturen erlaubt es diese Methode die elektrischen Eigenschaften dieser biologischen Zellen zu untersuchen. Basolaterale Überwachung der Impedanzspektroskopie von Caco-2 Zellen wurde schon mit Hilfe von flachen Kammelektroden durchgeführt [Fischeneder 09].

Die hier präsentierte Arbeit hat eine transzelluläre Elektrodenkonfiguration mit einer Elektrode im apikalen Kompartment und einer Elektrode im basolateralen Kompartment zum Ziel. Die transzelluläre Elektrodenkonfiguration ist speziell dafür geeignet, die Konfluenz einer Zellschicht zu messen und deren 'tight junctions' zu untersuchen. Das Ziel dieser Arbeit war es daher, die transepitheliale Impedanz von Caco-2 Monolagen unter Verwendung von mikrostrukturierten Elektroden zu überwachen. Ein angepasster Messaufbau um die Impedanz in Zweipunktkonfiguration zu messen wurde geplant und entwickelt. Zwei Sorten von Elektroden, apikale und basolaterale Elektroden, wurden hergestellt und analysiert. Ein Multiplexer wurde implemeniert um jede gewünschte Verbindungen zwischen den einzelnen verfügbaren Messelektroden herzustellen. Ein LCR-Meter wurde dazu verwendet ein Messsignal mit Frequenzen zwischen $50\,Hz$ und $100\,kHz$ zu senden und die resultierende Impedanz zu messen. Die speziellen Anforderungen einer nicht invasiven Beobachtung des transepithelialen Widerstandes der Caco-2 Zellen wurden evaluiert und im experimentellen Messaufbau umgesetzt. Der endgültige Messaufbau wurde sowohl in Hinblick auf Funktionalität als auch in Hinblick auf Reproduzierbarkeit der Messergebnisse getestet. Die Ergebnisse dieser Test zeigen die Eignung des Messaufbaus zur Messung der transepithelialen Impedanz. Die Biokompatibilität konnte für alle Materialien, die in Kontakt mit den Caco-2 Zellen stehen, bestätigt werden. Es konnten Impedanzspektra von acht Zellkulturen gleichzeitig während der gesamten Wachstumsperiode aller Kulturen gemessen werden. Es konnte gezeigt werden, dass die transepitheliale Impedanz einer Caco-2 Monolage während eines Zellzyklus um das zwei- bis achtfache anstieg. Signifikante Vorkommnisse während des Zellzyklus wie der Austausch des Nährmediums konnten charakteristischen Peaks im gemessenen Impedanz Spektrum zugeordnet werden.

Die Ergebnisse dieser Arbeit helfen nicht nur dabei, den genauen Zeitpunkt der Konfluenz einer Zellschicht für pharmazeutische Studien zu bestimmen, sondern haben auch zu einem besseren Verständnis der elektrischen Eigenschaften der humanen Epithelzelllinie 'Caco-2' geführt.

1.2 Abstract

For the screening of new prospective drugs and testing the effectivity of known medicaments, pharmaceutical transport studies are increasingly important. These studies use epithelial cells grown on membranes to measure the transport of pharmaceutical agents from one compartment to another. One of the adherent cell lines used for these studies is the human colon cell line Caco-2. The Caco-2 cell line, due to its functional differentiation properties, is recognized as a model for the human small intestine as reported in [Press 08] and [Weissenboeck 04]. Uptake and absorption of pharmaceutical agents can be efficiently scanned by transport studies. The Caco-2 cell culture differentiates to form a dense monolayer. Pharmaceutical transport studies rely on the confluence and a high density of the epithelial monolayer.

To test for the confluence as well as the cell density, the transepithelial electrical resistance (TEER) is a widely used parameter. The TEER value gives the transepithelial specific impedance of a cell layer, measured in Ωcm^2 at the frequency of $12.5\,Hz$ retrieved during a singular measurement. The conventionally used measurement is invasive to the cell culture as the cell culture has to be removed from its growth environment.

To avoid disturbance of the cells during measurement, an adapted measurement setup was designed and fabricated to monitor the cells impedance noninvasively. The concept of transepithelial resistance was extended to the range up to $100\,kHz$ and to investigate the electrical properties of the Caco-2 cell layer in detail because Caco-2 cells are epithelial cells that do not generate electrical signals themselves. In contrast to neuronal cell lines, they have to be considered electrically passive cells. Nonetheless, their biological structure and behavior electrically influences the cell's environment. These influences can be detected by impedance measurements [Coster 96]. The cell layer itself can be considered a passive electrical circuit with variable capacitors and resistors.

Complex electrical circuits like the mentioned cell layers can be investigated through impedance spectroscopy. This method is capable of collecting information on the resistive, capacitive, inductive and diffusive characteristics of a tested system. When applied to adherent Caco-2 cell cultures, this method allows investigation of the electrical properties of these biological cells. Basolateral monitoring of the impedance of Caco-2 cells has been performed using interdigitated planar electrodes [Fischeneder 09],

The presented work addressed a transwell configuration with one electrode in the apical compartment and one electrode in the basolateral compartment. The transwell configuration is an excellent method to measure the confluence of the cell layer and to evaluate the tight junctions. The aim of this work was to monitor the transepithelial electrical impedance of Caco-2 monolayers using microstructured electrode arrays. An adapted electrical setup for a two terminal configuration impedance measurement was designed and fabricated. Two types of electrodes, apical and basolateral electrodes were fabricated and analyzed. A multiplexer was implemented to establish any desired pairing of available measurement electrodes. An LCR-

meter imprinted a signal and measured the impedance in the range of $50\,\mathrm{Hz}$ to $100\,kHz$. Specific requirements of a non-invasive continuous monitoring of the Caco-2 cells' transepithelial impedance spectroscopy were evaluated and implemented into the setup. The final setup was then tested for functionality as well as for accuracy. Results proved this suitable to measure the transepithelial impedance. Biocompatibility was confirmed for all materials in contact with the Caco-2 cells. Monitoring of the transepithelial impedance spectroscopy for eight wells simultaneously was performed during the complete growth period of a cell culture. The transepithelial impedance of a Caco-2 monolayer was found to be increased during growth period by factors ranging from two two eight. Significant events of the cells growth cycle such as exchange of nutrient medium could be correlated temporally to characteristic peaks of the measured transepithelial impedance.

The results of this work do not only help in detecting the exact time of a cell layer's confluence for pharmaceutical transport studies but have also lead to a better understanding of the electrical properties of the human epithelial cell line 'Caco-2'.

Chapter 2

Introduction

2.1 Motivation

In pharmaceutical studies, an increasingly important field of research is scanning and testing of pharmaceutical agents using epithelial cell cultures. Various pharmaceutical methods have been reported in literature [Fischer 08; Shi 08]. The reported methods vary from testing the toxicity of substances with specific cell lines to transport studies exploring the intestinal absorption of certain substances by an organism. These transport studies are particularly interesting as their results deliver valuable information on the efficiency of medications on the biomolecular level.

A widely used cell line for these transport studies is the Caco-2 line, which is an immortalized human epithelial cell line. Due to its morphologic and functional differentiation as a distinct barrier for biologically active substances, the Caco-2 cell line as a cell culture system is an acknowledged model for the human small intestine [Bogner 06]. Transport studies using Caco-2 cells investigate the transport of pharmaceutical agents through the epithelial cell layer. The studies are performed under reproducible ex-vivo conditions in standardized cell containments. The cell cultures are grown on artificial membranes and cultivated in an incubator.

An essential parameter for transport studies is the cell layer's confluence and intactness. If the cell layer is confluent, only active transport of agents across the cell layer is feasible. Substances are absorbed on one side of the cells and excreted on the other side. If there is an undetected 'leak' in the cell layer, an agent may also pass the cell layer via this leak thereby disturbing the measurement. Therefore, it is essential to know whether the grown cell layer fully covers the available area as an intact and confluent cell layer. A common method used in pharmaceutical studies to test for the cell layers confluence is to measure the transepithelial electrical resistance TEER. A commercially available testing device [Mil 09] measures the impedance of cell layers grown on permeable membranes at

a sensing frequency of 12.5 Hz. The TEER value quantifies the transepithelial transport of agents by measuring the electrical resistance of cell layers across the cell membrane. It characterizes especially the formation of so called tight junctions. These junctions are cell to cell connections that seal the intercellular interspace and form an impermeable transport barrier for intercellular transport. This significantly influences the transport of ions across the epithelial cell layer. Generally, the statement 'the higher the TEER, the better the cell layers confluence' holds for many cases but this method can only deliver results corresponding to the distinct frequency of 12.5 Hz at a certain time of measurement. It neither takes into account the frequency dependent character of an epithelial cell's impedance nor fluctuations in time. Furthermore, this method is invasive as the cell culture has to be removed from its culturing environment to perform the measurement. Therefore, TEER measurement of an epithelial cell layer is limited to very few points in time and only one point on the frequency scale.
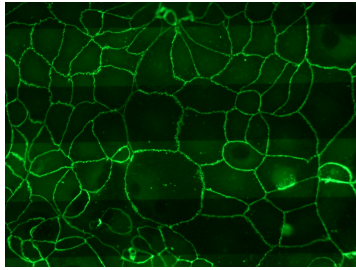
(a) Confocal microscopic image of Caco-2 cells. The immunofluorescence staining (green) of proteins shows the tight junctions between the cells [Bogner 06].
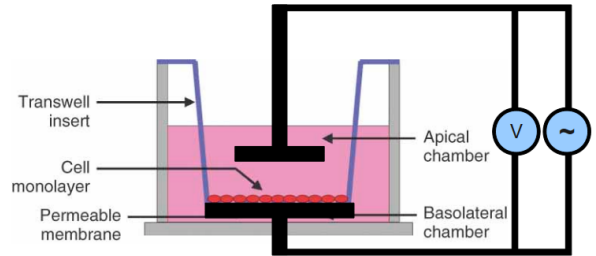
(b) Schematic illustration of a transwell setup with (transwell) electrode pair: planar basolateral electrodes covered with adherent cells and a top electrode in the apical compartment.

Figure 2.1: Fluorescence image of tight junctions in a Caco-2 cell layer and schematic illustration of the transwell configuration to measure the impedance across the cell layer.

Another method to analyze the transepithelial impedance of biological cell layers overcoming these previously mentioned limitations is to measure the impedance spectroscopy of the cell culture. Impedance spectroscopy is an electrochemical method that characterizes intrinsic electrical properties of any material and its interface. This method is capable of analyzing the frequency dependent response to an electrical excitation signal of the investigated cell layer. The most important advantage of this method is the fact that it is a non-invasive and non-destructive method that can be used for continuous monitoring.

In this work, a setup to monitor the transepithelial impedance spectroscopy of the Caco-2 cell layer during the growth cycle is presented. To measure the transepithelial impedance, the Caco-2 cells were directly grown onto the electrodes. These cells need a fluid environment to grow. A standardized silicone confinement was used to provide a containment for the nutrient medium. Electrodes, adapted to the geometry of this confinement were fabricated using methods and procedures of micro structuring such as optical lithography and sputter

deposition. The approach to use micro structuring methods also allows for miniaturization of the measuring electrodes. A miniaturized setup could also be used to measure spatially resolved transepithelial impedance spectroscopy.

The presented interdisciplinary approach will not only help detect the time of a cell layer's confluence for pharmaceutical transport studies but will also lead to a better understanding of the electrical properties of the human epithelial cell line 'Caco-2'.

2.2   Objectives

The objective of the presented work is to investigate the feasibility of monitoring the growth and confluence of Caco-2 cell layers by a two-terminal transwell setup using lithographically structured electrodes. This objective can be reformulated into tree key questions.

Question 1: Is an impedance measurement for a transepithelial configuration feasible?

A setup to measure the transepithelial impedancy spectrum of Caco-2 cells will be designed and constructed. It will be investigated whether it is mechanically and electrically possible to create a measurement setup capable of measuring the transepithelial impedance while the cells are still in their habitual environment. It is assumed that an adequate measurement setup can be composed of instruments and procedures common in microelectronic fabrication and testing. This assumption leads to the second question.

Question 2: How can the developed measurement be optimized?

This measurement setup for transepithelial impedance spectroscopy of Caco-2 cells will be composed of several components, so any limitations in components will affect the performance of the complete setup. Therefore, specifications for each component will be evaluated and optimized if necessary. The electrical properties of the electrodes themselves will be tested. For reference purposes impedance of several electrolytes will be measured to find whether the measurement setup's accuracy is good enough. Provided the results of these test are successful, the tasks explicitly related to Caco-2 mono layers can be addressed.

Question 3: Is the presented setup suitable to measure the impedance of biological cells?

The special demands of biological cells such as a fluid environment and biocompatibility of the used materials as well as the uncertainties inherent in biological probes such as unknown cell numbers or influences of biological side products require careful and stepwise proceeding. The first step will evaluate whether the cells' nutrient medium can be characterized electrically. The next step will be the evaluation of the biocompatibility of the used materials. If all previous steps have produced satisfactory results, the measurement setup will be used for in-situ monitoring in an incubator and the impedance of Caco-2 cells will be investigated continuously during growth. By gradually increasing the number of varied parameters per experiment the final configuration is intended to monitor the transepithelial impedance in a frequency range of 50 Hz to 100 kHz for several days simultaneously at eight measurement positions at the same time.

Finally, the question as to whether characteristic points of the impedance measurement can be correlated to distinctive events during the growth and differentiation of the Caco-2 monlayers will be evaluated.

Chapter 3

Theory

The aim of this work is to develop an approach to monitor the transepithelial electrical impedance of Caco-2 monolayers on a planar electrode array. Theoretical input to handle the task can be found in several fields of natural sciences. The theory presented in this chapter will follow the structure shown in figure 3.1.
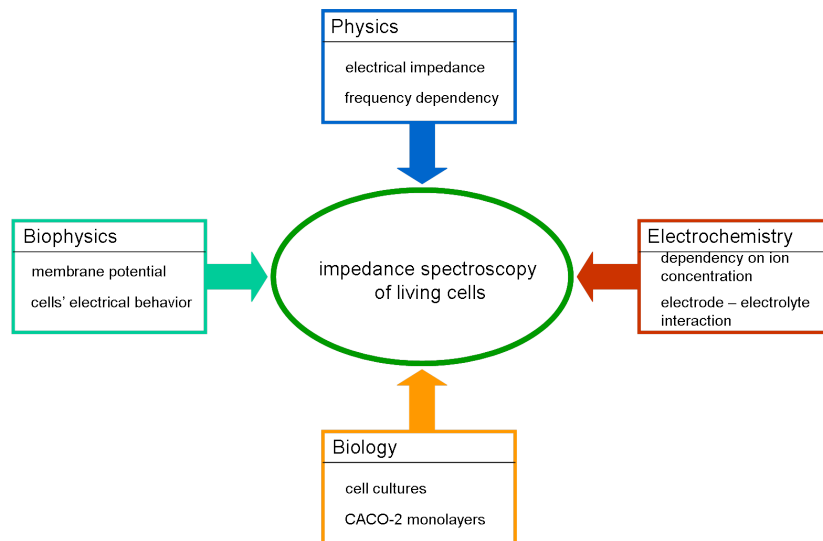
Figure 3.1: Overview of the theoretical input considered to measure the transepithelial impedance spectroscopy of Caco-2 cell cultures.

The theory chapter starts with an explanation of relevant mechanisms and expressions regarding epithelial cells and continues with a description of the Caco-2 cell culture. A section on electrical impedance in general and impedance of electrolytes in particular prepares for the understanding of the cells' electrical properties. A measured impedance signal is composed of several components. Some of them are static, resulting from sensors' properties such as electrode geometry, electrode material, electrolyte composition and chosen frequency. Other components of the measured impedance result from the cells metabolizing, cloning themselves and growing to confluence. These components are accessible to research by impedance spectroscopy as concluded in the last section.

3.1 Epithelial Cells

'omnis cellula e cellula' [Virchow 59]

Cells, the fundamental units of life, generally have a common layout and structure. This cell structure will be the key element of the electrical measurement of this work. Therefore, this section gives a detailed information on elements of epithelial cells necessary to understand the impedance of Caco-2 cells. In all eucaryotic cells a membrane encapsulates the nucleus and the cytoplasm. The nucleus stores and synthesizes DNA, the cytoplasm transports materials (O_2, CO_2) or signals and produces secretions. There are various types of cells, in this work epithelial cells are used. Epithelial cells form layers that cover the surface of the body and line its internal cavities, such as lungs and intestine. These cells typically have a diameter of 5 - 100 μm. The measurements presented in this work will use electrodes considerably larger than the cells' diameter.
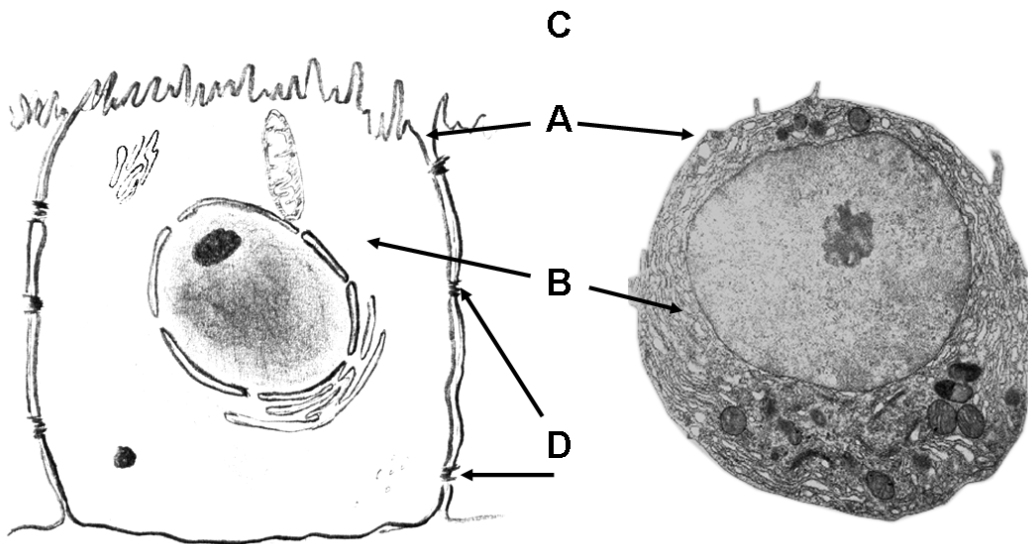
Figure 3.2: Epithelial Cell, schematically and TEM image [Thews 99] showing A = membrane, B = cytoplasm, C = extracellular medium, D = tight junctions

Epithelial cells are polar cells. Polar, in this context, means that these cells can distinguish between 'upper side' and 'down side'. Their apical side ('up') is orientated towards the epithelial surface, the basal ('down') side connects epithelial cells via a membrane, the basal lamina, to the tissue beneath. General information on cells can be found in [Alberts 04] and [Bolsover 04]. Figure 3.2 shows a schematic picture of an epithelial cell and a picture, retrieved by transmission electron microscopy. A to D in this figure are the structures of interest to measurement of transepithelial impedance:

A) Plasma Membrane

The plasma membrane defines the boundary of the cell. This 5 nm sheet regulates the

bidirectional transport of molecules and ions.

(a) Cytomembrane, a phospholipid bilayer.   (b) Transmembrane diffusion of uncharged molecules.
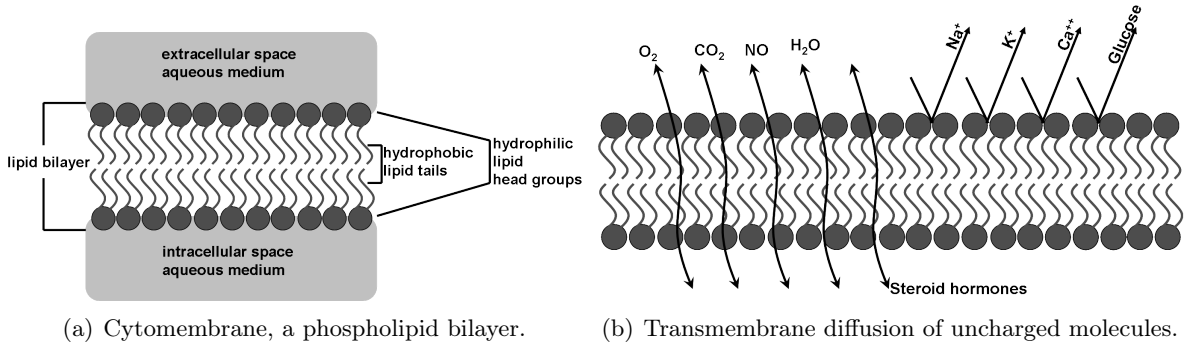
Figure 3.3: Cytomembrane, images according to [Bolsover 04].

The primary structure of the plasma membrane is a phospholipid bilayer. The phospholipids are arranged in two layers, their hydrophobic tails directed towards the center of the membrane. Small uncharged particles like O_2, CO_2, H_2O, NO may pass the bilayer by diffusion. In contrast, charged ions such as Na^+, K^+, Ca^{++} have hydration shells. They cannot dissolve in hydrophobic environments and therefore cannot diffuse through the membrane. This fact is essential for electrical measurementsChannels and carriers, proteins integrated into the bilayer, facilitate ion transport. These proteins control the extra- and intracellular concentration of charges and generate a membrane potential of about 70mV given by the Nernst equation 3.17 as shown in Section 3.5. Electrically, the cytomembrane represents a capacitor studded with resistors.

B) Cytoplasm

Cytoplasm is an aqueous solution of various dissociated ions, confined within the cytomembrane. Average concentrations of the most important ions are given in table 3.1. The concentrations in the cytoplasm vary over the cells' life cycle and depend strongly on the concentrations in the extracellular medium.

Ion	Cytoplasm $c\left[\frac{mmol}{liter}\right]$	Extracellular Medium $c\left[\frac{mmol}{liter}\right]$
Sodium Na^+	10	150
Potassium K^+	140	5
Calcium Ca^{++}	0.0001	1
Chloride Cl^-	5	100
Hydrogen ion H^+ (really H_3O^+)	$6.3 \cdot 10^{-5}$ or pH 7.2	$4 \cdot 10^{-5}$ or pH 7.4

Table 3.1: Typical concentration of ions in mammalian cytoplasm and extracellular medium according to [Bolsover 04].

When exposed to a strong DC electrical field, these ions feel a force along the field's direction. The resulting electrophoresis of cytoplasm is lethal to cells. Therefore, the presented

measurement setup uses alternating voltage and current.

C) Extracellular Medium

The extracellular medium is the fluid the cells need as a natural environment to be grown in. Table 3.1 shows concentrations of the most important ions present in the extracellular fluid. In Caco-2 cell cultures the extracellular medium is replaced by the nutrient RPMI medium (Roswell Park Memorial Institute Medium). The RPMI medium is an aqueous solution of glucose, salts, amino acids and vitamins, based on a bicarbonate buffering system. The pH indicator phenol red is added to track the pH value. Electrically the nutrient medium represents a physiological saline. From a chemical point of view the RPMI medium is a conducting electrolyte.

D) Tight Junctions

The electrical properties of the cells strongly depend on the density of a structure called tight junctions. As the cells in cell cultures are seeded on a substrate and grow to confluence, they establish a dense layer and connect to each other by so called tight junctions. Tight junctions are the crucial structures for this experiment. They are strong intercellular connections, exclusively established by epithelial cells. These connections inhibit transport or flow of materials through interstitial space, therefore induce trans cellular transport.
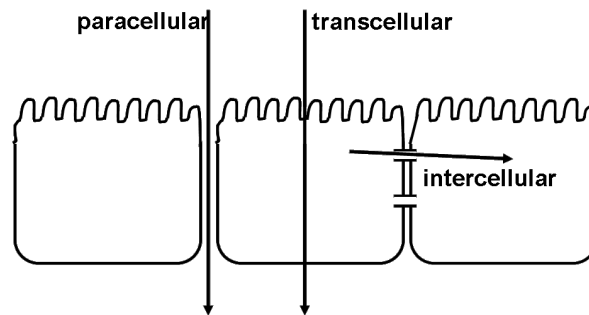
Figure 3.4: Pathways for molecules passing a layer of epithelial cells.

At the time of complete confluence all transport of ions through the mono layer is trans-epithelial. At this state the transepithelial current is lowest, thus the trans epithelial impedance is highest [Ranaldi 03]. This behavior will be assessed in the presented approach and will be investigated for monitoring the biological status of the cell layer.

3.2 Caco-2 Cell Cultures

Due to the distinctive barrier function for charged molecules and ions this cell type is especially suited for electrical impedance monitoring. Caco-2 cells are an epithelial colon cell line. This cell line is also of great importance for pharmaceutical studies. Due to their morphologic and

functional differentiation as a distinct barrier for biologically active substances, Caco-2 cells as cell culture systems are an acknowledged model for the human small intestine [Bogner 06]. The Caco-2 cell line was originally derived from a moderately well-differentiated human colon adenocarcinoma of a 72 years old man with blood group 0^+ [Fough 77]. When grown to confluence under normal culturing conditions, these cells differentiate spontaneously. Differentiation continues for about 12 - 14 days and leads to formation of a fully functional 'brush border' membrane with microvillis. The Caco-2 cell line was shown to undergo spontaneous in vitro enterocytic differentiation leading in 2-3 weeks to the formation of a viable, highly polarized monolayer. The cultured membrane corresponds to a large extend to normal intestinal epithelial cells. Furthermore, Caco-2 cells have ion transporters (Na^+/H^+ exchanger), a p-glycoprotein mediated secretion and several other active transport mechanisms [Hidalgo 86]. Therefore they are widely used for pharmaceutical in vitro studies to model the transport of drugs' or their components' absorption. During growth and differentiation also the permeability for charged species, and consequently the electrical properties of the cell layer, are subject to a gradual change. This change will be investigated using impedance spectroscopy monitoring.

(a) Epithelial cell of the intestine adhering to blood vessel.

(b) Cross section of the intestine covered with epithelium used for drug transport studies.
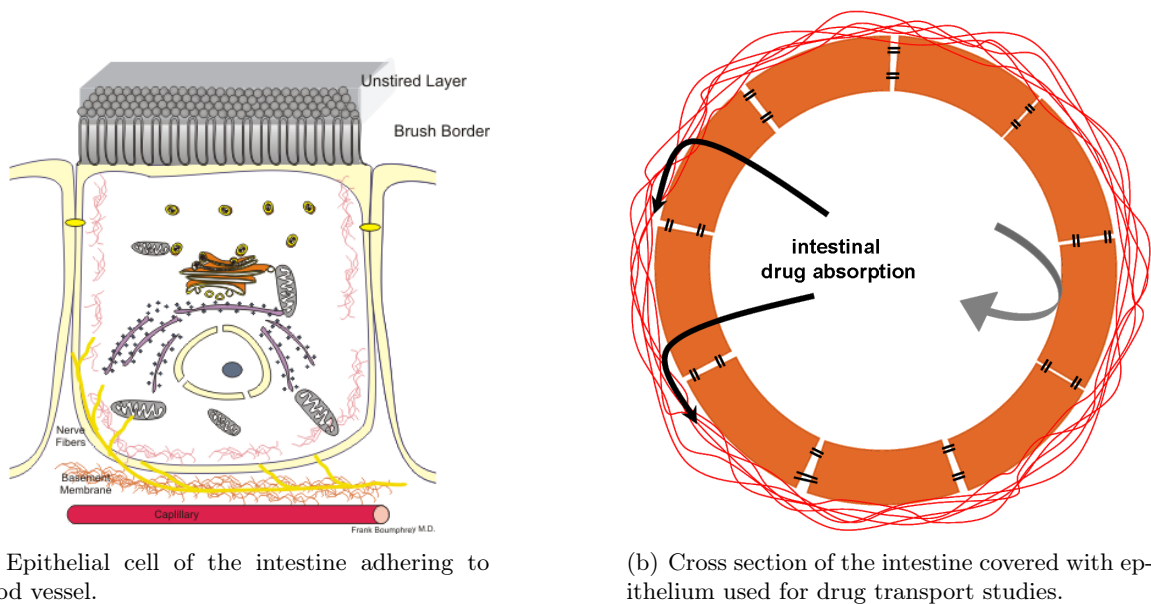
Figure 3.5: Schematic Caco-2 cell in the small intestine.

For these pharmaceutical transport studies it is essential to know whether the cells have built a dense confluent mono layer with an intact brush border or if gaps are left in the cell layer allowing for leakage of material and paracellular transport. An increased transport of charges leads to a measurable decrease of impedance. Confluence of Caco-2 cells, cultured on impermeable substrates, is characterized by the occurrence of domes. These domes can be detected via optical inspection. Another, widely used method to monitor the extent of the cells's confluence is the monitoring of transepithelial electrical resistance [Ranaldi 03].

These electrical measurements must be performed under suitable environmental conditions. Cell culturing requires sterile working and controlled environmental conditions. Caco-2 cells grow in nutrient medium at a temperature of $37°\,C$ and a CO_2 concentration of 95%. After they are seeded onto a growth substrate in small concentrations, these cells start reproducing untill a confluent layer covers the whole substrate.

3.3 Electrical Impedance

The electrical properties of biological specimen may be used for their investigation. For non-excitable cells such as Caco-2 cells the electrical impedance can be used as a parameter to monitor the status of cell layers. As alternating current my be generated over a wide range of frequencies, also the measured impedance can be recorded as an impedance spectrum over this frequency range of exciting signals. Electrical impedance is the complex resistivity of circuit elements exposed to alternating currents. These circuit elements may be parts of a complex network of passive devices, where they react individually to the applied alternating current.

Resistor	Inductor	Capacitor
$U\left(t\right) = R\,I\left(t\right)$	$U\left(t\right) = L\,\frac{dI(t)}{dt}$	$C = \frac{dQ(t)}{dU(t)}$ $I\left(t\right) = \frac{dQ(t)}{dt}$ $I\left(t\right) = C\frac{dU(t)}{dt}$ $U\left(t\right) = \frac{1}{C}\int I\left(t\right)\,dt$

Table 3.2: Description of passive electrical devices.

[Kohlrausch 85] If the alternating current as well as the voltage is periodical in time, they can be expressed as a linear combination of sines and cosines:

$$U(t) = U_0(\cos\omega\,t - i\,\sin\omega t) = U_0 e^{i\,\omega\,t} \tag{3.1}$$

A convenient way to visualize this periodical relation is the arrow diagram in the Gaussian plane. Figure 3.6 shows an arrow of length U_0 is rotating with rotational speed ω. The right horizontal axis shows the development in time.
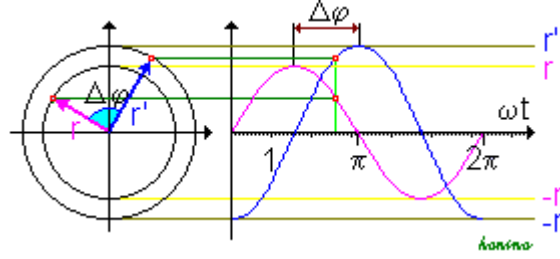
18

Figure 3.6: Schematic illustration of an arrow diagram.

If sinusoidal potential modulations are applied to passive circuit elements, the responding currents will experience changed amplitudes and phases.

Biological cells with their cell membrane and the cytoplasm show capacitive and resistive characteristics. Therefore, inductive behavior can be neglected in the present discussion of impedance.

$$U(t) = U_0 e^{i\omega_u t} \tag{3.2}$$

$$I(t) = I_0 e^{i\omega_i t} = \frac{U(t)}{Z(t)} \tag{3.3}$$

On the lines of Ohm's law, the voltage is proportional to the current at any time. Proportional constant is the impedance Z.

$$Z = \frac{U(t)}{I(t)} = \frac{U_0 e^{i\,t\,\omega_u}}{I_0 e^{i\,t\,\omega_i}} = \frac{U_0}{I_0}\, e^{i\,(\varphi_u - \varphi_i)} = |Z|\, e^{i\,\varphi} \tag{3.4}$$

The impedance may be characterized by it's absolute value $|Z|$ and the phase component φ. In the cell layer $|Z|$ and φ are defined by the cytomembrane. To calculate the impedance of a capacitor $U = \frac{Q}{C}$ is differentiated in time. That gives

$$\frac{dU}{dt} = \frac{1}{C}\frac{dQ}{dt} = \frac{1}{C}\,I \tag{3.5}$$

For a periodic signal $U = U_0 \cdot \cos \omega t$ that is $I = \omega C \cdot U_0 \cdot \cos(\omega t + 90°)$ and using $I_0 = \omega C U_0$ gives the complex resistance of a capacitor:

$$Z_C = \exp^{-i\pi/2} \frac{U_0}{I_0} = -i\,\frac{1}{\omega C} = \frac{1}{i\,\omega C} \tag{3.6}$$

The capacitive impedance Z_C depends on the frequency of the applied voltage. It decreases as ω increases and becomes sufficiently small at a cutoff frequency. The overall impedance of an epithelial monolayer can be approximated by a highpass circuit. An electrical highpass is a circuit that transmits high frequencies ω undamped, but suppresses low frequencies. Figure 3.7 shows a realization of a highpass.
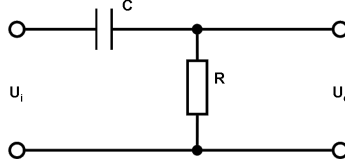
19

Figure 3.7: Equivalent circuit diagram of a capacitive highpass.

The capacitive behavior of the cell membrane leads to strong frequency dependence of the overall impedance. This dependence can be explored using the methods of impedance spectroscopy. [Demtroeder 99]

3.4 Impedance of Electrolytes

In the system under investigation the medium and it's impedance is an essential component. The medium is a salt solution with organic components (eg. proteins) and may be treated as an electrolyte. The transport of charges, as performed by an electrolyte solution is proportional to the electrical field $\vec{E}$ and therefore proportional to the potential difference along the charge's path. [Hamann 05].

$$I = LU \tag{3.7}$$

The constant of proportionality L is the conductance. The unit of conductance is $1\Omega^{-1} = 1\,Siemens$, it is the reciprocal of resistance. Electrolytic conductance depends on concentration and mobility of ions in the electrolyte. An applied voltage generates an electrical field $\vec{E}$ which accelerates the dissociated ions. Due to friction forces, these ions will move with a terminal velocity $\vec{v}^{\pm} = u^{\pm}\vec{E}$, where $u^{\pm}$ denotes the ions' mobility. The unit of ion mobility is usually $\left[\frac{cm^2}{Vs}\right]$. The terminal current of a salt solution generated by the movement of all the cations and anions of the salt is given by

$$I = I_+ + I_- = e_0 A(N_+ v_+ + N_- v_-) \tag{3.8}$$

N is the number of ions, v is the terminal speed of ions, e_0 the elementary charge of $1.6{\cdot}10^{-19}$C and A is the cross section the ions are transiting. With $N_+ = N_- = cN_A$, N_A being the Avogadro number and $F = 96487\left[\frac{C}{mol}\right]$ the Faraday constant, equation 3.8 can be written in terms of the ions' concentration c:

$$I = cAF(u_+ + u_-)\left|\vec{E}\right| \tag{3.9}$$

20

The common parameters found in literature, like [Adam 03], are the specific conductivity λ and equivalent conductivity Λ

$$\lambda = \left| \frac{(I/U)\, l}{A} \right| = c\, F(u_+ + u_-) \tag{3.10}$$

$$\Lambda = \frac{\lambda}{c} = F(u_+ + u_-) \tag{3.11}$$

Due to interionic forces, the equivalent conductivity is dependent on the electrolytes concentration c. With $\Lambda_0 = \lim_{c \to 0} \Lambda(c)$ and $a = f(c) \cdot c$ being the electrolyte's activity. For strong electrolytes the Kohlrausch law states the equivalent conductivity to be:

$$\Lambda(c) = \Lambda_0 - a\sqrt{c} \tag{3.12}$$

Theoretical background for these empirical relations is based on the Debye-Hückel-Onsager-Theory [Hamann 05].

A system inherent challenge is, that a measurement of the impedance of electrolytes is accompanied by the effects at the metal-electrolyte interface. An electrochemical double layer, represented by a capacitor with a distinct cutoff frequency, builds up at charged electrodes. The impedance of any medium in between the electrodes can only be measured directly for frequencies higher than the cutoff frequency of this capacitor. Below the cutoff frequency, the measured impedance is dominated by a serial circuit including the Helmholtz capacitor. The electrochemical double layer is formed from the solutions' ions as effect of an electric fluid. Excess charges on the electrodes' surfaces attract solvatized ions of opposite sign. These solvatized ions tend to minimize the distance to the opposite charged layer, the electrodes' surface. Therefore, a planar double layer with the thickness of the hydrated ions effective radius r_h is formed. This layer is called the Helmholtz layer, electrically represented by a charged capacitor

$$C_H = \frac{\epsilon\, A}{r_h} \tag{3.13}$$

Figure 3.9 visualizes the ions' positions and their hydration shells. On the cathode's surface excess charges, and eventually anions bound by van der Waals forces, form the inner Helmholtz plane. The attracted cations, surrounded by their hydration shells form the outer Helmholtz plane. On an anode an analogous layer sequence with the opposite charge is formed. In addition to this rigid double layer, a diffuse double layer C_D is formed by unoriented H_2O dipoles and solvated ions [Orazem 08]. The thickness of the diffuse layer can be estimated as

$$r_d = \sqrt{\frac{\epsilon\, k\, T}{e_0^2 \sum z_i^2\, n_i^\infty}} \tag{3.14}$$

Where ϵ is the permittivity of the medium, $k = 1.380\,6504 \cdot 10^{-23}$ J/K is the Boltzmann constant, T is the absolute temperature in Kelvin, $e_0 = 1.602 \cdot 10^{-19}$ is the elementary charge and

z_i is the number of charges per ion. The rigid Helmholtz layer and the diffuse layer both effect the total capacity.

(a) Helmholtz double layer.

(b) Hydrated ion with effective radius r_h.
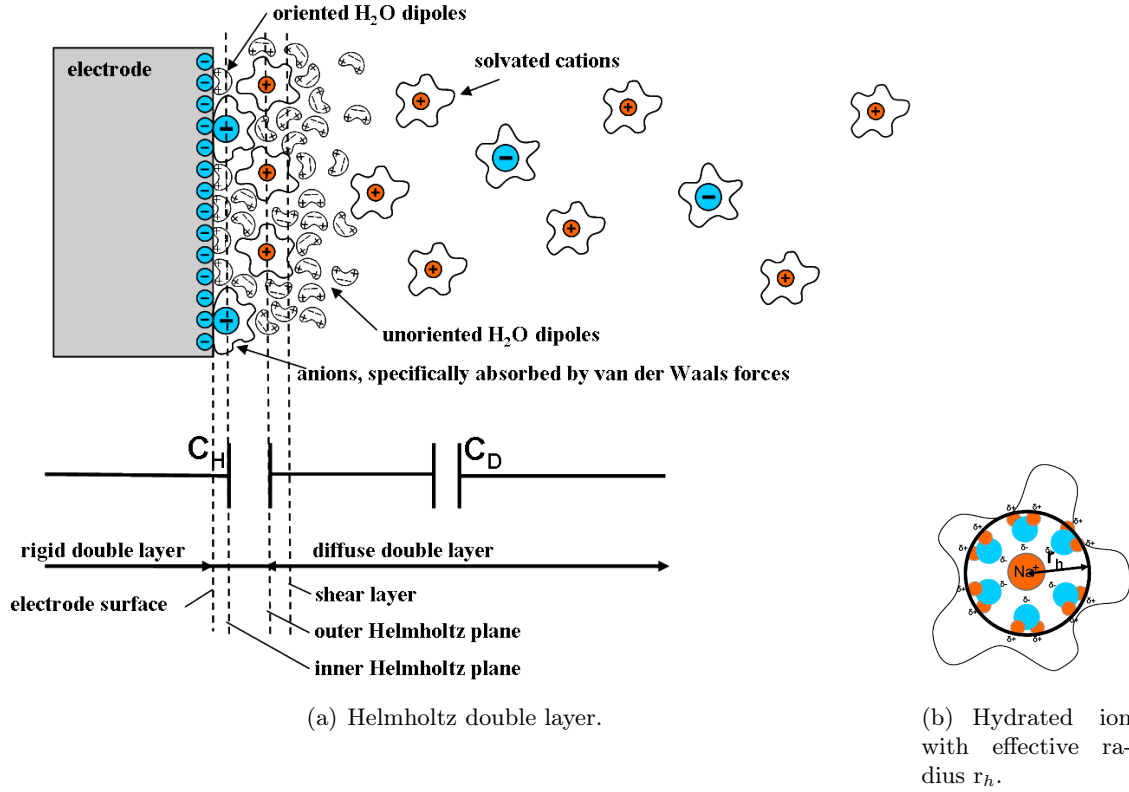
Figure 3.8: Ions in the electrolyte attach to the electrode, forming the electrochemical double layer. Image inspired by [Fafilek 09].

C_H and C_D are connected serially and sum up to the overall capacity

$$C = \frac{C_H \, C_D}{C_H + C_D} \tag{3.15}$$

Several models (Stern-Grahame, Bockries) have been established to take into account on the one hand various events at the metal/electrolyte phase border and on the other hand varying dielectric permittivities ϵ. The real configuration can be very complex and has to be explored for the present setup. Usually, this electrode‑electrolyte impedance is referred to as constant phase element (CPE) [Bisquert 98] and it's impedance Z_{CPE} can be expressed as:

$$Z_{CPE} = \frac{1}{Q} \left(i\omega \right)^{-n} \tag{3.16}$$

$$with \ 0 \ < \ n \ < \ 1$$

Where Q is a constant with the dimension $\left[F \, s^{n-1} \right]$. When $Q = C$ and $n = 1$ the constant phase element represents an ideal capacitor.

3.5 Electrical Properties of Caco-2 Mono Layers

The main component of interest in our system is the Caco-2 cell layer and it's electrical properties. Epithelial cells are electrically inactive. They do not produce an action potential, as neurons do, but they may generate static potential differences by regulating ion concentration gradients between extracellular space and intracellular space. Living cells influence the impedance of the extracellular medium by changing the concentration of ions that are also carriers for the transport of electrical charges.

Also other components of the cell or the cell medium - such as proteins - may act as carriers of electric charge. Living cells metabolize their nutrient medium. While growing, they break up complex molecules to smaller charged particles, leaving an increased number of ions. Simultaneously, they also transport ions into the intracellular medium. This way they may change the concentration of ions in the electrolytes and therefore influence the measured impedance [Adam 03].

A biological cell, due to it's morphology, builds up a complex electrical system. The cell's membrane divides the fluid volume into extracellular and intracellular compartments. The membrane is selectively permeable to several ions. As there are ions responsible for creating an osmotic equilibrium, there will also develop an electrochemical equilibrium. The Nernst equation [Bolsover 04] allows to calculate the equilibrium voltage of an ion species across a membrane.

$$U_{eq} = \frac{R\,T}{z\,F}\,\ln\left(\frac{[Ion_{outside}]}{[Ion_{inside}]}\right)[V] \tag{3.17}$$

Where $R = 8.3\left[\frac{J}{Kmol}\right]$ is the gas constant, T[K] is the absolute temperature, z is the charge on the ion in elementary charge units and $F = 96487\left[\frac{C}{mol}\right]$ is the Faraday constant. If there are more ion species striving for equilibrium, each ion's contribution adds to the overall voltage, weighted according to their concentration.

$$U_{eq} = \frac{R\,T}{z\,F}\,\ln\prod_{i=1}^{k}\{a_i\}^{\nu_i} \tag{3.18}$$

In living cells potassium has the highest intracellular concentration (see table 3.1) of all ions, responsible for the equilibrium. The diffusion potential is therefore dominated by potassium, $U_{eq}(K^+) \approx 70mV$. Electrically, the membrane of a cell behaves like a charged capacitor. It prevents any transport of charges into or out of the cells. But there are proteins which transport certain charged molecules. These carriers or channels can be represented by variable ohmic resistors [Asphahani 07]. An epithelial cell can be modeled as an electrical circuit, composed of capacitors and resistors. Figure 3.9 shows a circuit model of a single Caco-2 cell.
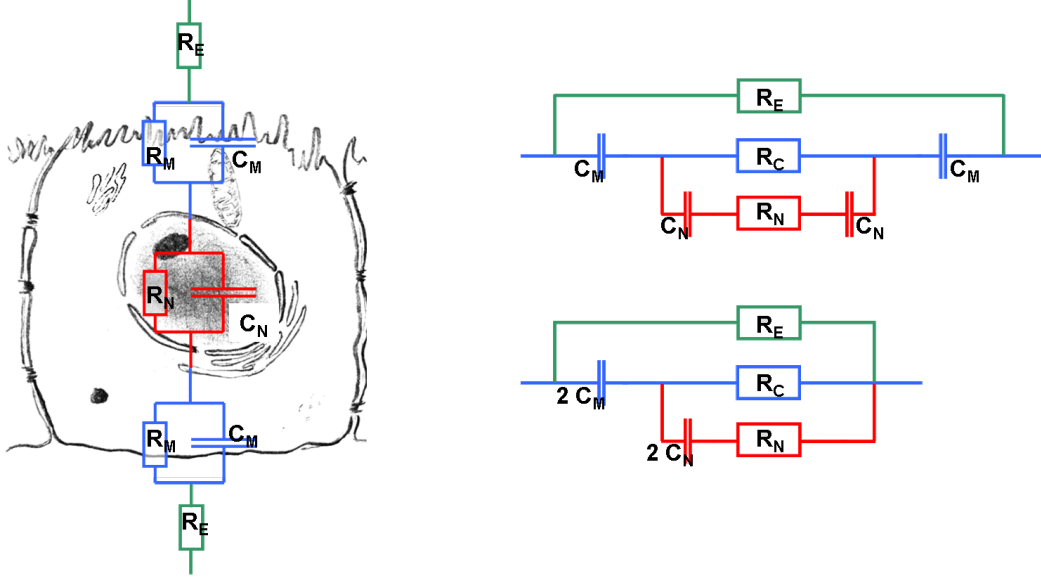
Figure 3.9: Circuit model of a single epithelial cell, inspired by [Fafilek 09].

R_E is the resistance of extracellular medium, R_M is the resistance representing ionic transport through the cells membrane, C_M is the capacitance representing the cells membrane. R_N and C_N belong to the nucleus. The model can be simplified as shown in the right side in figure 3.9 by merging the membranes resistance and the resistance of the cytoplasm to R_C and assuming the capacity of the apical membrane being equal to the capacity of the basal membrane. As long as the cells are separated, overall impedance is dominated by extracellular medium, an electrolyte with reasonable high conductivity. After several days of cell growth, epithelial cells form confluent mono layers with all cells closely connected. Within these mono layers, the membranes of Caco-2 cells connect tightly to each other via tight junctions. A tight junction is a connection between the cells' membranes which is no longer permeable to ions. As the Caco-2 cells differentiate to form a functional intestinal membrane, they morphologically polarize. Due to different ionic concentration an electrical potential forms between the apical and basal side. Apical and basal capacities and resistances generally differ from each other. An equivalent circuit diagram of an epithelial monolayer is shown in figure 3.10. Besides the cellular impedance as defined in figure 3.9 an additional component, the paracellular resistance R_{para} has to be considered. R_{para} may be considered as a measure for the confluence of a cell layer and for the status of the tight junctions between cells. The impedance of a cell layer is a combination of serial and parallel elements resulting in a total transepithelial impedance of an epithelial cell monolayer:

$$Z_{monolayer} = \left(\left(\frac{R_A}{1 + R_A\, i\, \omega\, C_A} + \frac{R_B}{1 + R_B\, i\, \omega\, C_B} + R_{cyto} \right)^{-1} + R_{para} \right)^{-1} \qquad (3.19)$$
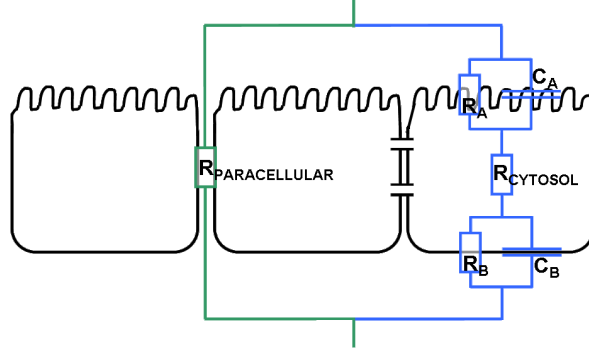
Figure 3.10: Equivalent circuit diagram of Caco-2 mono layers.

which can be simplified to

$$Z_{monolayer} = \frac{R_A\,B\,+\,R_B\,A\,+\,R_{cyto}\,A\,B}{A\,B\,+\,R_{para}\,(R_A\,B\,+\,R_b\,A\,+\,R_{cyto}\,A\,B)} \qquad (3.20)$$

with the frequency-dependent contribution included in

$$A\,=\,1\,+\,R_A\,i\,\omega\,C_A \qquad (3.21)$$

and

$$B\,=\,1\,+\,R_B\,i\,\omega\,C_B \qquad (3.22)$$

Provided the ideal case that the mono layer is confluent, R_{para} does not contribute to the total impedance any more and the cell layer may be treated as a quasi-single intracellular compartment, comprising all cells in the network. In the case of a total confluence of the cell layer the transepithelial impedance is high for lower frequencies and decreases as the frequencies rise. This can be identified as a high pass behavior of an electrical circuit [Thein 10]. Various research groups have used impedance spectroscopy to fit parameters such as capacitance and resistance numerically to their measured data. They found that these values strongly depend on the cells contact to the substrate they are cultured on.

3.6 Basolateral and Transepithelial Impedance Measurement

Impedance Spectroscopy (IS) is an electrochemical method to characterize intrinsic electrical properties of any material and its interface. The basis of IS is the analysis of the impedance (resistance of alternating current) of the observed system as frequency-dependent response to the exciting signal. Impedance analysis provides quantitative information about the conductance, the dielectric coefficient. Impedance spectroscopy also offers the advantage, that it can be easily implemented in microfluidic devices and lab-on-chip devices [Iliescu 07]. One of the most remarkable aspects of impedance spectroscopy is the fact that it is a non-invasive and non-destructive method that can be used for continuous monitoring.

A wide variety of applications has been reported, especially in bioscience where sensitivity to invasive probing methods is inherent. [Coster 96]. It is commonly used for general studies of biological tissue for characterization [Dean 08]. General consistency has been found between the electrochemical impedance response and the morphological observation, therefore impedance spectroscopy has proven to be a reliable method for monitoring growth and cytotoxy of mammalian cancer cells [Guo 06]. Impedance analysis can be applied for different cell types ranging from bacterial cells [Varshney 09] to human cell cultures. Impedance spectroscopy was used for investigating the behavior of endothelial cells on substrate coated by a fibronectin layer and in presence of cytotoxicants lipopolysaccharide [Bouafsoun 08] and also necrotic cell response could be detected with this method [McRae 99]. In effect, there are two distinct configurations to measure a cell layer's impedance: the basolateral and the transepithelial configuration. Lo et. al. [Lo 99] have compared both methods and found considerable differences in the measures impedance values.

(a) Basolateral impedance measurement. (b) Transepithelial impedance measurement.
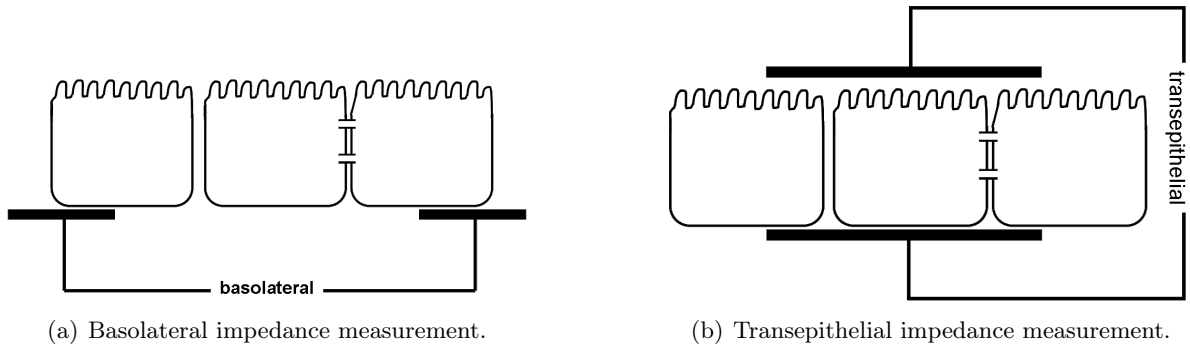
Figure 3.11: Two methods for impedance measurement.

Basolateral impedance measurement (figure 3.11 (a)) uses planar electrodes at the basal lamina of adherent cell cultures. Various implementations of this type can be found in literature, such as 'Electric cell-substrate impedance sensing' ECIS [Liu 09] and 'interdigitated electrodes' (IDEs) [Varshney 09], [Fischeneder 09]. Transepithelial resistance setups (TER, TEER; figure 3.11 (b)) measure the impedance of cell cultures across the epithelium. Assess-

ment of the transepithelial electrical resistance value is a method widely used in biotechnology and pharmaceutical studies to analyze the permeability of biological barriers, such as the blood-brain barrier or the intestinal epithelium. A commercially available implementation [Mil 09] measures the impedance of cell layers grown on permeable membranes at a sensing frequency of 12.5 Hz. The TEER value quantifies the transepithelial transport of agents by measuring the electrical resistance of cell layers across the cell membrane. It characterizes especially the barrier function of tight junctions.

This work presents the development of an approach including a setup to measure the transepithelial impedance in a wide range of frequencies (50 Hz to 100 kHz) over the complete growth cycle of Caco-2 cells. The measurement will be performed using microstructured electrodes.

Chapter 4

Experimental Setup and Procedures

Continuous monitoring of the cells' impedance spectroscopy provides information about the cell culture's state. The sensing device to measure the transepithelial impedance of adherent Caco-2 monolayers is a two terminal setup configuration as shown in figure 4.1. Figure 4.2 shows a schematic image of the setup for the transepithelial measurement. The main components are the electrodes, the multiplexer, the LCR-meter and the operating LabView program. For the measurement the whole setup is placed in an incubator to provide the necessary environment for the cell cultures. The measurement setup is designed for 8 wells so that 8 cell cultures may be grown and measured simultaneously. Both basolateral (bottom) and apical (top) electrodes are fixated on a specimen holder which is electrically connected via a 32 lead ribbon cable to a multiplexer so all available electrode configurations can be measured sequentially. Several measuring configurations in different wells have to be addressed consecutively. This task is accomplished by the multiplexer explained in section 4.2.1. The MUX is located outside of the incubator. The multiplexer loops the measurement's signal through to an LCR meter, see section 4.2.2. The LCR-meter, connected to the multiplexer, measures the impedance and forwards the data to a LabView program for data collection and evaluation. Impedance spectroscopy is recorded in a frequency range of 50 Hz to 100 kHz. In return the LabView instance sets parameters such as measurement frequency at the LCR meter and operates the multiplexer. For this purpose a data cable links the PC to the LCR meter and to the multiplexer.
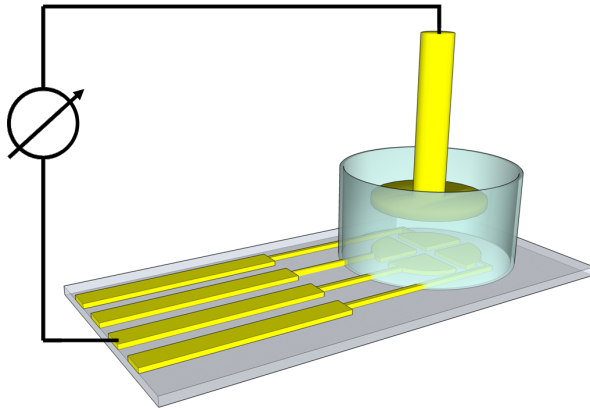
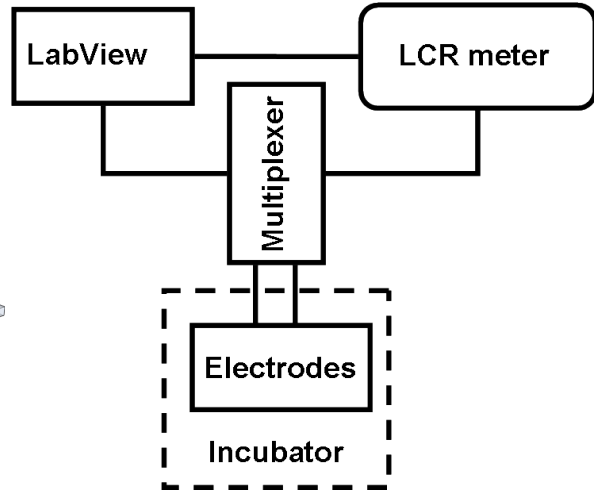Figure 4.1: Schematic illustration of a well with electrodes.

Figure 4.2: Overview of the measurement setup.

The most important criterion for choosing the method for sensor fabrication was the possibility to miniaturize and replicate the sensor. Therefore, methods and materials of microelectronic fabrication as described in section 4.1 were used.

Borosilicate was used as substrate to allow for optical inspection using inverted microscopy. Basic requirements for the used materials and procedures are their biocompatibility and conductivity. Therefore, noble metals such as gold were selected. Gold was chosen for the planar electrodes due to it's electrochemical persistence. For adhesion a thin biocompatible titanium layer was used as interface layer between gold electrodes and the substrate.

To fabricate planar gold electrodes optical lithography was used. This technology allows to transfer thin layers of a wide range of materials onto surfaces and to create precise structures. The demand to monitor the cells' state non-invasively defines the requirements for the measurement setup as described in section 4.2. To realize a sensor for impedance of adherent cell cultures, planar electrodes on borosilicate plates were fabricated. Cells need a fluid environment for living. They have to be confined in wells, therefore a silicone containment was attached onto the planar electrodes, which is depicted in section 4.3.3. For online monitoring of cell growth the cells and electrodes need to be placed within an incubator.

4.1   Sensor Fabrication

The entire sensor consists of basolateral (bottom) electrodes fabricated on planar substrates and apical (top) counter-electrodes fabricated as macroscopic pin electrode of $5\,\text{mm}$ in diameter. The following sections describe the fabrication of the bottom electrode. The miniaturized electrodes were fabricated lithographically under cleanroom conditions using the processes and parameters discussed in the following sections.

4.1.1 Concept and Design of the Photo Mask

The planar electrodes were designed using AutoCad07. A layout was designed to meet the specific requirements of a transepithelial impedance measurement of biological cell. The exact requirements and solutions according to these requirements are discussed in section 5.1.1. Figure 5.2 shows the result of the design of the electrodes layout. For the creation of photomask holding the desired patterns was purchased commercially. A photo mask contains the desired patterns as a combination of transparent and opaque areas. The transparent glass substrate of the photomask is covered partially by an opaque chrome layer. The photomask designed for this purpose contained several arc shaped structures, forming the planar bottom electrodes. Therefore, a photomask with very low roughness of lines was required. A mask meeting the required criteria was purchased from the company 'ML&C GmbH' in Jena. The photomask design, created via AutoCad, was sent as a Drawing Interchange File Format (dxf) and a mask with the specifications listed below was received.

substrate material	Sodalime
opaque areas	Chromium
size	4 inch x 4 inch x 0.06 inch
roughness of lines	$< 100\,\mathrm{nm}$
width of structures	$20\,\mu\mathrm{m}$

Table 4.1: Specifications of the photo mask.

4.1.2 Optical Lithography

Optical lithography was used to fabricate planar gold electrodes on a (5 x 5) cm^2 borosilicate glass substrate. Optical lithography copies patterns from a photo mask onto the sample. This method was used to produce feed lines for the electrodes with a width of 150 μm and creates very accurate, reproducible structures.

To transfer the patterns from this chrome photo mask to the glass substrate several steps of optical lithography were optimized and performed as visualized in figure 4.3. For pattern transfer a Karl Suss MJB3 Photomask Aligner a mercury arc lamp producing high intensity light with wavelengths of 365 nm (i-line), 405 nm (h-line), and 435 nm (g-line). It is optimized for mask sizes of 4 inch x 4 inch x 0,06 inch and 3 inch x 3 inch is the maximal wafer size that can be fully exposed. An overview and explanation of each procedure is given below. Extensive information on optical lithography can be found in literature [Campbell 96].
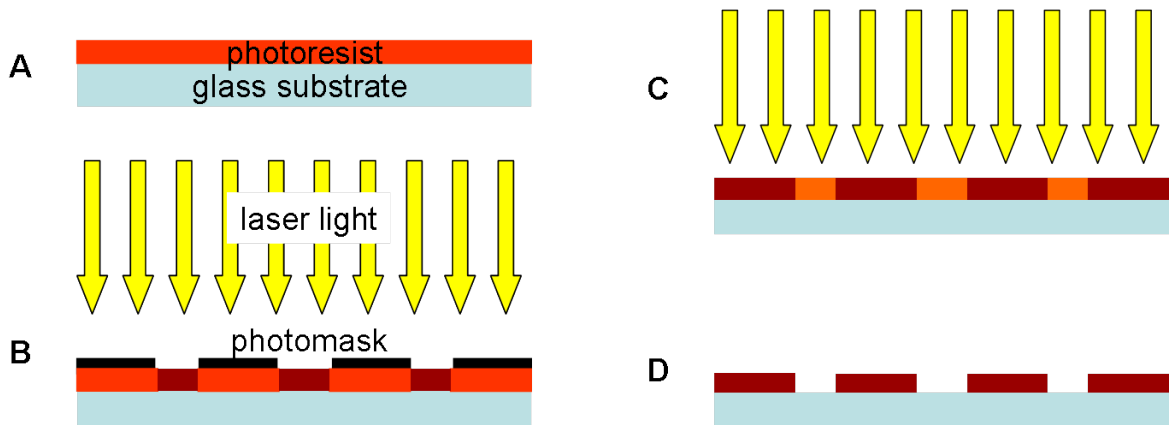
Figure 4.3: Visualization of lithographic process sequence: A = spin coating, B = structure exposure, C = flood exposure, D = development

0) Cleaning

Proper cleaning of the working sample at several stages of the process is indispensable for a good result. At first dust particles were removed with high pressure nitrogen. Then the sample, immersed in distilled H_2O, was placed into ultrasonic bath for several minutes. Subsequently, the sample was immersed in acetone, a polar aprotic solvent, to remove residues. Acetone is volatile at room temperature and tends to produce stains while evaporating. To avoid these stains, the sample was rinsed immediately in isopropanol. High pressure nitrogen was used to dry the sample and to remove drops. This cleaning procedure was repeated until no particles could be detected optically.

Cleaning agent	boiling point
Acetone	56°
Isopropanol	82°
distilled water	100°

A) Spin Coating the Photoresist The liquid photoresist AZ 5214 E (Microchemicals) is distributed uniformly across the sample using a spinner. The spinner's speed of rotation determines the thickness of the photo resist. It was varied from 3000 rpm to 4000 rpm for 35 seconds, which gives, according to the calibration curve shown on the right hand, layers of $1.62\,\mu m$ to $1.4\,\mu m$. Subsequently the sample was heated to $120°\,C$ and prebaked for 50 seconds. The lacquer's adherence also depends on the substrates material. For the used borosilicate substrate it was necessary to use a sputtered chrome layer for undercoating to assure the photo resist's adherence on the substrate.
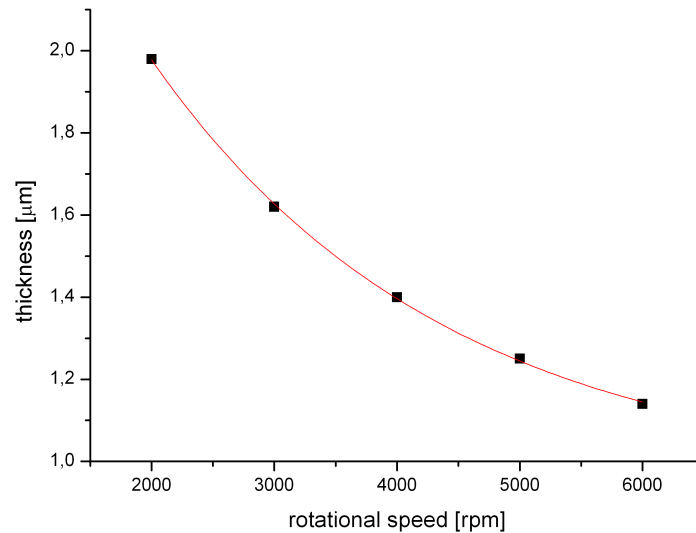
Figure 4.4: Dependency of the photoresist's thickness on rotational speed [Clariant].

A pattern is transferred from photo mask to substrate by mapping the pattern onto the light sensitive lacquer. The photoresist AZ 5214 E has it's spectral sensitivity in the range of 310 nm to 420 nm. A mercury arc lamp, emitting 356.4 nm (I-line) and 404.7, nm (H-line) was used to harden the desired structures.
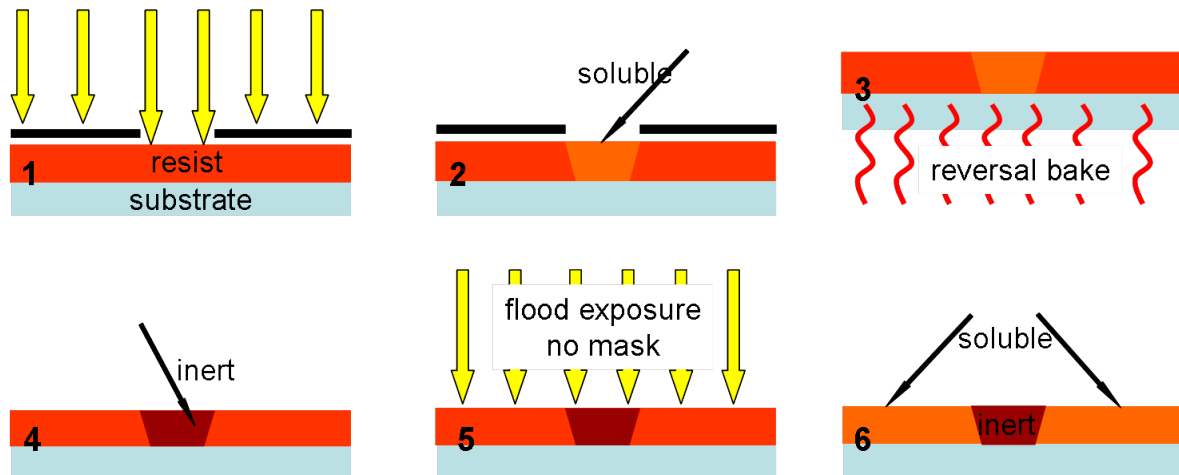
Figure 4.5: Schematic illustration of the steps while processing the 5214 AZ image reversal photo resist.

B) Resist exposure

Light exposure causes the 5214 photoresist to rearrange it's molecular structure. Photo resists can be categorized as either positive or negative resist. Exposed areas of positive photo resists will dissolve faster than unexposed areas during the development process. With positive resists the resulting wall profile has a positive slope of 75° to 85°. Negative photo resists

'harden' in consequence of light exposure. Therefore, also negative slopes of more than 90° are feasible. The 5214 photo-resist combines both features. Figure 4.5 illustrates the states during processing of reversal photo resists. For structure exposure the photo mask is placed onto the lacquer covered sample. In this work contact exposure with a Karl Suss MJB3 was performed, so that the minimal distance between photo mask and photoresist allows to to reduce artifacts caused by stray light. After alignment of the photo mask of the planar electrode arrays and sample the photoresist was exposed for 3.5 seconds at a wavelength 356 nm. This step generates structures of soluble and inert areas within the photo resist.

Image reversal bake In figure 4.5 the image reversal processing is visualized. Part 3 denoted the image reversal bake. This step was necessary to invert the previously soluble areas of the 5214 photo resist to inert areas. A second heating, the image reversal bake, combined with a flood exposure inverts these structures in so called 'reversal photo resists'. The sample was hardbaked for 50 seconds at $120° C$.

C) Flood exposure After structure exposure the entire specimen is exposed to ultraviolet light a second time using the MJB3 without the photomask. This step (step 5 in figure 4.5) in combination with the so-called image reversal bake (step 3 in figure 4.5) inverts inert and soluble areas of the photo resist. Flood exposure at $356\,nm$ for 25 seconds makes the invert structure of the mask soluble in the developer and hence defines the final structures which can be elaborated in the developer. This kind of reversal structuring is necessary to form sharp edges at the boundaries of structures. After step 'D Development' a sharp angle between substrate and the edge of the photo resist is created. This angle enables clean lift off after sputter deposition.

D) Development

The specimen is now immersed in an developer for AZ5214. This developer MIF 726 is a metal ion free developer based on tetramethylammoniumhydroxide [AZ 06] The MIF 726 was allowed to remove soluble parts of the photo resist by immersion over a time of 60s to 90s. Exact Development times depend on the developer's activity. At this step in the process those predefined areas on the substrate, which will be covered with electrodes, remain unprotected. To stop the development, the sample was immersed into distilled water and subsequently rinsed in fresh distilled water, then dried with high pressure nitrogen. At this stage of the process the photoresist forms an etch mask. It is no longer susceptible to light so the quality of the etch mask was checked using optical microscopy.

Chrome Etch During the lithographical processing, chromium was used as an undercoating for the photoactive lacquer. In contrary to noble metals like gold and titanium, this material is potentially damaging for the Caco-2 cells. Therefore, chromium had to be removed from the sample completely. It was removed by wet chemical etching.

Figure 4.6: Illustration of the chrome etching process. Chemical etching removes unprotected chrome on the surface of the sample.

Chrome layers protected by the photoresist stay unchanged. The chrome etch process was performed twice to remove all chrome from the sample. The sample is immersed in chrome etch for 40 seconds to remove the chrome layer in areas not covered by the photo resist. To stop the etch process, the sample was immersed into distilled water and subsequently rinsed in fresh distilled water, then dried with high pressure nitrogen. This step is particularly critical as water drops tend to leave stains on the sample surface in the subsequent evaporation step. At last the residual chrome between the Ti/Au structures was removed by a second chrome etch for 40 seconds to protect the Caco-2 cells from chrome residuals.

Thin Film Electrodes This step produces the planar electrodes. Titanium was sputtered onto the glass samples with photo resist mask for 120 seconds with 75 Watt at a working pressure of $8 \cdot 10^{-3}$ mbar. The top metal layer was a gold layer, created by sputtering for 30 seconds under argon atmosphere on top of the titanium layer with a working power of 100 Watt.

E) Liftoff
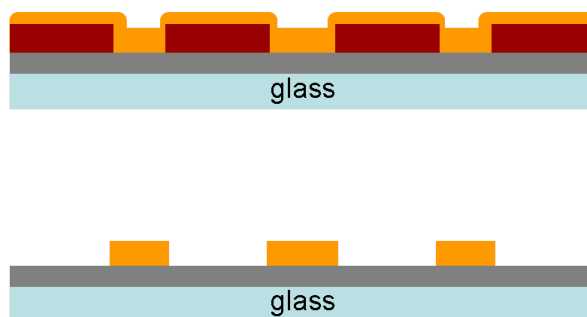
Figure 4.7: Illustration of the liftoff step in MEA production.

The titanium and gold layer on the photo resist mask was then removed during the lift-off step by immersing the sample in acetone for 30 minutes leaving only the metal electrodes and interconnect lines.

4.1.3 Sputter Deposition

To provide biocompatible planar electrodes for the cells to adhere on, sputter deposition was used in this work to fabricate thin layers of gold and of titanium on the borosilicate substrate.

Sputter deposition is a physical vapor deposition method which produces uniformly thin films of a desired material. For the presented work the Ardenne LS 320 S sputter system, (figure 4.8 (a)) was used.
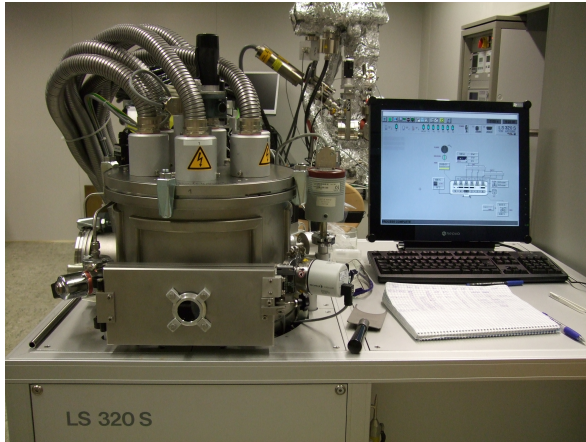
(a) Ardenne LS 320 S sputter system.

(b) Schema of a sputtering system using argon as an inert gas and gold as target material.

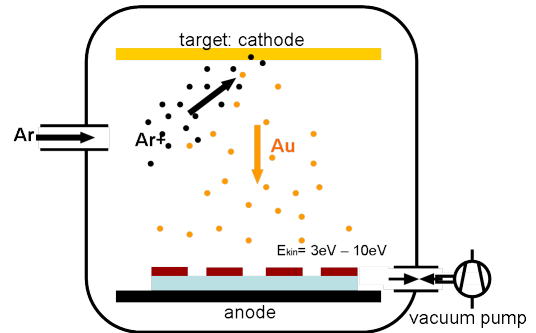Figure 4.8: Schematic illustration of sputter deposition used to fabricate the thin film electrodes on the borosilicate substrate.

The system was pumped to a base pressure of $2 \, 10^{-5}$ mbar. The sputtering process was started at a pressure of $8 \, 10^{-3}$ mbar with a glow discharge to generate argon plasma. To fabricate the planar electrodes chromium, gold and titanium targets were sputtered at argon pressures of 10^{-1} to 10^{-3} mbar with RF powers of 60 to 100 watt for 15 to 60 seconds. The resulting gold layer is a uniformly thin film of biocompatible, conducting and mechanically resistive material. The first layer deposited onto the glass surface was a chrome layer, generated by sputter deposition applying 100 Watt for 15 seconds under argon atmosphere at a working pressure of $8{\cdot}10^{-3}$ mbar. This resulted in a chromium layer with an estimated thickness of 16 - 20 nm. The chrome layer acts as an agent for the photoresist.
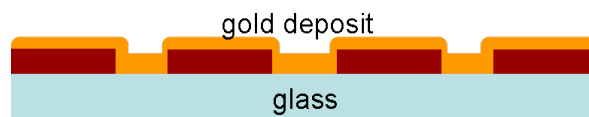
Figure 4.9: Schematic illustration of the substrate with photoresist and deposited gold after sputtering.

The distribution of the sputtered materials' incident angles has it's maximum at 90°, therefore predominantly substrate areas facing the target are covered whereas shadowed areas are kept free of sputtered material. In combination with the use of a reversal photo resist in the lithography process this fact facilitates a clean lift-off of unwanted material.

4.2　Electrical Setup

4.2.1　Multiplexer (MUX)

In the presented setup several electrode configurations have to be scanned sequentially. The switching between measurement channels is performed by a multiplexer. Each measurement position (microwell) contains two to six planar electrodes and a top electrode. A pair of electrodes is always used to measure the impedance in a two terminal configuration. For each measurement of two electrodes must be connected to the LCR meter. For each electrode the MUX provided one electromagnetic switching relay. The number of possible combinations is a sum of possible combinations for planar electrodes and of possible planar - top combinations. This number is calculated by the binomial coefficient, for k=2 it gives the number of a two-elemental subset out of an n-elemental set.

$$\binom{n}{2} = \frac{n!}{2\,(n-2)!} \tag{4.1}$$

Well	Number n of electrodes	combinations
A, G	2	1+1
B, H	6	15+15
C, E	3	3+3
D, F	4	6+6
Sum	**30**	**50**

Table 4.2: Number of pairs (k=2) for planar electrodes.

In total 80 combinations of electrodes exist which may be used for a two-terminal impedance measurement. To minimize systematic errors the established connections have to transport the analogue measurement signal free of losses and interferences from the measurement electrodes to the analyzer. The multiplexer designed to meet these requirements is a circuit of 72 electromechanical relay switches. It is operated via RS232 port by a LabView program and connected via a 9-pole null modem cable to the COM port of a personal computer. The 72 switches are distributed to nine 8-way relay boards, which are controlled by the PC via a connected board. Each relay can be activated individually via the serial interface on the relay board. Figure 4.10 shows the layout of one relay board. Each board measures 160 mm in length and 100 mm in width. The maximum relay switching power is limited by 24 V maximum voltage and 7 A maximum current.
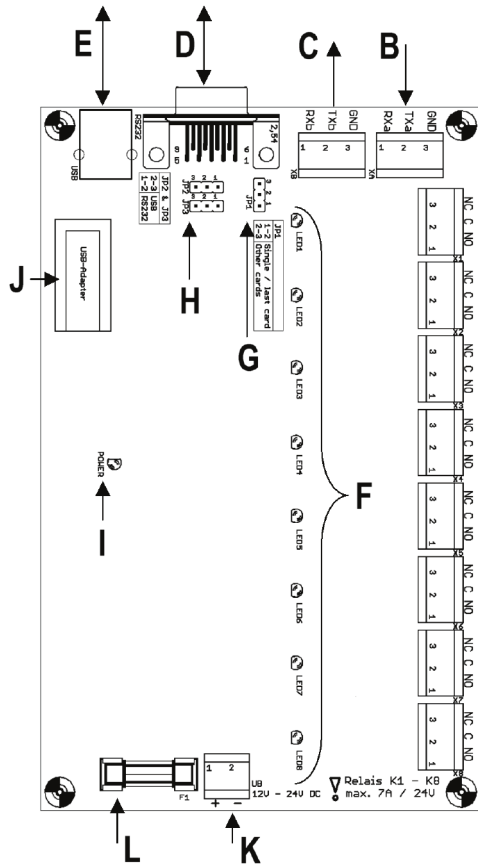
Layout:

A 8 changeover contact switching outputs,

B Serial input from previous relay board or from control computer

C Serial output to next relay board

D Serial connection to control computer via null modem cable (9-pole)

E USB connection to the control PC via USB cable

F LEDs signal the switching status of relays

G JP1 to 1-2 (single board or last relay board), 2-3 all other relay boards

H Connection type to control computer: RS232: JP2 + JP3 to 1-2

I Power LED

J Slot for RS232 USB converter for USB operation

K Supply voltage 12V/DC to 24V/DC

L Fuse 5 * 20mm, 250V / 1A, slow-blow

Figure 4.10: Layout of a relay board with eight monostable relay switches [Con 10].

An adapted circuit was designed and fabricated, it is described in the section 5.1.2 of this work. Once the multiplexer has established a programmed connection, an LCR meter performs the measurement with any pair of electrodes connected to the LCR-meter via the multiplexer. Other electrodes are disconnected and at flooding potential.

4.2.2 LCR Meter

The measurement setup instrument for the samples impedance is the main component of the system. For impedance measurement a high frequency resolution LCR meter, 'Hioki 3522-50 LCR HiTESTER', was used. This instrument measures impedance, phase, inductivity, capacitance, resistance and quality factor of an passive electrical network. As measuring mode either constant current ($10\,\mu$A to $100\,$mA rms) or constant voltage ($10\,$mV to $5\,$V rms) or constant current with limited voltage or constant voltage with limited current can be selected. Either mode can be used to apply a sinusoidal test signal with frequencies in the range of $100\,$mHz up to $100\,$kHz. To set the other measurement parameters, the LCR meter may either be manually operated via touch panel or operated by PC control via the GP-IB interface.
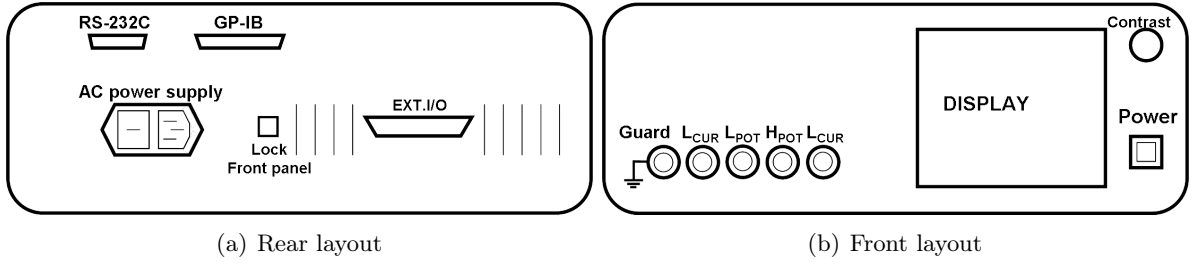
(a) Rear layout   (b) Front layout

Figure 4.11: Front and rear view of the Hioki 3522-50 LCR meter.

Several terminals are located on the rear side. RS-232C interface and GP-IB interface can be chosen to set up the data connection to an automatic operator. An external trigger signal may be connected to the EXT.I/O interface. On the front side, next to the guard connection, are 4 BNC connectors: L_{CUR}, L_{POT}, H_{POT} and H_{CUR}. L_{CUR} and H_{CUR} refer to measurement current, L_{POT} and H_{POT} refer to measurement voltage. The display shows current measurement parameters and measured values. Figure 4.2.2 shows the layout of front and rear view of an Hioki 3522-50 LCR meter. The ranges and accuracies of measured values are shown in table 4.3. More detailed information can be found in the Hioki data sheet [Hio 05].

parameter	range	accuracy
source frequency	$1\,mHz$ to $100\,kHz$	$\pm\,0.005\%$
output impedance	$50\,\Omega\pm10\,\Omega$	
measurement signal level	$10\,mV$ to $5\,V$ rms	
	$10\,\mu A$ to $100\,mA$ rms	
measurement ranges for impedance	$100\,m\Omega$ to $200\,M\Omega$	$\pm\,0.08\%$
output range of phase	$+180°$ to $-180°$	

Table 4.3: Ranges and accuracies of Hioki's measurement parameters.

For the presented work the LCR meter was operated automatically by the LabView program via the GP-IB interface. The output signal was a sinus signal in a frequency range of $50\,Hz$ to $100\,kHz$ with symmetric level control at the zero point and with an amplitude of $\pm10\,mV$. Due to LCR meter's high sampling rate, one measuring cycle can be performed within $5\,ms$. This excitation signal was transmitted via coaxial cables to the multiplexer, which forwarded the signal to the measuring electrodes via a shielded flat band cable. In the measurement cell the excitation signal was alternated and shifted by interaction with the sample. The returned signal was received by the LCR meter after transfer from the multiplexer. The LCR-meter sent the data to the LabView program for collection and evaluation. A detailed description of the LCR meters connections is given in the following chapter.

4.2.3 Connections

This section summarizes the connections and interfaces between the single components of the experimental setup. Figure 4.12 shows a schematic overview to the used connections. A PC, running the LabView program, operates the LCR meter and multiplexer. Control signals for the LCR meter are sent via USB to GP-IB interface. In return the LCR meter sends the processed data from a measurement cycle to the PC.
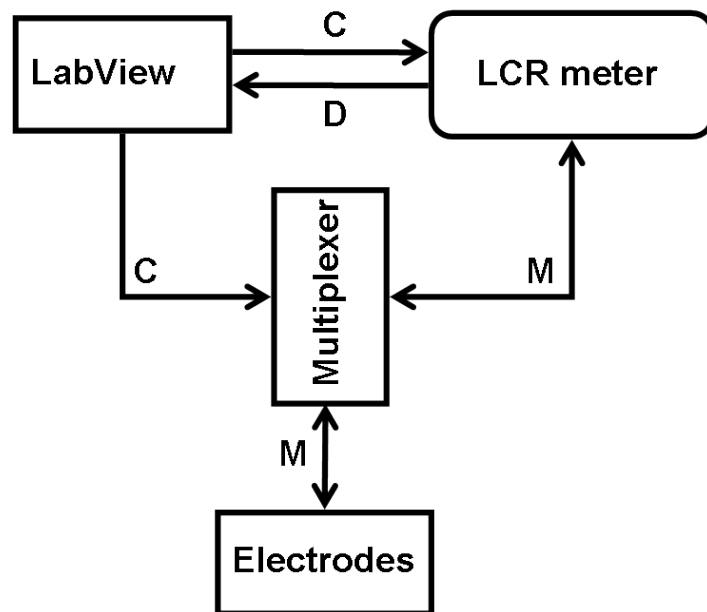
Figure 4.12: Connections of single components in the measurement setup:
C = control signal, D = data signal, M = measurement signal

Operating orders for the multiplexer are transported from the PC's COM port to the multiplexer via a RS-232C interface. The multiplexer then establishes a two way loop through connection for the measurement signal between the LCR meter and the designated measuring electrodes.

The measurement signal between the multiplexer and the electrodes is transported via a shielded 30-pole ribbon cable, whereas the measurement signal between the multiplexer and the LCR meter is transmitted by two coaxial cables connected to each device via BNC plugs. Table 4.2.3 gives an overview on the used connections and plugs.

Connection from - to	Signal	Plugs
PC - LCR meter	control signal	USB and GP-IB
LCR meter - PC	processed data	USB and GP-IB
PC - multiplexer	control signal	COM port and D-subminiature DE-9
multiplexer - relay card	control signal and measurement signal	D-subminiature DE-9; RS232
multiplexer - electrodes	measurement signal	D-subminiature DC-37
multiplexer - LCR meter	measurement signal	BNC

Table 4.4: Connections, plugs and parameters.

4.3 Cell Growth

The continuous electrical real-time monitoring of the growth of a cell layer of Caco-2 cells was the main objective of this work. The preparation of a cell culture and the required preconditioning of the cell cultures environment is described in the following sections.

4.3.1 Handling of Caco-2 Cell Cultures

The Caco-2 cells for this work were cultured under sterile working conditions to avoid micro-biological bacteria, mycoplasma or fungus contamination. All materials and devices used for culturing were sterilized with 70% alcohol. The planar electrodes were immersed for several hours in piranha solution, a mixture of sulfuric acid (H_2SO_4) and hydrogen peroxide (H_2O_2), to remove organic residues. Sterile conditions during preparation of seed suspensions were provided by a laminar airflow system.

To start a fresh Caco-2 cell culture the cells were subcultivated from previous cultures, using trypsin to cut the cell-cell connections. A suspension of Caco-2 cells was seeded onto the planar micro electrode array and transfered to the sterile incubator and cultured for at least ten days in the incubator 'NAPCO 6000 CO_2'. The water-jacketed incubator kept the temperature in the growth compartment at 37°C and humidity at 95%. The CO_2 concentration in inlet air was regulated to 5%. Proper CO_2 supply from the gaseous phase is necessary to enable the bicarbonate buffering system in the medium to maintain the correct concentration of carbonic acid in the culturing medium. During cultivation, the nutrient medium was changed regularly every three days to provide sufficient nutrition for the cells and to remove metabolic products.

41

4.3.2   Nutrient Medium

Cells were cultured in an RPMI (Roswell Park Memorial Institute Medium) Sigma R6504 medium. This medium is based on 10% fetal calf serum (FCS) with additives. The content of one liter RPMI medium is listed in table 4.3.2. It contains inorganic salts, amino acids, vitamins and also antibiotics. The medium enables cell proliferation, differentiation and typical cell functionality. In combination with sufficient CO_2 supply the added bicarbonate ($NaHCO_3$) works as a buffering system to regulate the pH value. To prepare one liter of medium, 10.4 grams of powder are required.

INORGANIC SALTS	g/L	AMINOACIDS	g/L	VITAMINS	g/L
$Ca\,(NO_3)_2\,4H_2O$	0.1	L-Glutamine	0.3	D-Biotin	$2 \cdot 10^{-4}$
$MgSO_4$	0.04884	L-Arginine	0.2	Choline Chloride	0.003
KCl	0.4	L-Cystine $2\,HCl$	0.0652	Folic Acid	0.001
$NaCl$	6	L-Isoleucine	0.05	myo-Inositol	0.035
Na_2HPO_4	0.8	L-Asparagine	0.05	Niacinamide	0.001
		L-Leucine	0.05	p-Amino Benzoic Acid	0.001
OTHERS		L-Lysine HCl	0.04	D-Pantothenic Acid	$2.5 \cdot 10^{-4}$
D-Glucose	2	L-Serine	0.03	Pyridoxine HCl	0.001
Glutathione	0.001	L-Tyrosine	0.02883	Riboflavin	$2 \cdot 10^{-4}$
Phenol Red Na	0.0053	L-Glutamic Acid	0.02	Thiamine HCl	0.001
$NaHCO_3$	2	L-Aspartic Acid	0.02	Vitamin B-12	$5 \cdot 10^{-6}$

Table 4.5: Table of ingredients in RPMI 6504 medium [Sigma-Aldrich 09].

Prior to usage, the entire medium was sterilized by membrane filtration. This procedure guaranties that there are no particles larger than $0.22\,\mu$m left in the medium. Monitoring of relevant changes of the medium's pH value was facilitated by adding the indicator phenol red. At the beginning of a culturing cycle the medium's pH value is 7.5 and tends towards acidic milieu due to metabolic processes of the cells. The change of pH value indicates the time for exchanging the medium. The change of the pH value may also influence the measures impedance signal in this work. This medium was used (i) for preparing initial cell suspensions for seeding and (ii) for replacing consumed medium during ongoing cell growth.

4.3.3 Cells' Containment

During growth on top of the planar sensing electrodes the cells and their nutrient medium need to be confined in a fluid-tight reservoir . The silicone containment 'flexiPERM micro 12' from 'Greiner Bio-One' was used for this purpose. This multiwell containment is of rectangular shape, 60 mm in length, 25 mm in width and 10 mm in hight. Twelve holes with diameters of 6.5 mm form twelve wells for cells. Each well can hold a fluid volume of 0.35 ml [Greiner 04]. When attached to smooth surfaces such as glass slides, the silicone confinement adheres tightly onto the surface due to adhesion forces. A close contact between the surface and the confinement prevented the cells' nutrient medium from leaking. The figure below shows the confinement's dimensions.

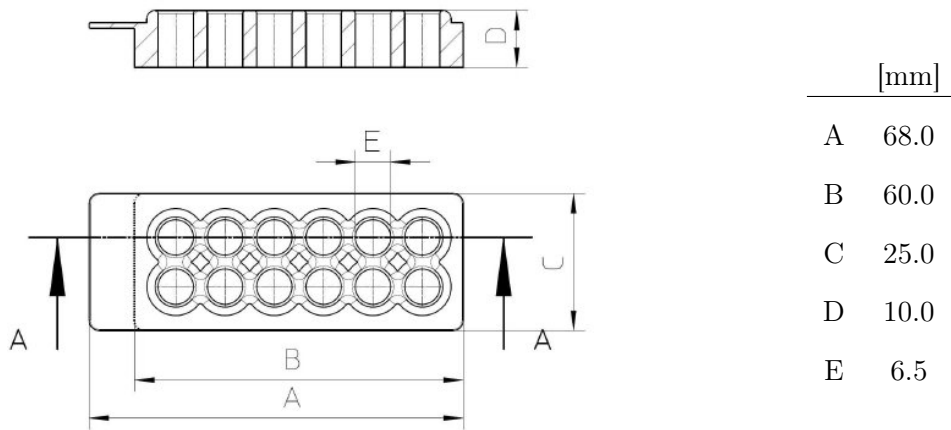|	[mm]
A	68.0
B	60.0
C	25.0
D	10.0
E	6.5

Figure 4.13: Schematic illustration of the silicone confinement, source: [Mil 09].

Periodicity and diameter of the wells defined the layout for the planar electrodes. The silicone confinement was placed onto the sample. It was necessary to fixate the confinement with slight pressure to the sample, therefore a specimen holder was developed and is described in the results section 5.1.3. For growth of cell cultures on the microelectrode arrays the 'Flexiperm' cell confinement was mounted on top of the glass substrate and filled with a cell suspension. With all electrical connections established the impedance of cells mas measured. The following section derives the standard procedures used for evaluation of the data.

4.4 Data Evaluation Procedures

Electrical monitoring of Caco-2 cells by impedance spectroscopy results in a large amount of data. Various effects like material aspects, geometry of the electrodes and chemical influences of the medium will contribute to the measured absolute impedance values. While cells are growing on the electrode they will alter their environment and contact to the electrodes.

Therefore, the measured signal caused by the Caco-2 cells will change in time. To display the specific influence of Caco-2 cells on the measured signal, a parameter Z_{rel}, hereafter referred to as 'relative change' or 'change factor', was chosen. To capture this specific fracture of the impedance each measured signal is evaluated in relation to the impedance value measured at starting time t_0. This evaluation procedure allows to immediately see the relative change caused during growth of cell layers.

$$Z_{rel}(\nu_i, t_j) = \frac{Z(\nu_i, t_j)}{Z(\nu_i, t_0)} \tag{4.2}$$

The collected data is visualized in three dimensional graphs, showing the relative change as an interpolated surface function $Z_{rel}(\nu, t)$ of the frequency ν and the time t post seeding. The sampling points in the frequency range of the impedance spectroscopy are evenly distributed on a logarithmic scale. This fact and the large amount of raw data resulting from cell monitoring over a period of several days requires stable algorithms also capable of interpolating not equidistantly distributed data. Two interpolation algorithms were tested: 'Weighted Average' and 'Renka Cline'.

The weighted average method calculates the weighted average of the points within a specified search radius r weighted with1/r.

$$\langle Z_{rel} \rangle = \frac{\sum_{k=1}^{n} \frac{1}{r_k} Z_{rel,k}}{\sum_{k=1}^{n} \frac{1}{r_k}} \tag{4.3}$$

If there is no value within the search radius, the radius is increased until at least one point is encountered. This algorithm also works for large amounts of randomly distributed data and produces smooth surface plots. Increasing the search radius may cause loss of fine details.

The Renka Cline gridding method is based on the algorithm of Renka and Cline [Renka 84]. Three steps in sequence are performed; triangulation, gradient estimation and interpolation:

1. Triangulation is performed on the sampling rate in frequency range (X) and time range (Y).

2. The gradient in the X and Y direction is estimated for each node as the partial derivatives of a quadratic function.

3. For an arbitrary point Z the interpolated value is calculated using the data values and gradients estimated at each of the three vertices of the triangle containing Z.

Both algorithms give reasonable results. The Renka Cline method is more sensible to faster changes, it is suitable to display the changes of impedance spectroscopy caused by the Caco-2 cells. The data matrix $Z(\nu,t)$ collected during continuous real -time impedance spectroscopy was recalculated to yield the relative change of impedance. The relative change $Z_{rel};\nu;t)$ was transfered into interpolated data using the 'weighted average' or 'Renka Cline' method.

Chapter 5

Results and Measurements

The previous chapter presented the procedures and experimental devices available to address the task of measuring the transepithelial impedance spectroscopy of Caco-2 cell cultures. The used devices had to be adapted and new components had to be added according to the requirements of a impedance spectroscopy of living cell cultures. A transepithelial electrode configuration was developed. The following chapter describes the results of experimental work performed and relates their evaluation with the central researching question of this work. A schematic overview over the results is is illustrated in figure 5.1.

Issue	Approach and Results	Section
Adapted measurement setup	Basolateral electrodes: planar microelectrodes Apical electrodes: zinc coated top electrodes Monitoring of 8 wells simultaneously: Mux Maintain growth environment: Specimen Holder	5.1
Functionality and performance of the measurement setup	Parasitic impedance <1.5 Ohm Resistance of feed lines ~ 200Ohm Reproducibility of measured impedance: 50 Hz – 900 Hz : σ < 3% 900 Hz – 100 kHz: σ < 1% Sensitivity: Δ|Z| ≈ 40 x Δc at c = 0.004% NaCl	5.2
Monitoring of cell growth	All construction materials are biocompatible Impedance of RPMI ≈ Impedance 0.9 % NaCl, equal at 9.5 kHz Significant change of impedance at cell growth increase of 230% after 11 days detection of physiological characteristics Cells signal bandwidth: 500 Hz – 5 kHz	5.3

Figure 5.1: Overview and summery of the results.

5.1 Measurement Setup

5.1.1 Fabricating of the Planar Basolateral Electrodes

The layout of the planar electrodes was developed to meet the following requirements:

- Optimum geometry to be used for the planar electrodes

- Optimum contact to the planar electrodes on the borosilicate plate

- Optimum spacing of conductive areas on the substrate

- Low resistance of the thin film electrodes

- Multiple electrode arrays within one well to facilitate locally resolved measurement

The aim of this work was to develop a sensor to monitor the transepithelial impedance of Caco-2 cultures for potential use in pharmaceutical studies. In this field of research it is necessary to monitor several cultures at once, so that a sensor with several microwells with individual measurement positions are required. Therefore, the layout of the planar electrodes was optimized for eight sensor areas which can be addressed sequentially. Figure 5.2 shows the resulting layout for the sensor plate holding the planar electrodes, that considers all design reqirements discussed before.
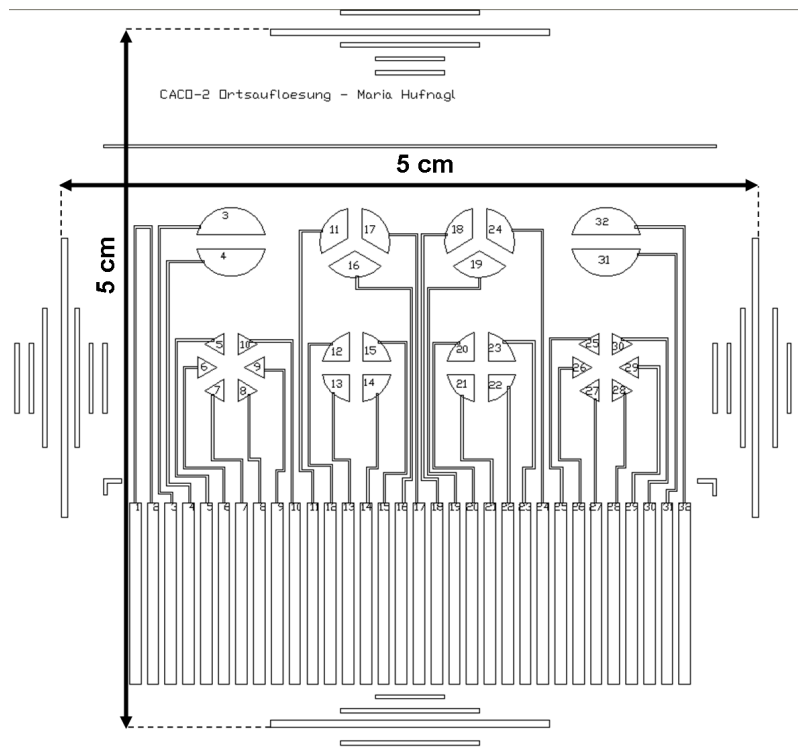

Figure 5.2: Layout of the planar electrodes.

Placement and diameters of the sensor areas were adjusted to the aperture diameter of the used microwells of the silicone confinement (see section 4.3.3). Each sensing area covers a circular area with a diameter of 6.5 mm on the planar sensor chip. Four different electrode geometries were used to monitor the impedance of varying cell-covered areas. The layout was designed symmetrically to generate parallel sets of identical sensor areas. Table A in the appendix lists the different sensor areas, the number of electrodes per measurement position and the electrodes' areas.

The resulting layout contains four main parts in an area of 5 cm x 5 cm:

- Alignment marks for alignment during the lithographic process, indicating an area of $(50 \times 50) \, \text{mm}^2$

- 32 contact pads $(0.82 \times 27.6) \, \text{mm}^2$ to connect the probe to a PCI slot

- 30 measurement electrodes of variable size distributed over 8 sensor areas

- 1 closed interconnect loop (contacts 1.2) for resistance measurement

To establish a connection between electrodes and measurement electronics, a system of interconnect wires on the chip guides the measurement signal to the contact areas on one edge of the sensor plate. The borosilicate plate with the sensor areas and the interconnects is then connected via a PCI (Peripheral Component Interconnect) slot to a 32 pole ribbon cable. The position of the contact pins in the PCI slot require a periodicity of 1.27 mm. Therefore, the spacing between contacts for the PCI connector was set to 0.45 mm and width of the contacts was 0.82 mm. The contacts positioned at the rim of the sensor plate are connected to the electrodes via interconnect lines with a width of 0.15 mm. To avoid capacitive crosstalk between the interconnect lines their spacing was maximized within the limited space. Limitations were given by the silicone confinement's layout: All interconnect lines had to be placed completely beneath the silicone material of the 'flexiperm'. Hence, the resulting interconnect lines have spacing between the lines of 0.25 mm and 0.45 mm. Interconnect lines as well as the contact areas are thin films of metal, fabricated by sputtering. Due to process-related fluctuations, slight variations of film thickness might occur. The layout was therefore designed to measure the resistance of interconnect lines separately. The resistance of several sensor plates was measured, the results of this measurement are presented in section 5.2.2.

The designed microelectrode sensor was then fabricated using optical lithography and sputter deposition according to the process parameters discussed in section 4.1. Figure 5.3(a) shows areas of the interconnect lines after lithographic structuring of the photresist. The photoresist at this stage was removed partially at areas that were covered by the gold layer using sputter deposition.
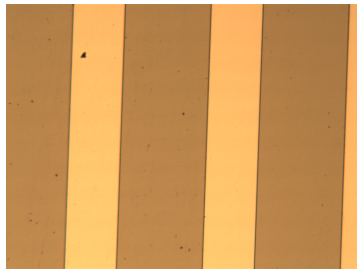
(a) Image of interconnect lines after lithographic structuring of the photoresist.
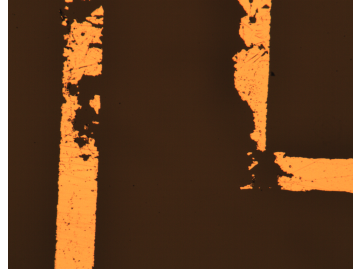
(b) Image of corroded and interrupted interconnect lines due to insufficient adherence of the gold layer.
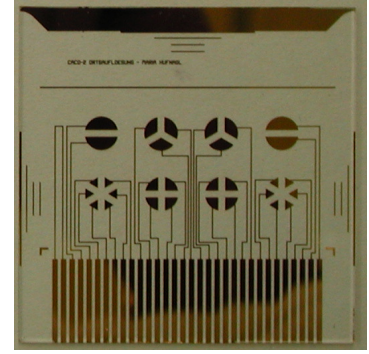
(c) Picture of the planar electrode structures on 5 cm x 5 cm borosilicate substrate transfered as metal layer from photomask.

Figure 5.3: Images of the planar basolateral microelectrodes during fabrication process.

A problem arising during the fabrication process was that the sputtered gold layer tended to lift partially as illustrated in figure 5.3(b). This resulted in interrupted interconnect lines between electrode areas and contact pads. Further investigation of the fabrication process revealed that the adherence problems of the gold layer were caused by an insufficient titanium layer. The titanium layer was sputtered onto the borosilicate substrate to enhance the gold layer's adherence to the glass substrate. A titanium layer of increased thickness was found to solve the problem. The sputter duration for the titanium layer was therefore set to 120 seconds and the RF power was set to 75 Watt. A pause after 60 seconds allowed for cooling of the substrate to avoid deformation of the sputtered layer due to thermal effects. Figure 5.3(c) shows the final microelectrode chip. The structures were transfered from the photomask onto the borosilicate plate. These structures were used in the measurement setup as the planar basolateral electrodes to measure the transepithelial impedance of 8 Caco-2 cell cultures simultaneously. The Caco-2 cells were grown directly onto the planar electrodes, adhering tightly to the surface. Aspects of biocompatibility will be discussed in section 5.3.2. Of these electrodes either two electrodes within one well or one electrode in combination with the corresponding top electrodes can be chosen to establish a two terminal electrode configuration for impedance measurement. This task was performed by the multiplexer which is discussed in the following section.

5.1.2 Circuit Diagram of the Multiplexer

From the 32electrodes on the sensor chip and the 8 top electrodes always a set of 2 electrodes had to be connected to the LCR-meter for reading the impedance spectrum. Selection of the two active measurement electrodes and the connection to the measurement equipment was performed by the multiplexer.

The multiplexer was used to establish a programmed connection between any pair of electrodes and the LCR-meter to measure the impedance.It was necessary to design and fabricate an adapted circuit to enable the combinations of 32 planar electrodes plus eight top electrodes. The chosen method for measuring the impedance was the two-point setup. Figure 5.4 shows a schematic diagram of the relay cards in the multiplexer and their connections. Each relay card holds eight switches which can be activated individually to establish or exclude the programmed connection.
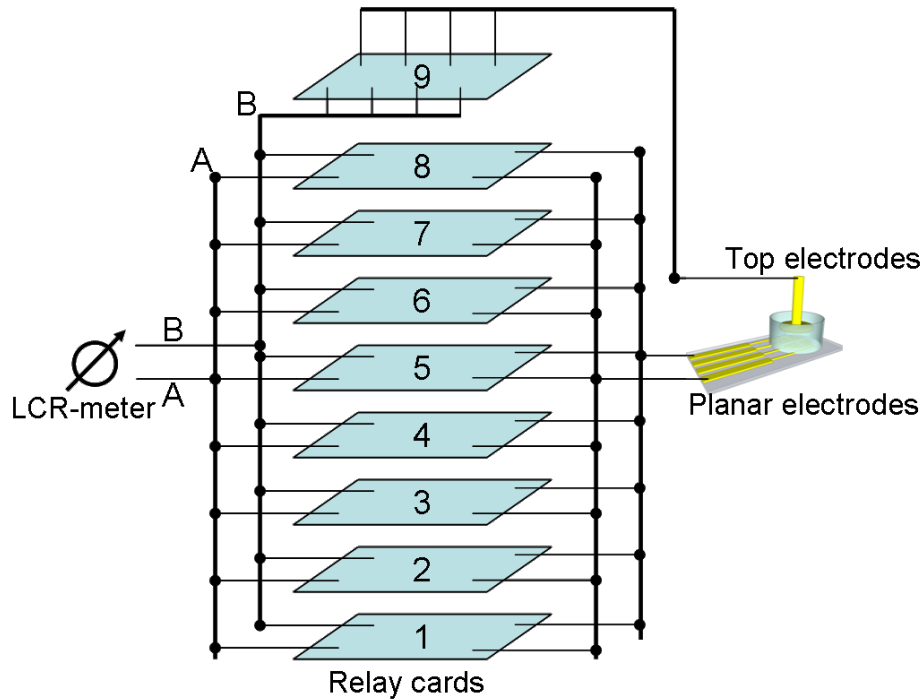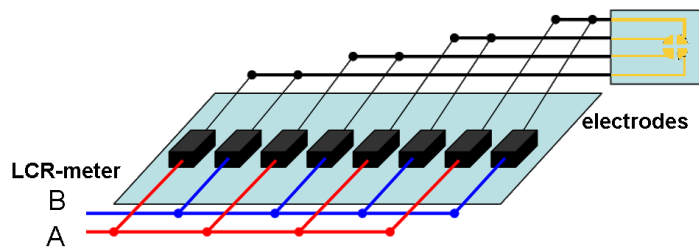

Figure 5.4: Schematic illustration of the multiplexer's internal connections between the 9 relay cards.

As indicated on the left side of this figure the LCR-meter measures the impedance in a two terminal configuration of the electrical signals transported in the lines A and B. Line A is connected to the relay cards 1 to 8, whereas line B is connected to all boards. The boards 1 to 8 are responsible for the planar electrodes, the ninth board is associated exclusively to the eight top electrodes. Each board holds eight switches. The internal wiring is sketched in figure 5.5. These switches can be addressed and operated individually by the relay board 1 which is itself operated by the LabView program. The wiring of the ninth board is less complex as every switch is responsible for one of the eight top electrodes only. Every switch of the ninth board is connected to line B on one port and to one of the eight top electrodes on the other port.

(a) Schematic illustration of the relay card's wiring of card 1 - 8.
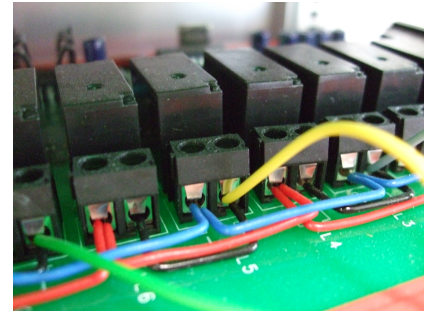
(b) Photographic image showing a selection of the relay cards with with cables connected.

Figure 5.5: Wiring scheme of the relay cards 1 to 8.

Part (a) of figure 5.5 shows wiring scheme of the relay card specified in section 4.2.1. One port of the first, third, fifth and seventh switch leads to measurement line A, the second port of these switches leads to one of the measuring electrodes. Measuring Line B is connected to the first port of the second, fourth, sixth and eighth switch. The other port of these switches leads to one of the measuring electrodes. Part (b) of the figure shows the practical realization of the depicted circuit.

By operating these switches appropriately, any pairing of two planar electrodes as well as any pairing of one planar electrode to one top electrode can be established to transport the electrical signals between microelectrodes on the chip and the LCR-meter.

5.1.3   Specimen Holder

the microelectrode sensor setup consisting of several components has to be operated unattended within an incubator. For this reason a mechanically robust holder was built. The specimen holder provides a stable platform for fixating the planar electrodes, the top electrodes, the 'flexiperm' cell containment, and all the cable connections. The images in figure 5.6 show the complete specimen holder with the planar electrodes on borosilicate substrate, the silicone wells and the electrical connections.
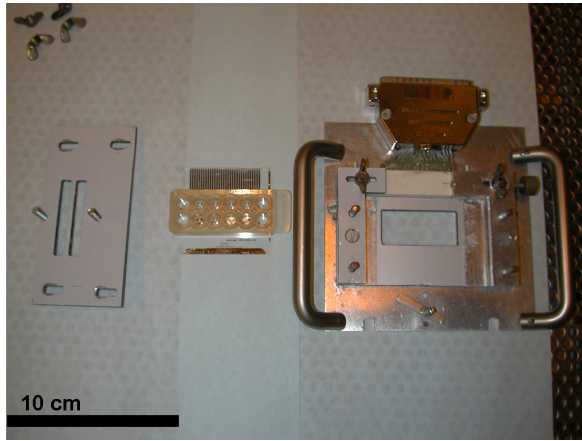
(a)
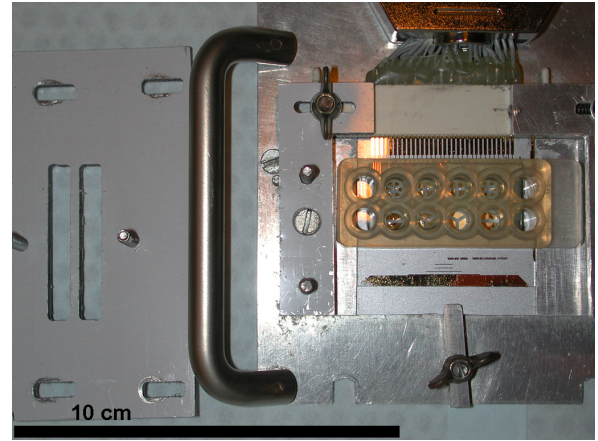
(b)
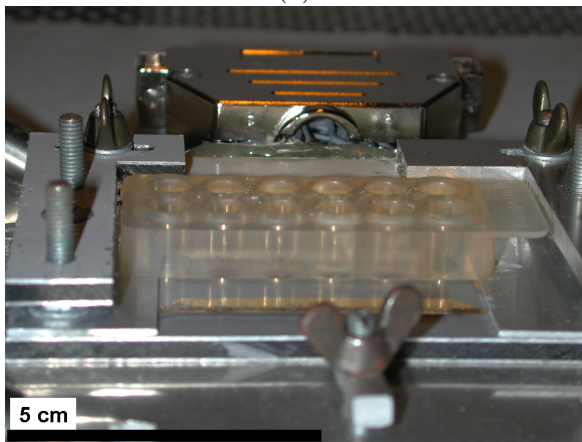
(c)

(d)

Figure 5.6: Detailed images of the specimen holder.

The specimen holder is basically fabricated from aluminum and composite plates of aluminum and polypropylene. The base plate made of aluminum measures 120mm x 120mm x 8mm. An aperture in the base plate of 50mm x 16mm size allows for optical investigation of the Caco-2 cells while they are grown on the planar electrodes. The position of this aperture is beneath the position where the borosilicate chip will be placed. The cable connections are fixated mechanically on the base plate, and s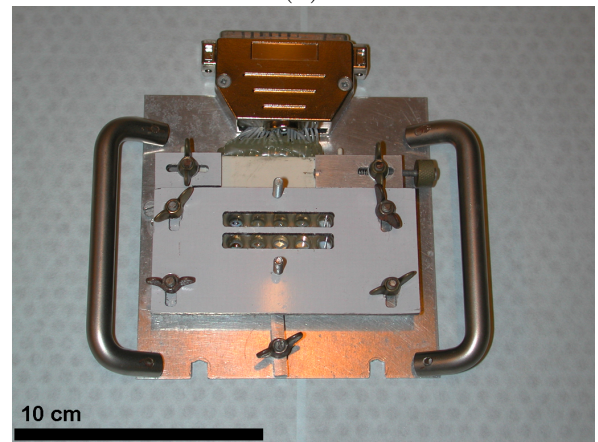o is the sub D plug. When mounted, the borosilicate plate with the planar electrodes is placed on the base plate and directly inserted into the sub D plug. The silicone containment with 8 microwells for the cell suspension and their nutrient medium is aligned to the planar electrodes and fixated to the borosilicate by slight pressure from the top frame. A top plate fixates the silicone confinement to the borosilicate plate. The top frame also is the base to fixate the top electrodes at their positions. Sketches of the specimen holder containing the exact measurements are attached in the appendix A.The electrodes on the microelectrode plate are contacted by a PCI-plug as shown in figure 5.6 (d). A 35-port Sub-d plug is connected to the PCI-plug on one side and connects each measurement

line individually to the multiplexer. As second 9-pole sub-D connects the top electrodes via a wire and links each electrode to one switch of relay board '9' of the multiplexer. The top electrodes are described in the next section.

5.1.4 Design and Fabrication of the apical Top-Electrodes

For a transepithelial measurement also top electrodes covering the apical region of the cell layer are required. The eight top-electrodes are large-area electrodes positioned approximately 3 mm above the planar electrodes probing the basolateral region. Figure 5.7 shows an outline of the top-electrodes. Each top-electrode is contacted individually and can also be addressed individually by the multiplexer. The top-electrodes were fabricated from conventional M5 screws made of zinc coated steel. The screw head was grinded on the top to yield a planar, smooth surface. Even after prolonged exposure to the cell medium, no corrosion effects were observed on the electrode surface by optical inspection.
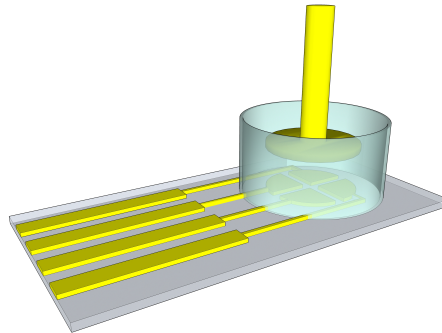
Figure 5.7: Schematic illustration of a microwell with a set of 4 planar basolateral electrodes on a glass carrier and a large top electrode in the apical region.

The areas of these electrodes were chosen large enough to cover all microelectrodes in the opposite planar electrode plate of one well. Each top-electrode has a diameter of 5 mm which gives an effective area of $78.5\,\text{mm}^2$. The hight of the top electrodes can be adjusted with a thread providing a thread lead of 0.8 mm. One 180° changes the distance between the top electrode and the planar electrode for 0.4 mm.
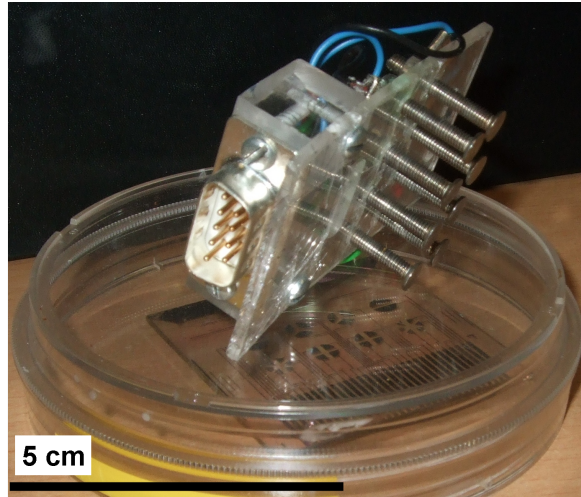
Figure 5.8: Image of eight top-electrodes in a holder plate with the sub-D port mounted on top.

Figure 5.8 shows an image of the eight top electrodes used to measure the transepithelial impedance of the Caco-2 cells. These top electrodes are placed into each single well of the cells' confinement and build a counter electrode for one of the planar electrodes. Each top electrode is connected via a copper cable to one pin of the DE-9 subminiature plug. The measurement signal is linked from there via the MUX to the LCR-meter. The combination of all components discussed in the previous sections builds the fully functional measurement setup. The resulting measurement setup developed to monitor the transepithelial impedance spectroscopy of eight Caco-2 cell cultures simultaneously is composed of the two electrode sets (top and bottom), the specimen holder they are mounted on, the 'Flexiperm' cell containment, the multiplexer, the LCR-meter and the LabView program operating all components. The next section will focus on the qualitative and quantitative testing of single components as well as the combinations of the single components.

5.2 Functional Evaluation of Measurement Setup

The entire setup was designed for impedance measurement of a confluent, adherent cell layer. The functionality of the entire setup was evaluated before the first biological samples were tested, as biological samples extend the parameter range and make the identification of problems related to the technical setup more difficult. This pre-testing was performed with physically well defined systems and is reported in the following sections.

The primary question before starting the final experiments with biological cells was whether the measurement setup explained in section 4.2 including the developed adaptations described in section 5.1 operates properly and delivers measured signals with an acceptable accuracy.

53

Figure 4.12 shows the devices used for the presented setup. All these devices are connected electrically; Section 4.2.3 shows, that the measurement signal is transported along cable connections between the LCR-meter and the Multiplexer, as well as along the cable connection between the MUX and the measurement electrodes. The overall path length the signal is transported sums up approximately to 3 m. The parasitic impedance of every component along this path has to be tested. All connectors were designed and fabricated especially for the presented measurement setup and the correct contact has to be checked. The LCR-meter as well as the multiplexer are operated by the LabView program. It has to be checked, whether the operation of these component runs according to the specifications. To test for these questions several experiments were performed.

5.2.1 Electrical Testing of the Measurement Setup

The series of experiments was started with a simplified setup of the LCR meter and the multiplexer. Basic functions and reliability of these components were tested. At a first experiment the behavior of the measurement system was tested using shortcut circuits. The shortcut circuits were realized mechanically by connecting all pins by a soldered wire.

Parasitic Impedance:
The Impedance along the Signal's Way to the Planar Electrodes including the Multiplexer was measured. The cable connection between the LCR-meter and the Multiplexer is established by two coaxial cables, each with a length of one meter, connected to each device by BNC connectors. To measure the impedance along this path the multiplexer was connected to the LCR meter. Both devices were operated by the LabView program. The multiplexer was operated in such a way to establish a shortcut circuit by connecting the first switch to both measurement lines, i.e. line A on port one and line B on port two. The LCR-meter measured the impedance in the frequency range from 50 Hz to 100 kHz. Figure 5.9 shows the result of this short-circuit measurement.
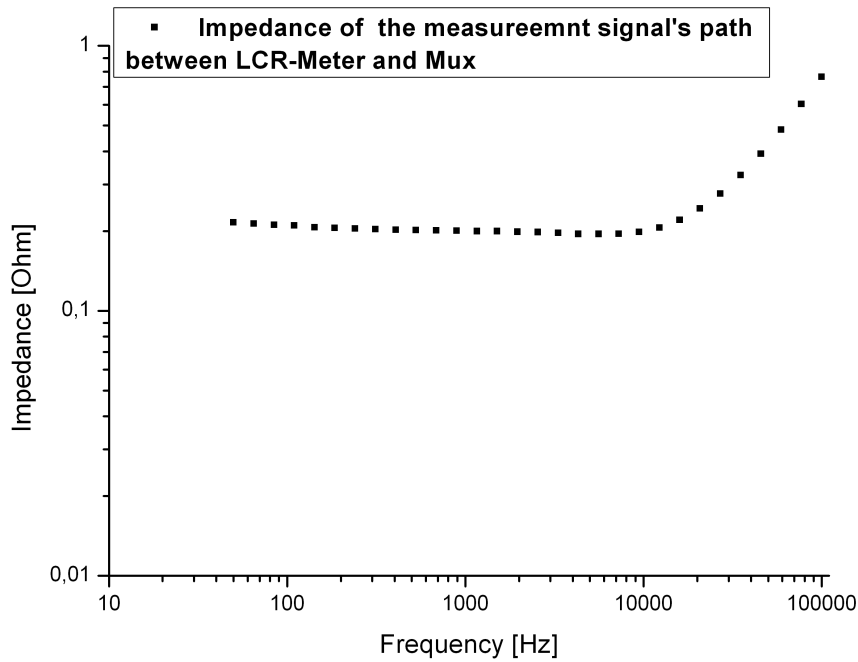
Figure 5.9: Graph displaying the impedance of each connection established by the MUX, including cable.

The x axis shows frequency in the range of 10 Hz to 100 on a logarithmic scale. The y axis is scaled logarithmically as well and shows the measured impedance in a range of 10 mOhm to 1 Ohm. The measured impedance has a mean value of 203.24±6.85 mOhm for frequencies lower than 15 kHz and increases slightly for larger frequencies. Section 5.2.3 will show that the parasitic impedance is less than 50 % of the standard deviation in this frequency range. Due to the small contribution the effect of these parasitic impedances may be neglected in further evaluation and needs no special treatment. The maximal impedance measured was 762.7 mOhm at the frequency of 100 kHz. The result of this measurement proves that the connection could be established properly. The measured impedance shows constant values for low and middle frequencies. The slight increase of impedance at larger frequencies might be caused by the connections within the MUX. The increase of 0.5 Ohm will be proven to be negligible in section 5.2.2 as the resistance of the microelectrodes is assumed to be much higher.

Impedance along the Signal's Way to the Planar Electrodes including the Multiplexer and the Cables:
To measure the impedance along this path the multiplexer was connected to the LCR-meter and the cable leading to the measuring electrodes was attached to the multiplexer. A short-circuit for each contact was established by a shortcut connector plug directly at the position of the MEA connector with all pins connected by a soldered wire at the end of the cable. The

impedance for each contact was measured separately. Figure 5.10 shows the magnitude of the measured impedance for all 31 connections.
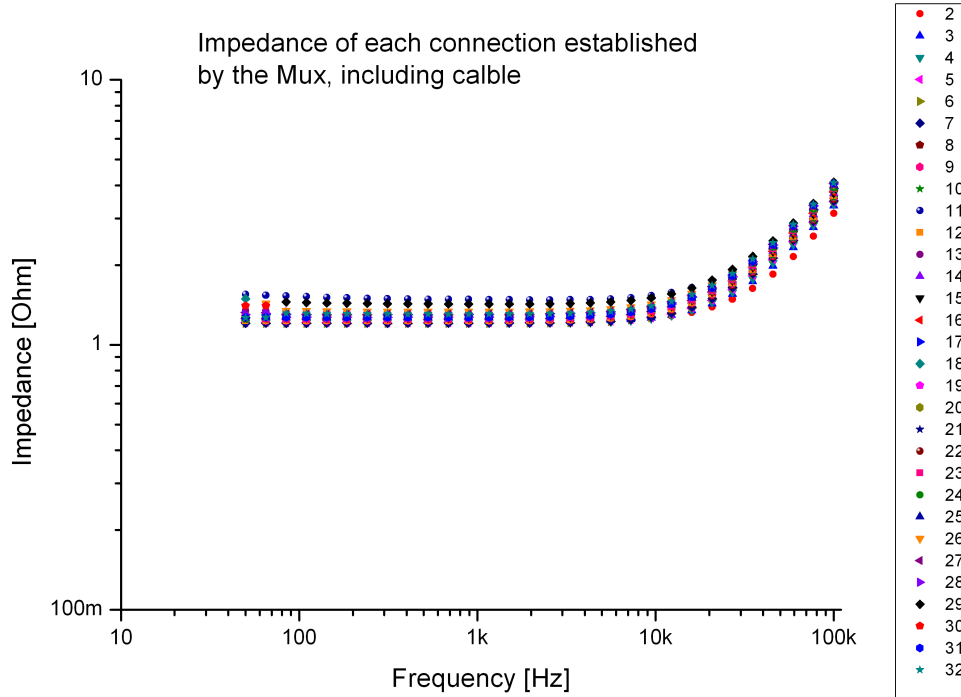

Figure 5.10: Impedance for each contact of LCR meter, multiplexer and cables with short-circuit at the point of the sensor chip.

The x axis shows the frequency from 10 Hz to 110 kHz on a logarithmic scale, the y axis shows the measured impedance in the range of 100 mOhm to 10 Ohm. For frequencies smaller than 10 kHz the measured impedances are in the range of 200 mOhm to 1.5 Ohm with a mean value of 1.2±0.2 Ohm. This shows that the impedance of the connector cable between Multiplexer and sensor chip adds ≈1 Ohm. The measured impedance increases slightly for frequencies larger than 10 kHz and reaches a maximum of 2.3 Ohm at a frequency of 100 kHz. This measurement proves that all contacts are connected properly. Each combination of electrodes can be addressed by the multiplexer. For the most frequencies the established connection including the cable have a low impedance of 1.2 Ohm. Due to the low value (only in the range of one standard deviation in the corresponding range of frequencies) this contribution to the overall impedance can be neglected.

Shortcut detection by Open-measurement

As another task it was evaluated, if there are unintended shortcuts in the plugs or the wiring. The next experiment was performed to test for eventual undesired shortcuts in plugs or cables. An open circuit was realized by leaving connectors at the position of the sensor chip floating by leaving all ends unconnected. The impedance was measured for frequencies from 50 Hz to
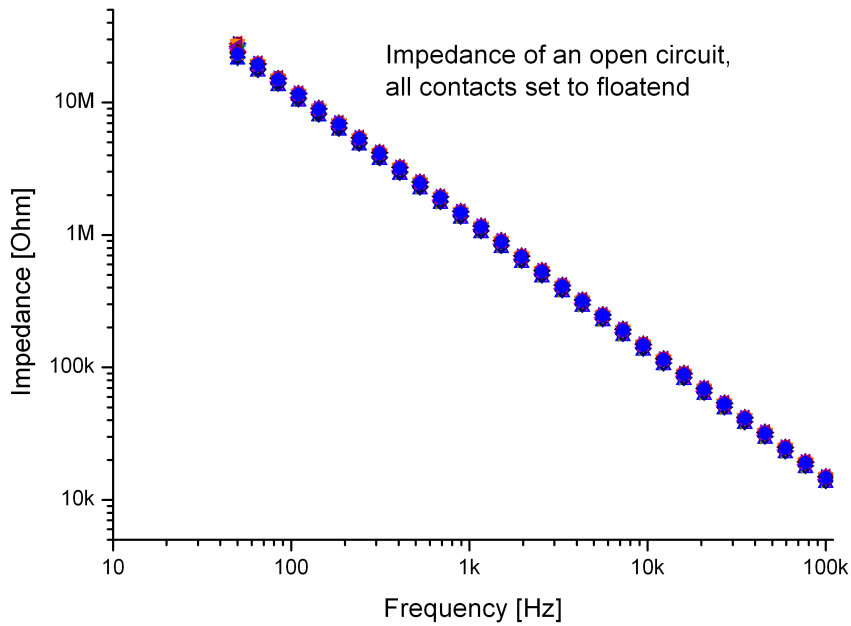
100 kHz.

Figure 5.11: Graph of the impedance spectrum measured at an open circuit.

Figure 5.11 shows the measured impedance as all contacts were set to floatend. The graph is a double logarithmic plot with the measurement frequency plotted on the x axis from 10 Hz to 110 kHz and the measured impedance plotted on the y axis in the range from 5 kOhm to 50 MOhm. The data points are corresponding to each other for the complete range of frequencies. All measured impedances start at very high values of $2.78 \cdot 10^7$ Ohm at 50 Hz and decrease to a value of 13 kOhm at a frequency of 100 kHz. This behavior corresponds to the expected behavior of a capacitor and displays the fact that all ends are floating. There is no undesired contact that could be detected by its lower impedance.

Impedance Measurement in Fluid Environment:
The experiments described above were performed without the fabricated planar electrodes and top electrodes. An experiment to test these components has to be proceeded in fluid environment. Influences of the fluid electrolyte have to be considered and can only be minimized. Therefore, a fluid was chosen which has a low conductivity. Distilled water was chosen for the experiment described below. Two measurements were performed, one of them measured the impedance of distilled water in a well of the 'flexiperm' silicone confinement and the other measurement was carried out with an empty well. The planar electrodes, the top electrodes and the fluid - tight silicone confinement were mounted onto the specimen holder. The LCR-meter and the MUX were connected according to the description in section 4.2.3.

The impedance was measured for frequencies from 50 Hz to 100 kHz. Figure 5.12 shows the results of both measurements. Both axes are display a logarithmic scale. The x axis shows the impedance from 10 Hz to 100 kHz and the y axis shows the measured impedance from 200 Ohm to 200 kOhm.
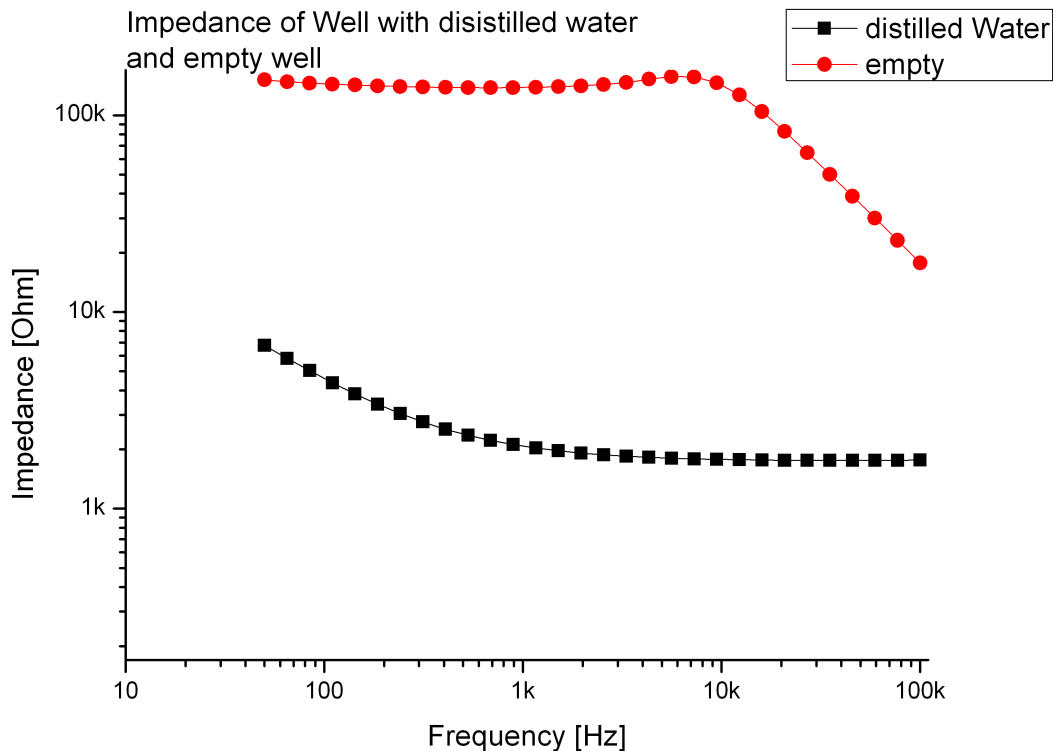
Figure 5.12: Graph of the impedance spectrum of a well filled with distilled water compared to the impedance spectrum of an empty well.

The curve plotted with the circles shows the measured impedance of an empty well. The black squares show the measured impedance of the well filled with distilled water. As expected, the curve of the empty shows a much higher impedance than the curve of the distilled water. It was possible to measure the impedance of an electrolyte (distilled water) and obtain a significant difference (10^3 Ohm) of the measured value when compared to the impedance of an empty well.

In the experiments described above, the functionality of the complete setup was shown. It was proved that the introduced setup including the planar (bottom) electrodes and the top electrodes is suitable to measure impedances of fluids. This is an essential finding and paves the way for measuring the impedance of Caco-2 cell cultures which are grown in a fluid environment. The next sections will focus on the properties of the sensor electrodes.

5.2.2 Conductivity of the planar electrodes

For electrical probing of the basolateral area microstructured planar electrodes were used, with interconnect feed lines between contacts and electrodes of $150\,\mu$m width. The planar electrodes were fabricated from titanium and gold sputtered onto the borosilicate glass substrate. The resulting conductive pathways are very thin films. Their conductivity had to be tested. The conductivity of the setup was investigated as this impedance adds to the impedance of the cell layer. To test the conductivity of the feed lines, extra feed lines with a defined geometry were designed and fabricated as described in section 5.1.1. These extra feed lines are shown in figure 5.2 and the corresponding contacts are labeled with '1' and '2'. This test fees line forms a closed circuit of a length analogous with the test electrode. The area of the feed lines as well as the area of the electrodes can be found in table A of the appendix. The area of the extra feed lines is $6.11\,$mm^2. Figure 5.13 shows the impedance and the phase of one of these feed lines.
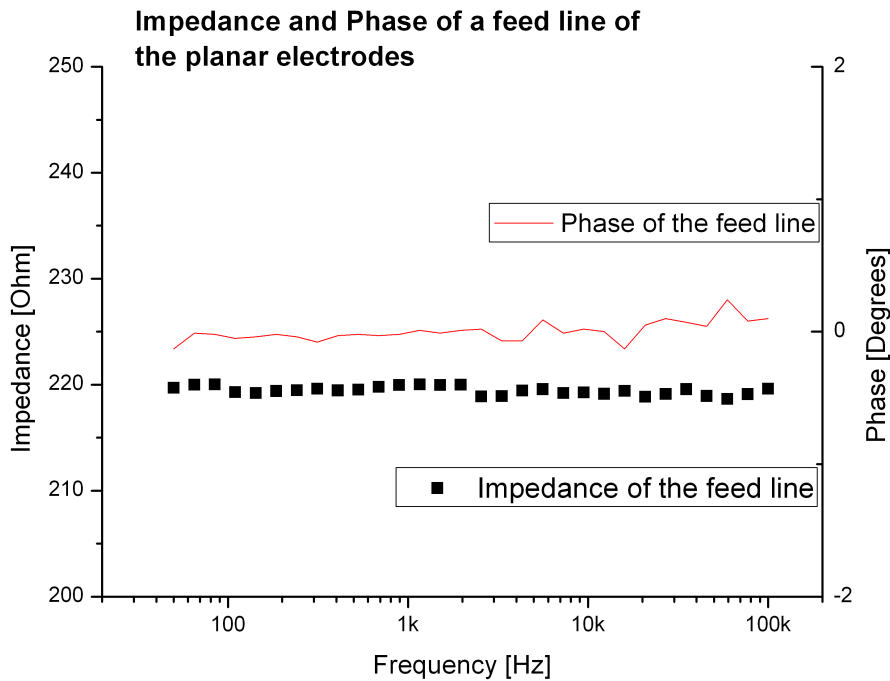
Figure 5.13: Graph displaying the impedance and phase of the feed line.

In this figure the x axis displays the logarithmically scaled frequency in the range of $10\,$Hz to $110\,$kHz. The left y axis displays the measured value of impedance. It is scaled linearly and an impedance in the range of $200\,$Ohm to $250\,$Ohm. The curve corresponding to this y axis shows the measured impedance of the feed line of one sample. The right y axis shows the scale of the phase this feed line is. This axis is scaled linearly and displays a range of -2° to 2°. Both curves plotted are perfectly stable for the complete range of measured frequencies which

indicates a purely ohmic impedance. The impedance of the tested feed line is 219.4±0.4 Ohm. The phase is equally stable for the complete range of frequencies, it varies from -0.13° to 0.24°. This data proved that the feedline behaves as an ohmic resistor.

Several samples were fabricated and used for measuring the impedances in the experiments described in the following sections. Figure 5.14 shows their impedances averaged over the measurements at frequencies in the range of 50 Hz to 100 kHz.

Figure 5.14: Bar graph displaying the impedances of several samples, averaged over the complete frequency range.

The impedances of these samples are in the range of 100 Ohm to 226 Ohm. This is result shows that the fabricated planar thin film electrodes can be reproduced with comparable qualities. As suggested in 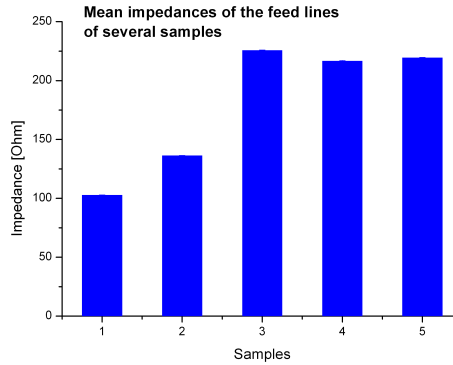section 5.2 the impedances of cables and the MUX are negligible compared to the impedance of the gold electrodes. The next section will explore the accuracy of the measurement. As length is always constant and width is given by lithography the varying impedance of the feed lines is caused by changes of the thickness of the thin film electrodes or impurities of the sputtered material. These changes may by caused by process variations during sputtering or impurities of the base material used for sputtering.

5.2.3 Reproducibility of the measured values

To explore the reproducibility of the measurement setup including the planar electrodes and the top electrodes, a series of experiments was carried out. The planar electrodes were placed in the specimen holder, the counter electrodes were mounted on top. To examine the reproducibility of measurements the impedance of physiological saline was retrieved in repeated measurements. New saline was used each time to exclude possible influences of impurities in the electrolyte resulting from corrosion products of the electrodes. In section 5.2.6 this effect is investigated in detail. Prior to measurement the electrodes were cleaned with distilled water. 0.1 ml of physiological saline was filled into the well formed by the silicone confine-

ment. Impedance spectroscopy was measured in the frequency range of 50 Hz to 100 kHz. The impedance spectroscopy was measured using the transwell configuration configuration of one top electrode and one of the planar electrodes in one well. This procedure was repeated several times. The well was emptied of the saline solution and cleaned with distilled H_2O after each run. Figure 5.15 shows mean value and standard deviation of these measurements.
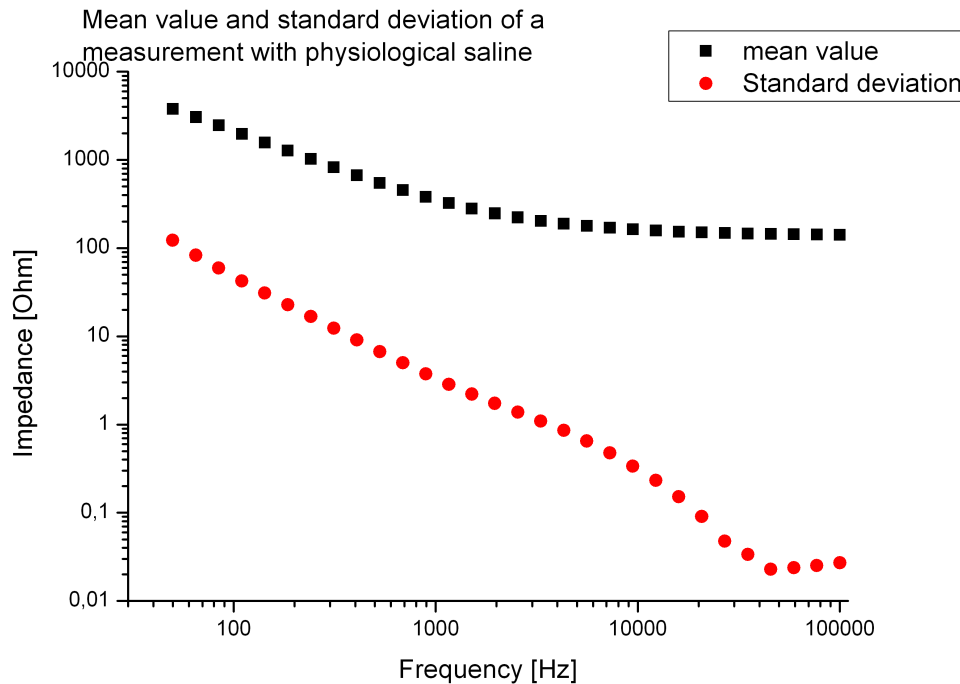
Figure 5.15: Mean value and standard deviation of repeated measurements of 0.9%NaCl in transwell configuration, logarithmic scaling.

The frequency is shown on the x axes, whereas the y axes shows the measured impedance. Both axes have logarithmic scales. The black squares show the mean value of measured impedance of the physiological saline and the red circles show the corresponding standard deviation. Note that due the logarithmic scaling of both axes smaller values appear to be larger than they actually are. Values of the standard deviation start with a value of 123.07 Ohm at low frequencies and decline with rising frequency to very small values with a minimum of 0.02 Ohm. This allows to conclude that when measuring the cell cultures impedance, changes as small as 4 Ohm for frequencies of 1 kHz can be reproducibly shown as significant changes. For higher frequencies even changes below 1 Ohm can be measured reproducibly.

The impedances that will be measured in following experiments will have impedance values in a very wide range. It is therefore also interesting to know the reproducibility of a measured value compared to the absolute value. Figure 5.16 shows therefore the standard deviation as percents of the corresponding mean value.
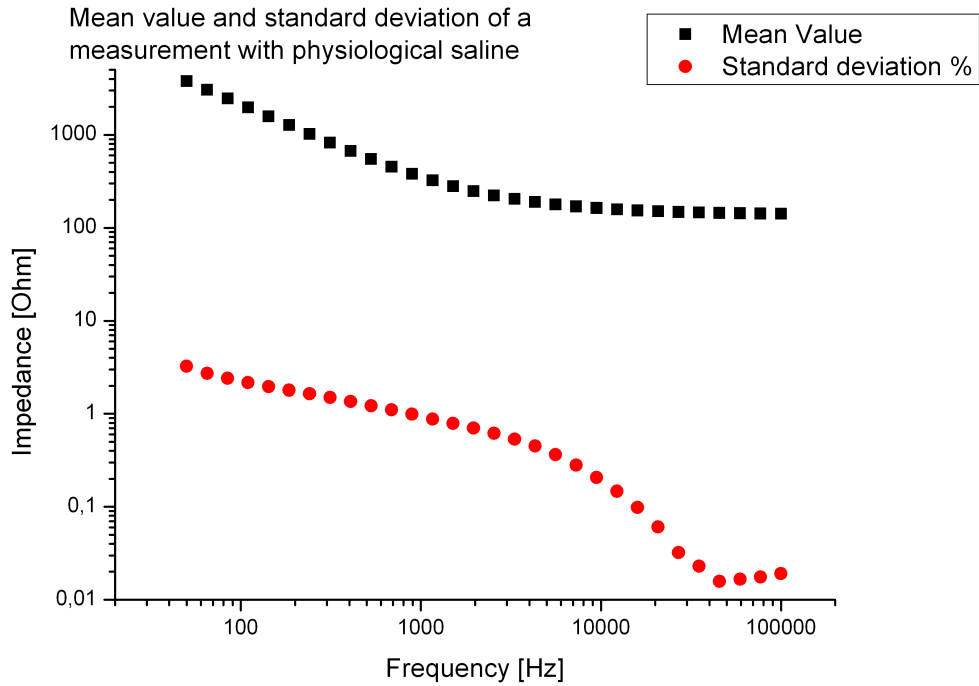
Figure 5.16: Mean value and percentual standard deviation of a measurement series with physiological saline (0.9%NaCl) in transwell configuration.

Standard deviation of the presented measurement is generally very low, at frequencies larger than 893.5 Hz the standard deviation is smaller than 1 percent. This allows to conclude that also for small frequencies changes of the cell layers' measured impedances larger than 3% can be interpreted as a significant change. For middle and high frequencies even changes of 1% of the measured impedance can be considered as significant. For the transepithelial impedance of Caco-2 cell layers impedance values in the range of 100 Ohm to 1 MOhm are expected. The results from abouve indicate that changes of the measured impedance smaller than 3 Ohm are significant changes due to changes of the Caco-2 cell layer. These results imply a high sensitivity of the presented transwell configuration setup to measure the transepithelial impedance of Caco-2 cells.

5.2.4 Concentration Series

In the previous section distilled water was used as an electrolyte, in this section electrolytes with different concentrations of NaCl are tested to address the following questions:

- The concentration of ions in the extracellular medium is known to change due to metabolism of the epithelial cells.
  Can the presented setup detect the varying concentration of ions?

- Are there differences of the measured impedances as the frequency varies?
  The formation of the Helmholtz layer is dependent on the ions in the electrolyte. This layer can be represented electrically by capacitor which would induce a frequency dependent change of the measured impedance in addition to the impedance due to the concentration of anions and cations in the electrolyte.

To answer these questions the setup as described in the previous sections was used again. The impedance was measured in a transwell configuration using one top electrode and one planar electrode. Previously, the silicone confinement and the electrodes were rinsed with distilled water to remove residues from previous measurements. The electrolytes for this test were prepared as dilutions of the physiological saline. Four different dilutions were produced. The corresponding concentration in terms of mass fraction was calculated using the following equation:

$$\omega = \frac{m_{NaCl}}{m_{NaCl} + m_{H_2O}} * 100\% \tag{5.1}$$

Where ω is the mass fraction in percent of the diluted component, m_{NaCl} is the mass of the NaCl salt in grams and m_{H_2O} is the mass of the solvent H_2O added for the diluted solution. Table 5.1 lists the dilutions of the physiological saline and the resulting concentration of NaCl in H_2O as percents of the dilutions' mass.

dilution	mass fraction NaCl
1:1	0.9 %
1:10	0.0818 %
1:25	0.0346 %
1:100	0.00891 %
1:250	0.00358 %

Table 5.1: Dilution ratios and mass concentration of NaCl in H_2O.

Starting at the smallest concentration each solution was pipetted into the silicone well. The measured electrolyte volume was 0.1 ml. The impedance for each electrolyte was measured

by the LCR meter with a maximum voltage of 0.1 V. Figure 5.17 shows the results of this experiment for several frequencies.
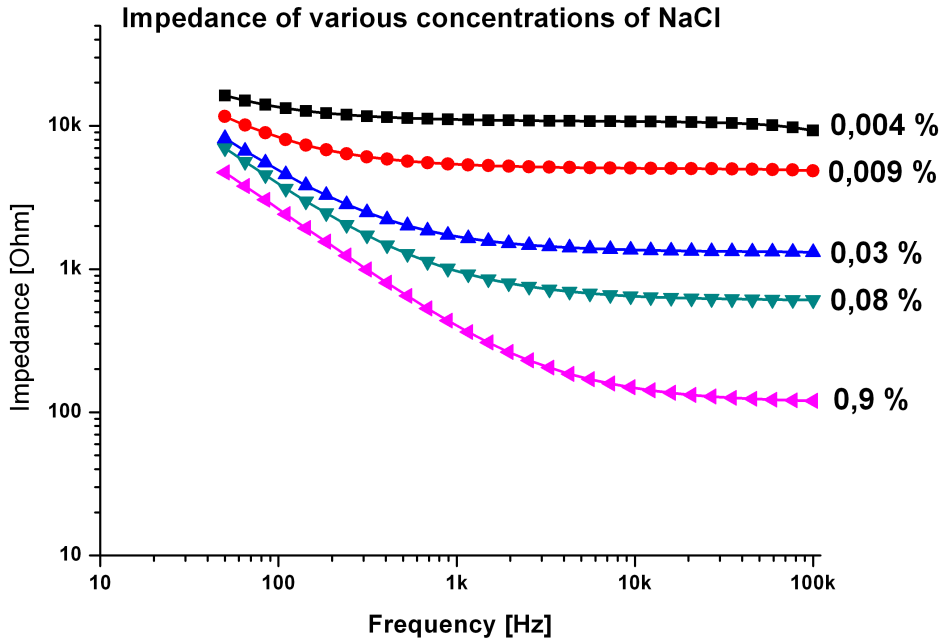

Figure 5.17: Concentration series of NaCl in distilled water, impedance varying with frequency.

This graph shows impedance values in the range of 10 Ohm to 50 kOhm on the logarithmically scaled y axis and the measurement frequency in the range of 10 Hz to 110 kHz on the x-axis. Five curves for different concentrations are plotted. All curves can be clearly distinguished. For frequencies larger than 9.5 kHz the smallest difference between two electrolytes was 525 Ohm measured for electrolytes containing 0.0818%NaCl and electrolytes containing 0.9%NaCl. Compared to the standard deviation of 0.34 Ohm this difference is obviously significant. For lower frequencies the differences of the measured impedances form varying electrolytes decrease wheras the standard devieation increases. For the lowest frequency measured, 50 Hz, the difference of the 0.9% NaCl electrolyte and the 0.0818%NaCl electrolyte is 2267 Ohm. The standard deviation at this low frequency is 123.07 Ohm. So even for the lowest frequency measured, the differences of impedance between two electrolytes with varying concentration is larger than 18σ. The topmost black squares display the measured impedances of the electrolyte with the lowest concentration of 0.004% NaCl in H_2O. The other curves correspond to increasing concentrations with the highest concentration of 0.9% NaCl. While the first curve displays only small dependance on the frequency, the lowest curve varies strongly with the frequency. For higher concentrations the measured impedance is lower, it is more strongly influenced by the Helmholtz layer capacity. All curves start at comperably

high imedances of $4.7\,\mathrm{kOhm}$ (0.9%) to $16.2\,\mathrm{kOhm}$ (0.004%). For frequencies larger than $2\,\mathrm{kHz}$ all curves except for the 0.9 % curve display stable impedance values. This result agrees to the theory explained in section 3.4. The impedance at a certain frequency varies with the concentration of an electrolyte. At higher concentrations the number of charged anions and cations is higher. This results in higher conductance of the electrolyte, thus lower impedance as shown in figure 5.17. The 0.9% curve has the lowest impedance. Compared to the other concentrations the frequency for measuring a stable impedance of this concentration is slightly shifted to a frequency of $10\,\mathrm{kHz}$.

5.2.5   Sensitivity of the Au Electrode

In the previous section the dependence of the measured impedance on the concentration of the measured electrolyte was proven. This section focuses on the sensitivity of the transwell setup towards this property of the electrolyte. The identical setup as presented in the previous section was used to test for the sensitivity of the electrodes. Figure 5.18 displays the dependence of the measured impedance values on the concentration of NaCl in H_2O.
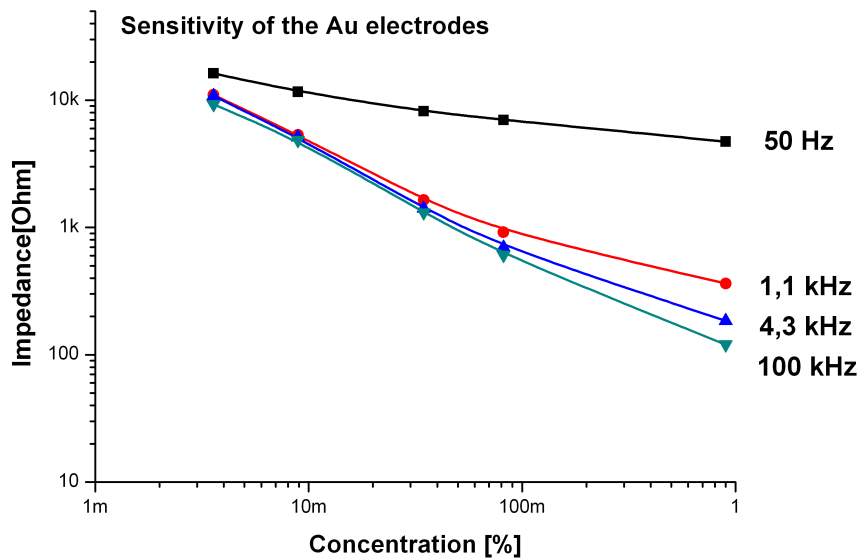
Figure 5.18: Concentration series of diluted NaCl in distilled water at significant frequencies, varying with mass fraction of dissolved NaCl in water.

The x axis in figure 5.18 plots the logarithmically scaled concentration given in percental mass fraction. The displayed range starts at the left end with a very low concentration of 0.001% of NaCl in H_2O and ends at 1% of NaCl in H_2O. This scale is plotted logarithmic. The y axis, displaying the measured impedance in logarithmic scale as well and shows a

range of 10 Ohm to 50 kOhm. The plotted lines in this graph display the impedance of the measured electolytes at four different frequencies. All four curves start at comparably high impedance values in the range of 9 kOhm to 16 kOhm and decrease with varying slopes as the concentration increases. The data measured at 50 Hz shows a lower decrease than the other three sets of data. Three lines collected at the frequencies 1.1 Hz, 4.3 kHz and 100 kHz exhibit very similar behaviour but the line for 100 kHz shows the strongest decrease in impedance as the concentration rises. Sensitivity of the transwell setup improves with increasing frequency. The best sensitivity shown in figure 5.18 was measured for 100 kHz. The measured data in this logarithmic representation can be approximized be the equation

$$\log Z = Z_0 + k \cdot \log c \tag{5.2}$$

where k is the slope, Z is the measured impedance, c is the concentration and Z_0 is the impedance for $c \rightarrow 0$. With this logarithmic representation the sensitivity is calculated by the slope of the logarithmized values plotted in figure 5.18

$$k \approx \frac{\Delta \log Z}{\Delta \log c} \tag{5.3}$$

k was calculated to be 1.6. A value for k=1.6 means that for a change of concentration Δc a change of impedance ΔZ of $10^{1.6} = 38.8 \cdot \Delta c$ can be measured. Compared to the standard deviation at 100 kHz of 30 mOhm a change of impedance for 60 mOhm corresponding to a change of concentration for 0.0015% mass fraction can be considered as significant.

5.2.6 Integrity of the Zn Electrode

The use of zinc coated steel for the top electrode was based on practicability considerations. However, zinc is a less noble element. The standard electrode potential E_0 in aqueous solution at 25°C is -0.76V [Ebbing 90]. the use of zinc for the top electrodes involves the risk of corrosion and decompensation of the electrode. Therefore, the integrity of the zinc electrode had to be evaluated under test conditions. So far the measurement setup was tested, the reproducibility of the measurement was confirmed and measurements of various electrolytes showed a good sensitivity for measuring concentration changes in the medium. All of these measurements were performed in fresh electrolytes for each experiment. This section reports on long time monitoring of impedance spectroscopy so effects occurring only after a prolonged exposure of electrodes and after repeated measurement cycles had to be considered. The most important factor to be evaluated is whether changes of the electrodes influence the measured impedance after some time. Therefore, a long time observation of the measured impedance was performed. 0.1 ml of distilled water was pipetted into the silicone well. This time the electrolyte stayed in the well for one hour. The impedance was measured every 15 minutes. Two series were performed: One measurement with a maximal voltage amplitude of 0.1 V

(peak to zero) and for the second measurement the maximal voltage amplitude was increased to 0.5 V (peak to zero). Both voltages are below the standard electrode potential $E_0 = -0.76$ V of the zinc electrode. Part (a) of figure 5.19 displays the results of the measurement for Voltages confined to 0.1 V.
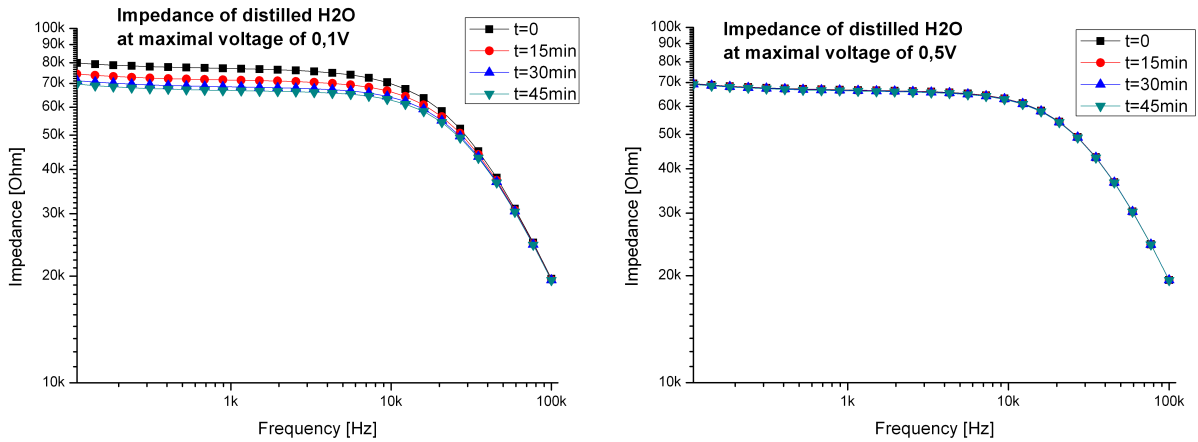
(a) Impedance of distilled water measured over a duration of 45 minutes with the voltage limited to 0.1 V.

(b) Impedance of distilled water measured over a duration of 45 minutes with the voltage limited to 0.5 V.

Figure 5.19: Impedance spectrum of distilled water measured several times during 45 min with the voltage limited to two different values.

Frequency is plotted logarithmically on the x axis, the impedance is plotted logarithmically on the y axis. The displayed curves show the impedance values of distilled water at different times. All curves show similar frequency dependence as observed before. However, each curve has a slightly different offset with a trend to lower impedance measured with proceeding time. After a long time the measured values would reach 70 kOhm like the curve in figure 5.19 (b). The second measurement with a measuring voltage of 0.5 volt was performed to check whether the effect is increased at higher voltages. Part (b) of figure 5.19 shows the results of this measurement. Plotting layout stayed unchanged compared to 5.19 (a) but the displayed data shows slightly differing behavior. For 0.5 V maximal voltage, the plotted curves overlap on the complete range of frequencies and the measured impedance in the low frequency range is about 10 kOhm smaller than the impedance measured at 0.1 V. To explore the differences of the two measurements, they are compared in figure 5.20 for a measuring frequency of 1.5 kHz.
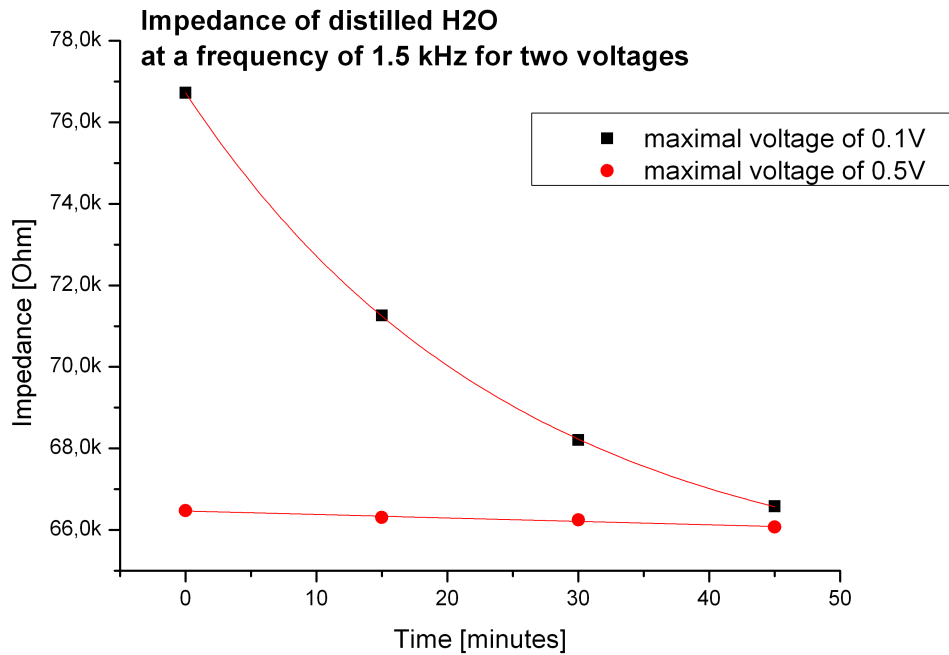
Figure 5.20: Measured impedance of distilled water at 1.5 kHz.

Both curves were fitted, the black squares representing the measurement confined to 0.1 V voltage was fitted exponentially and the second measurement corresponding to the measurement confined to 0.5 V voltage was fitted linearly. Table 5.2 lists the values calculated for both curves.

Impedance spectrum	0.5 V	0.1 V	
	y = a + b*x	y = y0 + A*exp(R0*x)	
a	66467.9	y0	64547.05
b	-8.47	A	12181.1
		R0	-0.04

Table 5.2: Fitting values for both curves.

In this figure, the impedance is plotted on the linearly scaled y axis in dependence of the elapsed time. Time is plotted on the linear x axis in the range of 0 minutes to 50 minutes. The black squares represent the measured impedance as the voltage was confined to 0.1 V. The first impedance measured at the beginning gave a result of 76 kOhm. After 15 minutes the impedance decreases to 71 kOhm which gives a decrease of 5.1 kOhm per minute. The difference of the impedance measured at t=30 min and t=45 is only 1.6 kOhm which gives a decrease of 0.1 kOhm per minute. The red circles show the impedance values measured with

a voltage of 0.5 V. These values hardly change at all. At t=0 the impedance is 66.5 kOhm, it decreases to 66.1 kOhm within 45 minutes. The curves appeared to to converge. This implies that the effect causing the decrease of impedance is the same for both curves. The curve corresponding to the measurement with the voltage limited to 0.1 V reaches its final state slowly whereas the curve corresponding to the measurement with the voltage limited to 0.5 V already shows low values of impedance at the beginning of the measurement. It is presumed that the impedance of the electrolyte is lowered for 10 kOhm due to Zn^{++} ions. The solid zinc immersed in water tends to establish a stable equilibrium at the electrode - electrolyte phase boundary. It is suggested that the impedance value of 66 kOhm points to this stable equilibrium.

5.3   Cell Culture Monitoring

The suitability of the presented setup and its sensitivity was evaluated. Several test were performed using varying electrolytes including physiological saline. Now we can proceed to the final goal of monitoring biological cell layers.

5.3.1   Comparison of the Culturing Medium to Physiological Saline

Experiments described in the previous section evaluated the electrical properties of the presented setup using distilled water and various concentrations of sodium chloride. As explained in section 4.3.2, Caco-2 cells need a nutrient medium to grow. The used RPMI1640 medium is a complex mixture of various ingredients listed in table 4.3.2. The osmolality is comparable to physiological saline, but contributions of other components (eg. proteins) added in the RPMI are unknown. The lead questions for this section were:

- How can the nutrient medium be characterized electrically?

- Is the physiological saline an adequate model for the RPMI medium from the electrical point of view?

The following chapter compares the impedance of an RPMI medium to the impedance of a physiological saline. To measure the impedance of these fluids the measurement setup including all components presented in previous sections was used. A transwell electrode configuration of one planar electrode and one top electrode was used. The planar electrode was a half circle. A borosilicate plate with the planar electrodes was placed in the specimen holder. The silicone confinement was used to form wells for containing liquids such as the physiological saline as well as the RPMI medium. The top-electrodes were mounted on top of the silicone confinement. Cable connections between the specimen holder, the multiplexer,

the LCR meter and the PC were established. The impedance of two electrolytes was measured separately. Table 5.3 lists the parameters for this experiment.

electrolyte 1	physiological saline 0.9% NaCl
electrolyte 2	cells nutrient medium RPMI1640
fluid volume	0.1 ml
frequency range	50 Hz to 100 kHz
maximal voltage	0.1 V

Table 5.3: Overview and parameters used in this experiment to compare physiological saline (0.9%NaCl) to RPMI medium.

Each fluid was pipetted into a clean well. The experiment was repeated several times after rinsing the electrodes and wells both with distilled water. Figure 5.21 part (a) shows the result of this experiment. The mean value of the measured impedances is plotted on the y axis in the range of 100 Ohm to 10 kOhm whereas the x axis shows the frequency in the range of 20 Hz to 200 kHz. Both axes are scaled logarithmically.
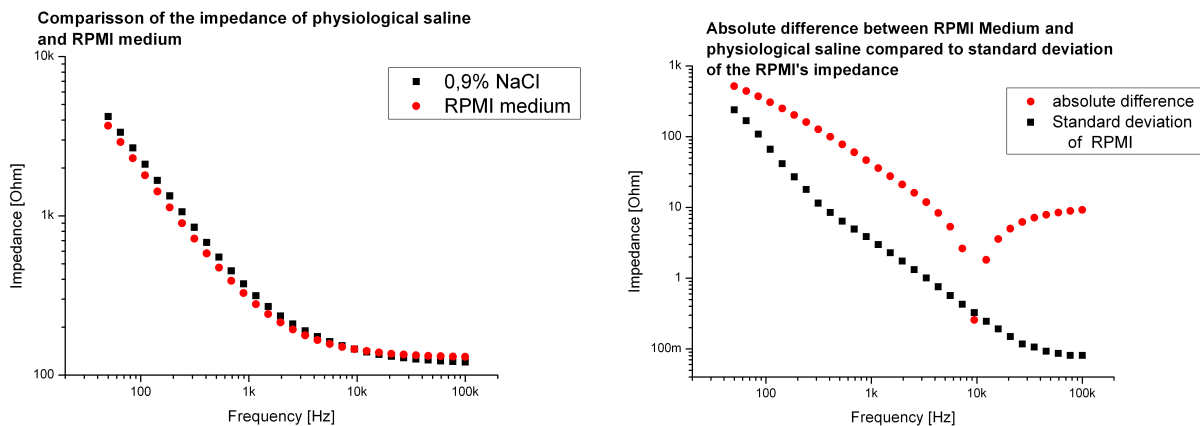
(a) Impedance spectrum of physiological saline and RPMI medium.

(b) Absolute difference of impedance ΔZ 0.9%NaCl to RPMI and standard deviatin of RPMI measurement.

Figure 5.21: Comparison of measured impedances of RPMI nutrient medium to physiological saline.

The black squares in part (a) show the measured impedance of the physiological saline, the red circles depict the measured impedance of the RPMI medium. Both curves are strongly decreasing for low frequencies. The slopes of the curves decrease with rising frequencies, so for middle and high frequencies the change of impedance is less intensive. Both curves correspond over the whole measurement range. In figure 5.21 (b) the absolute difference $|\Delta Z|$ of the two electrolytes' impedances is displayed and compared to the standard deviation of the RPMI's

impedance measurement. Where

$$|\Delta Z| = |Z_{RPMI} - Z_{NaCl}| \qquad (5.4)$$

The X axis still displays the logarithmically scaled frequency in the range of $20\,Hz$ to $200\,kHz$ and the y axis shows the logarithmically scaled impedance. But in the difference spectrum this axis only displays the impedance changes which are in a range of $40\,mOhm$ to $1\,kOhm$. The values of the difference between the two electrolytes' impedances, plotted as red circles, are only slightly higher than the standard deviation of the RPMI's impedance. So significant differences of the impedance between 0.9% NaCl and RPMI medium are hardly measurable. RPMI medium behaves similar to NaCl in our method. The minimum of the red curves at a frequency of $9.5\,kHz$ shows that the impedance of RPMI medium is almost equal to the impedance of physiological saline. In general, both curves overlap for the complete range of frequencies. Physiological saline can therefore be used as a model for the complex nutrient medium RPMI1640.

5.3.2 Biocompatibility of Materials in Contact with Caco-2 Cells

The planar electrodes were fabricated using materials and procedures common in microelectronic fabrication. The fabrication and layout of the planar electrodes were described in the previous sections, this section focuses on the biological aspects of the used materials. Table 5.4 lists the materials, which might have contact to the cells, and their relevance to the sensor.

| material	usage
borosilicate	substrate
chromium	temporal undercoating
titanium	undercoating, adhesion layer
gold	planar electrodes' surface
zinc	top electrodes
silicone	culturing wells

Table 5.4: Materials used for sensor fabrication.

To explore the biocompatibility of the used materials, several issues have to be addressed.

1. Do Caco-2 cells grow on the lithographically structures electrodes?

2. Do material properties inhibit or influence cell spreading or differentiation?

3. Is the substrate suitable for inverted microscopy and optical inspection?

To address these questions, the used materials were investigated and probed for their properties and effects on living cells.

Borosilicate substrates were used as support for the planar electrodes and to seed the Caco-2 cells on. Borosilicate glasses are chemically inert glasses with low dispersion and relatively low refractive indices (1.51-1.54 across the visible range). These properties facilitate optical inspection and inverse microscopy of the cell cultures. Borosilicate glasses have a very low thermal expansion coefficient, which is beneficial for sputtering. Chromium oxide was used as a temporal undercoating for better adhesion of photo resist during lithographical processing of the planar electrodes. This undercoating improved the photo resist's adherence to the borosilicate but in contrary to noble metals, chromium is toxic for Caco-2 cells. Studies showed that chromium intoxication caused significant decrease in membrane alkaline phosphatase and Ca^{++}-Mg^{++}-ATPase activities of intestinal epithelial cells [Upreti 05]. Therefore, chromium was removed completely by etching prior to finalization of the electrode structures. Titanium was used as a permanent adhesion layer for the top gold layer. The usage of titanium improved the adherence of the gold electrodes on the borosilicate significantly. No intolerance of Caco-2 cells to titanium has been reported. Gold was selected for the top layer of the planar electrodes due to it's high chemical resistivity and electrical characteristics. The response of Caco-2 cells to microelectronic materials was assessed in previous studies by [Wanzenboeck 04] and [Bogner 06] and showed good biocompatibility for gold and titanium. The top electrodes were fabricated from zinc coated steel. The effect of this material on the Caco-2 cells was inspected. To check on the biocompatibility of the combination of materials and their structures used in the presented work, Caco-2 cells were seeded onto the planar electrodes and grown in an incubator under standard conditions for 15 days. Figure 5.22 (a) shows a detail of a planar gold electrode.
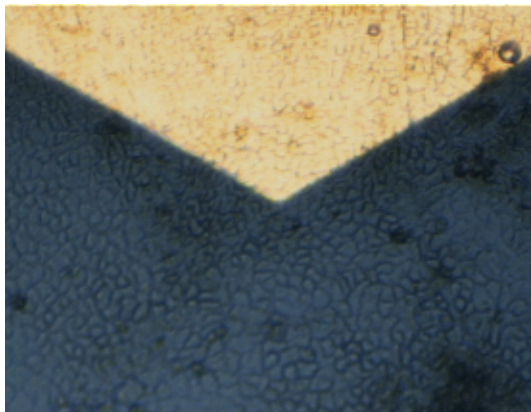
(a) Gold electrode and borosilicate covered with Caco-2 cells.
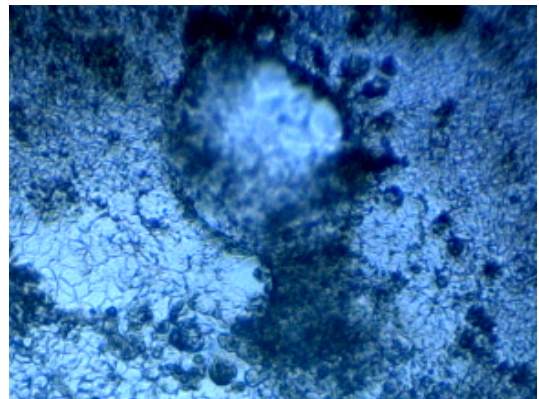
(b) Caco-2 cells on borosilicate forming a dome.

Figure 5.22: Microscopy image of gold electrode covered with cells.

Full Caco-2 cell coverage of gold electrodes as well as the borosilicate substrate has experi-

mentally proven the biocompatibility of these materials. Confluence of the Caco-2 monolayer was observed on these surfaces. Full differentiation of the Caco-2 cell culture can be assumed as the occurrence of domes as explained in section 3.2 was observed. Figure 5.22 (b) shows one of these domes. These facts indicate that neither cell growth nor differentiation were affected by the used materials.

5.3.3 Impedance Spectroscopy of Caco-2 Cells

The presence and the status of the Caco-2 cell layer was monitored by impedance spectroscopy. The characteristic features in the impedance spectrum and their use for online monitoring had to be evaluated.

- Which characteristic features of the impedance spectrum are related to the Caco-2 cells?

- Can impedance spectroscopy be used to monitor changes of the cell layer with progressing proliferation time of cells?

The setup described in section 5.1 was built to explore these questions. For this experiment the entire system was installed in the pharmaceutical laboratories. A PC running the LabView program as well as the electrical components (LCR-meter, multiplexer) were set up and connected according to the remarks in section 4.2.3. After seeding the cells the specimen holder with planar electrodes, silicone confinement and top electrodes was placed within the incubator to establish proper environment for the cells to grow. Cells confinement, specimen holder, top electrodes and cables were disinfected using 70% alcohol. The Caco-2 cells were then extracted from the previous passage and seeded onto the borosilicate plate under sterile conditions. 6 ml RPMI medium containing 636.000 cells were prepared and a volume of 160 μl distributed into the silicone wells. The specimen holder with the electrodes and the cells was then placed in the incubator where the Caco-2 cell culture was grown under standard conditions for two weeks. Their nutrient medium was refreshed every third day. For each time 160 μl of fresh RPMI1640 medium were used.

Table 5.5 gives an overview and lists the parameters used for measuring the impedance spectroscopy of Caco-2 cells. The transepithelial impedance of the Caco-2 cells seeded onto the gold electrodes was measured with the LCR-meter several times. When seeded onto the substrate at t=0 the cells in suspension do not adhere yet to the substrate. The cells may be distributed in the liquid or may as well sit loosely on the surface. There is no continuous cell layer yet. Only after some time the cells start to adhere to the substrate's surface and begin to cover the provided area.

electrolyte	cells nutrient medium RPMI 1640
cells	Caco-2 cells, passage 67
cell density	106.000 cells/ml
growth time	14 days
fluid volume	160 μl
electrode configuration	transwell, 1/4 bottom
frequency range	50 Hz to 100 kHz
maximal voltage	0.1 V

Table 5.5: Overview and parameters used in this experiment to measure the impedance spectroscopy of Caco-2 cells.

The impedance spectrum of a cell culture was measured directly after seeding (t=0) and a second time after ten days (t=10d). Figure 5.23 shows the results of this measurement at two different times. The curves illustrate the measured impedance values and their dependence on the measurement frequency. The x axis in figure 5.23 displays the frequency in the range of 10 Hz to 110 kHz and is scaled logarithmically. The y axis in this graph shows the logarithmically scaled impedance in the range of 100 Ohm to 110 kOhm.
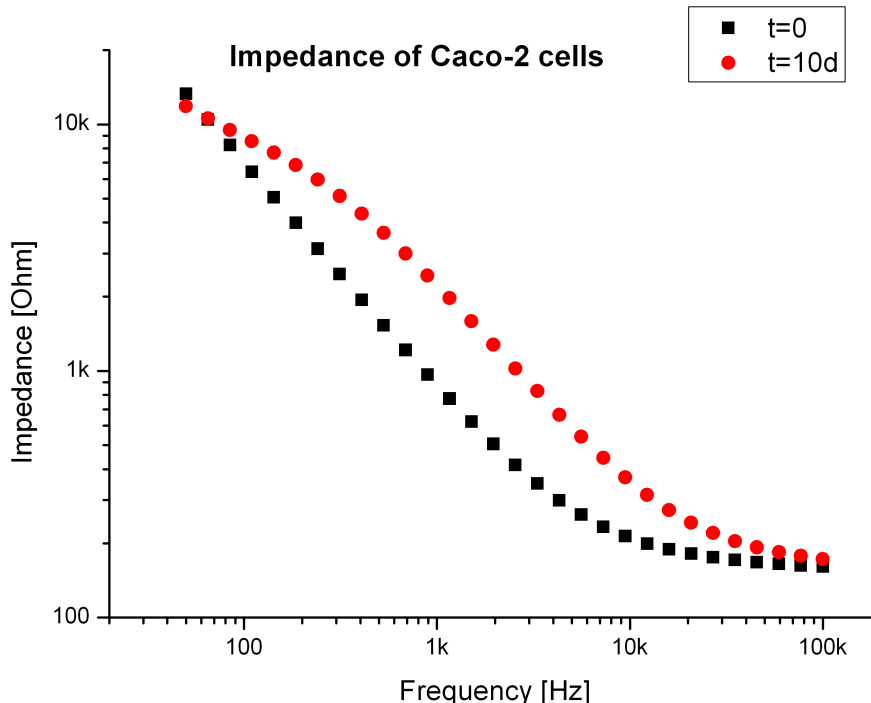

Figure 5.23: Impedance of Caco-2 cells seeded onto the borosilicate plate. Impedance was measured immediately after seeding (t=0) and after ten days of growth in the incubator(t=10d).

The results of two measurements at different stages of the cell layer's growth are plotted: The black squares depict the measured impedance values of the Caco-2 cells directly after seeding while the red circles show the measured impedance values of the cell culture ten days after seeding. As apparent in the graph, the values differ from each other significantly. At the time $t = 0d$ the impedance shows a rapid drop for small and middle frequencies but changes to a more flat slope for higher frequencies at $8\,kHz$. After ten days the curve shows a changed dependency of impedance on the measurement frequency. Significantly higher impedance values can be observed especially in the range of middle frequencies. For frequencies smaller than $100\,Hz$ no significant change can be observed in this curve. The difference of the measured impedance seems to be large in the frequency range of $100\,Hz$ to $1\,kHz$. But for large frequencies only little significant change can be observed. Figure 5.24 gives a closer look on the differences between the two curves. The impedance difference $|\Delta Z|$ is shown in this graph and was calculated by

$$|\Delta Z| \; = \; |Z_{t=10d} - Z_{t=0}| \hspace{4cm} (5.5)$$

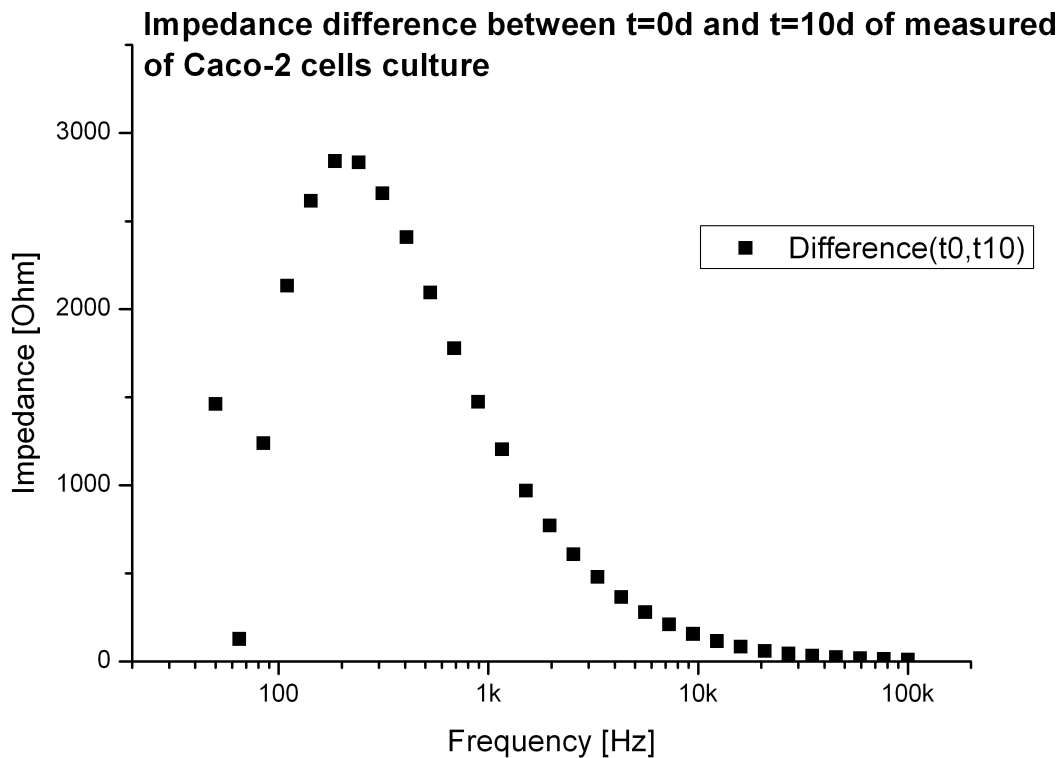Figure 5.24: Evolution of the cell culture's impedance between the time of seeding (t=0) and 10 days post seeding (t=10d).

The y axis in this graph displays again the logarithmically scaled frequency in the range of $20\,Hz$ to $200\,kHz$, whereas the y axis in this figure shows the absolute difference of two measured impedance values. The y axis is scaled linearly and displays values in the range of

75

0 Ohm to 3.5 kOhm. The curve depicted shows a clear maximum of 2.8 kOhm at a frequency of 185.4 Hz compared to the value at t=0 this is a 71%increase of impedance. At this frequency the the impedance of the cell culture after ten days of culturing is much higher than the impedance of the cell culture at the beginning of the experiment. A significant change of impedance with inrcreasing proliferation time could be measured.

To exclude artifacts due to any time dependent systematic errors from the measurement setup a reference measurement was performed at the same time. The measurement setup was identical to the one presented above but no cells were added to the medium. All parameters and procedures were applied as described before, including the change of medium every third day. The results of this reference measurement are shown in figure 5.25.
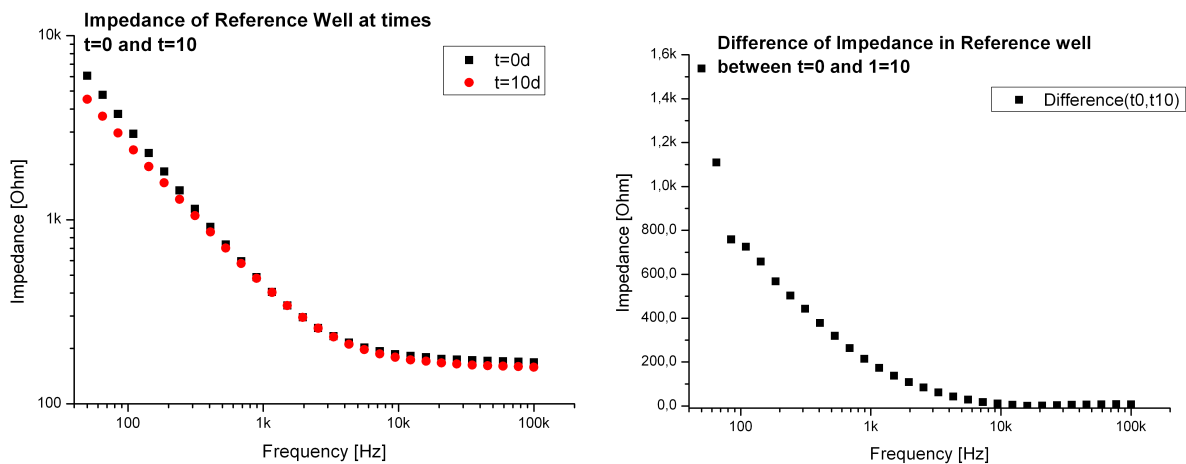
(a) Impedance spectrum of the reference well at t=0 and t=10d.

(b) Difference of the reference wells' impedance between time t=0 and t=10d.

Figure 5.25: Reference measurement of medium without cells, measured directly at the beginning of the experiment (t=0) and ten days later (t=10d).

Part (a) of the figure shows the measured impedance on the y axis in dependence of the measurement frequency on the x axis. Both axes are logarithmically scaled. Again, the black squares display the measured impedance directly at the beginning of the experiment while the red circles show the results of the measurement ten days later. The measured values lie in the range of 158.3 Ohm at the frequency of 100 kHz and 6 kOhm at the frequency of 50 Hz. Both curves correspond within the complete range of frequencies. Part (b) displays the difference between the measured values. In this figure the y axis is linearly scaled. It displays the absolute difference between the measured impedance values of the RPMI medium after seeding and ten days later. The maximal difference is 1.5 kOhm at the frequency of 50 Hz. The difference decreases with increasing frequencies. The difference of 1.5 kOhm at low frequencies is speculated to be caused by proteins in the medium adhering to the gold electrodes after a long exposure time. However, the difference of impedance occurring in measurement of the Caco-2 cell culture is still significantly higher than the smaller difference in the reference well.

5.3.4 Change of Cell Layers' Impedance within a Time Interval of Twelve Days

A significant difference of the measured impedance within 10 days proves that the transepithelial impedance of the investigated Caco-2 cell layer changed in time. The next step for investigation of this change was to continuously monitor the transepithelial impedance during the complete growth cycle in real time.

The measurement setup was installed as described in sections 5.3.3. The cells were seeded onto the planar electrodes and grown under standard conditions for 12 days in the incubator. $160\,\mu l$ of RPMI medium was used in each well and exchanged five times. Table 5.6 lists the days of medium exchange.

exchange number	days post seeding	consumption
1	2 d	incomplete consumption, pH > 6.8
2	4 d	full consumption, pH < 6.8
3	7 d	full consumption, pH < 6.8
4	9 d	full consumption, pH < 6.8
5	11 d	full consumption, pH < 6.8

Table 5.6: Exchange of RPMI medium, days post seeding.

The need to exchange the medium was indicated by the change of the pH value, visible due to the added phenol red. This substance changes it's color gradually from red to yellow when the pH value changes from above 8.2 to below 6.8. This change of pH value is caused by the cells metabolism. A pH value below 6.8 indicates the urgent need for an exchange of the medium to provide a physiological growth environment and sufficient supply of nutrient. Medium with an yellow color indicates the full consumption of the RPMI medium and its nutrients.

The transepithelial impedance of the Caco-2 cells was monitored for 12 days continuously. Every thirty minutes a full impedance spectrum was recorded. In figure 5.26 only a frequency of $9.5\,Hz$ was selected for the illustration of time-dependent change of impedance. As compared to figure 5.23 and figure B.1 this is a frequency where change of impedance could be observed and where the low standard deviation of $337\,mOhm$ allows measure even small changes of impedance. At this frequency significant differences between medium and cell culture were observed. Figure 5.26 shows the results of this online impedance monitoring. It has to be pointed out that this real-time impedance monitoring could be performed while the cell layer was formed without any disturbance by the electrical measurement. To monitor the transepithelial impedance a transwell electrode configuration was used. One top electrode was used as a counter electrode for the 1/4 bottom electrode labeled with the number 22 in figure 5.2.
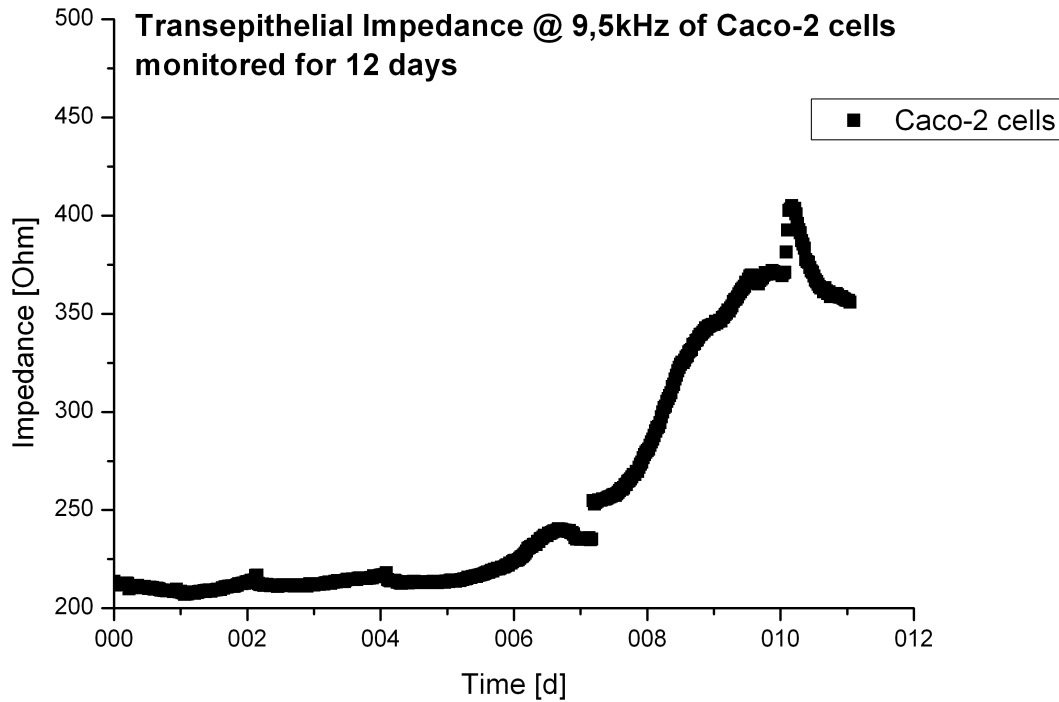
Figure 5.26: Impedance of Caco-2 cells monitored for 12 days using the transwell electrode configuration top electrode vs. 1/4 bottom electrode.

This figure shows the impedance of the Caco-2 cell layer growing on the planar gold electrodes, as monitored for 12 a duration of days. The x axis shows the time post seeding in days, the y axis is scaled linearly and shows the measured impedance in the range of 200 Ohm to 500 Ohm. When compared with figure 5.23 this value is in the expected range for impedances at 9.5 kHz. The plotted graph in general shows increasing impedance as the days pass and proliferation time increases. At the beginning the measured impedance is 214 Ohm and drops to 207 Ohm after one day. Then a gentle rise of the measured impedance starts and continues for several days. The increase of impedance is disrupted at several points. The first discontinuity appeared after two days, the second is visible after four days and a third can be seen between the seventh and eighth day. Eight days after seeding the impedance of this Caco-2 layer increased drastically and reached a maximum of 405 Ohm at a growth time of ten days and eight hours. Subsequently, the the impedance decreased again strongly to 350 Ohm. Compared to the start of the measurement, the impedance almost shows an increase by a factor of two. The singular jumps at the days 2, 4 and 7 days post seeding temporarily coincide with the exchange of medium. These steps may be either caused by the mechanical disturbance of the cell layer during the liquid manipulation or by the change of pH value directly after exchange of the medium. Generally, this set of measurements shows that the transepithelial impedance

of the Caco-2 cell layer rises for about eight days and also reaches a maximum after eight days. The temporal coincidence suggests that the maximal transepithelial impedance of a Caco-2 cell layer is at the time of full confluence and differentiation of the cells in the layer. As the cells are grown on a non-permeable substrate, they tend to ablate after this point in the growth cycle. The formation of domes has been reported on solid substrates and is due to the collection of metabolic products on the basolateral side. This fact might explain decrease of impedance ten days post seeding.

5.3.5 Relative Change of Transepithelial Impedance in Time

The monitoring of cell growth was repeated with several cell cultures. The absolute value of the measured impedance depends on several influences. Examples of these influences are the resistance of the electrical setup and the measuring electrodes, the geometry of the electrodes, the CO_2 content in the incubator or the passage number of the selected Caco-2 cells. Also the comparison of different measurement frequencies is difficult due to the large dynamic range of measured signals. For this reason a normalization of data and expression as relative value with regard to a calibration value was performed. As calibration value the impedance at t=0 was selected so that changes with increasing time as compared to the time of seeding can be evaluated. The parameter Z_{rel} was chosen to optimally display the effect of the cell layer on the measured impedance. The data evaluation to extract Z_{rel} from the measured data is described in section 4.4. This section presents the evaluation procedure using the example of the previous section.
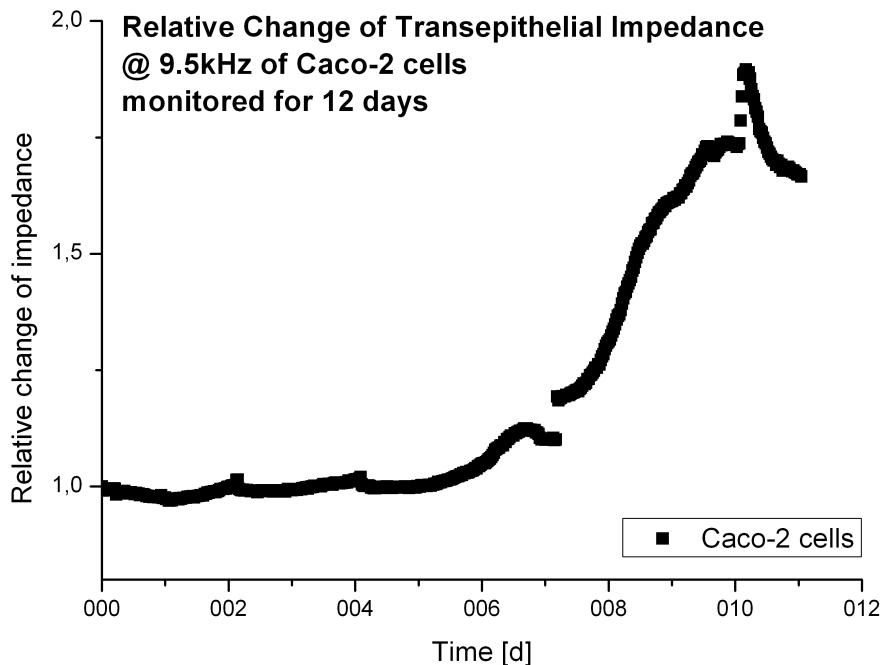

Figure 5.27: Relative change of impedance Z_{rel} of Caco-2 cells monitored for 12 days using the transwell electrode configuration top electrode vs. 1/4 bottom electrode.

Figure 5.27 shows the results of the previous experiment represented in terms of the relative change of impedance Z_{rel}. Figure 5.27 shows the impedance spectrum already displayed in figure 5.26 normalized to the impedance spectrum retrieved after seeding (t=0). This figure shows the time post seeding on the x axis in the range of zero days to twelve days. On the y axis this graph shows the relative change of impedance Z_{rel}. The axis is scaled linearly and shows a range of 0.8 to 2.0. Z_{rel} is a dimensionless factor that expresses the increase of the impedance compared to the impedance of the first measurement. It is generally calculated by equation 4.2. In figure 5.27 the frequency was constant so the evaluation function is

$$Z_{rel}(t_i) = \frac{Z(t_i)\,[Ohm]}{214\,[Ohm]} \tag{5.6}$$

Where $Z(t_i)$ is the measured impedance of this cell culture after t_i minutes post seeding. The resulting curve displays the identical characteristics as figure 5.26 but comes up with several advantages. First, it allows to compare the results of several experiments despite eventually system inherent varying offsets. The second advantage of this type of representation is the comparability of impedances at different frequencies despite of large differences in absolute values. The third advantage of this representation will be the possibility to recognize the amount of change at the first glance. The last two advantages will be particularly helpful in the next section, as this type of representation of values allows monitoring of the Caco-2 cell growth over the complete range of frequencies, from 50 Hz to 100 kHz.

5.3.6 Time resolved Impedance Spectroscopy during Cell Growth

Up to this point the complete measurement setup was tested for functionality, accuracy and biocompatibility. Measurement of the transepithelial impedance spectroscopy was gradually built up starting with the measurement of the impedance spectroscopy of cell free medium. Transepithelial impedance was measured for a range of frequencies to obtain an impedance spectroscopy. The transepithelial impedance of Caco-2 cells was also measured for a period of twelve days. An evaluation procedure was established to display the retrieved data in a clearly arranged, comparable manner. All these steps have demonstrated the feasibility and effectiveness of this method. This section will conclude these series of experiments by presenting the results of the monitoring of several separately grown Caco-2 layer's transepithelial impedance spectroscopy for the full growth period.

The measurement setup already presented in section 5.3.3 was installed at the pharmaceutical laboratories. The LCR meter to measure the impedance spectrum was connected via the MUX to the measuring electrodes. These electrodes, the planar basolateral as well as the apical top electrodes were mounted on the specimen holder. The 'flexiperm' cell confinement was placed on the borosilicate substrate containing the planar microelectrodes to form wells for the eight cell cultures. The Caco-2 cells were then extracted from passage 68 and seeded onto the borosilicate plate, equipped with the planar electrodes, under sterile conditions. 3 ml RPMI medium containing 318.000 cells were prepared and distributed into the silicone wells. After seeding the specimen holder with the electrodes and the cells was immediately placed in the incubator where the Caco-2 cell culture was grown under standard conditions for a duration two weeks.

electrolyte	cells nutrient medium RPMI1640
cells	Caco-2 cells, passage 69
cell density	106000 cells/ml
growth time	13 days
fluid volume	160 μl
frequency range	50 Hz to 100 kHz
maximal voltage	0.1 V
electrode configuration	transwell

Table 5.7: Overview and parameters used in this experiment to measure the impedance spectroscopy of Caco-2 cells.

Table 5.7 gives an overview and lists the parameters used for measuring the impedance spectroscopy of Caco-2 cells. Two wells were kept free of cells to allow for collection of reference

data. Cells were grown in six wells. Figure 5.28 shows the arrangement of wells. In this figure the wells are labeled alphabetically. A and B were chosen to be the cell free reference wells. C, D, E, F, G each contained 16960 cells at the time of seeding.
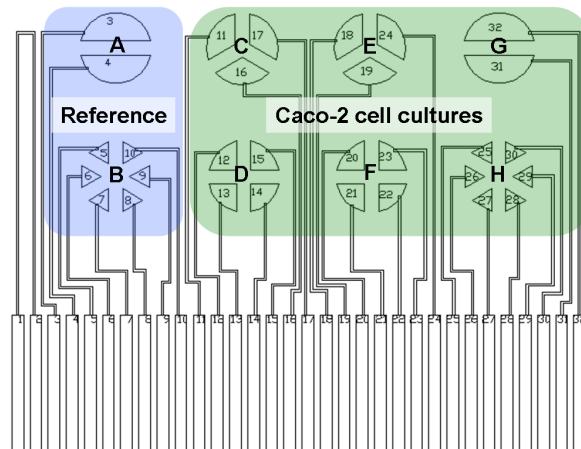

Figure 5.28: Layout of the planar electrodes with arrangement of the wells. Reference data was collected in wells A and B, Caco-2 cells were grown and monitored in wells C to H.

Culturing time was set to 15 days with a change of medium at least every fourth day. For each medium exchange $160\,\mu$l of fresh RPMI1640 medium were used. Table 5.8 gives information on the exchange of medium.

exchange number	days post seeding
1	2 d
2	4 d
3	7 d
4	9 d
5	11 d
6	13 d

Table 5.8: Exchange of RPMI medium, days post seeding.

Measurement data was retrieved continuously with a periodicity of thirty minutes. At the end of a growth period the sample containing the cells was unmounted and the cells were chemically fixated onto the substrate, to enable optical inspection.

The multiplexer subsequently established 32 connections to enable the serial measurement of the transepithelial impedance spectroscopy in eight wells. Table 5.29 shows an overview on several time resolved impedance spectra of Caco-2 cell cultures. Figure 5.30 gives a more
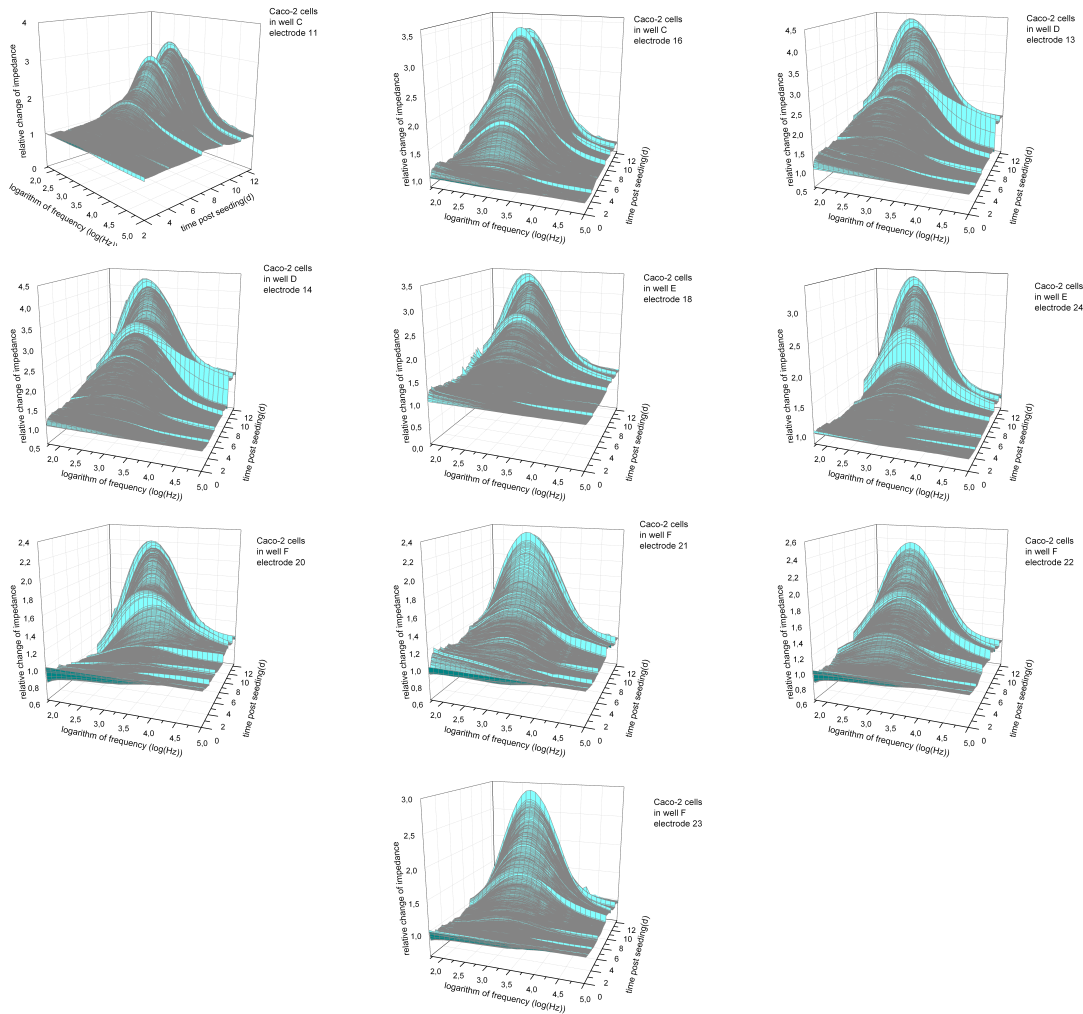
detailed view on a selected Caco-2 culture.

Figure 5.29: Graphs of monitored Impedance Spectra. Caco-2 cell cultures were monitored for 12 days, impedance spectra were retrieved with transwell electrode configurations. A detailed discussion of one graph can be found in section 5.3.6.

The following section will include a discussion of one time resolved impedance spectrum of a Caco-2 cell culture. Optical inspection approved good coverage in well 'C' where the cells' full differentiation could be confirmed by observation of domes at the end of the growth period. Figure 5.30 shows the relative impedance of Caco-2 cells grown on the electrode number 11 in well 'C'. This figure was chosen to represent the measurement from several electrodes and to discuss the observed effects. The results measured with well 'C' are representative of all other measurements and are discussed as example for all other measurements. The additional figures showing the results from the remaining measurements can be found in the appendix.
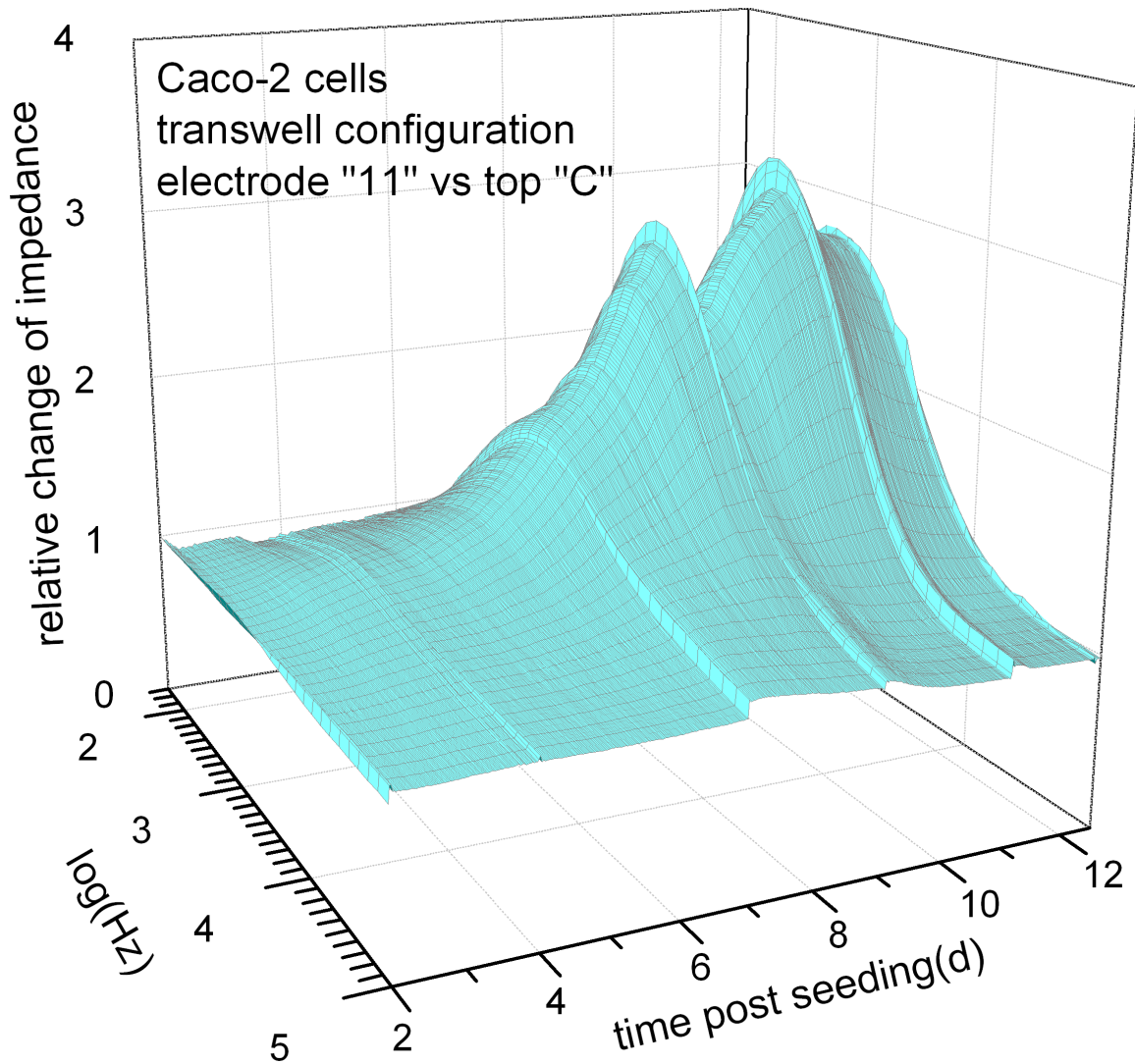
Figure 5.30: Caco-2 cells grown on electrode '11' on planar sensor as experimental parameters were set according to table 5.7. Monitored by impedance spectroscopy.

This three dimensional surface plot shows the logarithm of the frequency on the x axis, the time post seeding on the y axis and the relative change of impedance Z_{rel}(f,t) on the z axis. The surface was interpolated using the 'Renka-Cline' algorithm explained in section 4.4. The logarithm of the frequency is plotted on the linear scale in the range of 1 to 5. The days post seeding are displayed from the second day post seeding till 12.5 days post seeding. The relative change of impedance is plotted in the range of 0 to 4. It has to be noted that the relative change factor is a multiplier. A relative change of impedance below one represents a decrease of impedance compared to the impedance directly after seeding. A relative change larger than one represents an amplification by the factor displayed. The graph shows a slight decrease at the beginning, the minimum was measured to be 0.8 at a frequency of 50 Hz and a time of 3 days and 18 hours. This means that the impedance of 50 Hz decreased by 20%

compared to the value at the time of seeding. It is speculated that the decrease of impedance at the low frequency of 50 Hz is due to proteins from the RPMI medium adhering to the gold electrodes. After this minimum the relative change of impedance shows a constant increase. The most significant increase can be observed in the frequency range of 500 Hz to 5 kHz. The relative change reaches a maximum of 3.3 after 11 days and 3 hours at a frequency of 688 Hz. A relative change of impedance of 3.3 is equivalent to an increase of the impedance by 230%. For frequencies larger than 10 kHz ($\log10^4=4$) the measured impedance hardly changed at all. But the high frequence range is also sensitive to medium exchange as there are still leaps visible that can be correlated in their emergence to the time of the exchange of medium as listed in table 5.8. Appearently, the growth of Caco-2 cells can be monitored with the highest sensitivity in the frequency range of 500 Ohm to 5 kOhm. The transepithelial impedance showed a maximum amplification of 3.3 at the time of confluence predicted by the specifications of this cell layer. The electrical properties of the Caco-2 cell layer changes significantly and can be observed by transepithelial impedance spectroscopy. Figure 5.22 shows a detailed photograph of the planar electrodes in well C. The bright areas are the conducting gold electrodes and the darker zones are borosilicate areas. Full coverage of the gold electrodes could be observed after the thirteenth day. The size of single Caco-2 cells is typically between 10 μm and 20 μm, therefore the specimen was investigated using scanning electron microscopy. Figure 5.31 shows the SEM image.
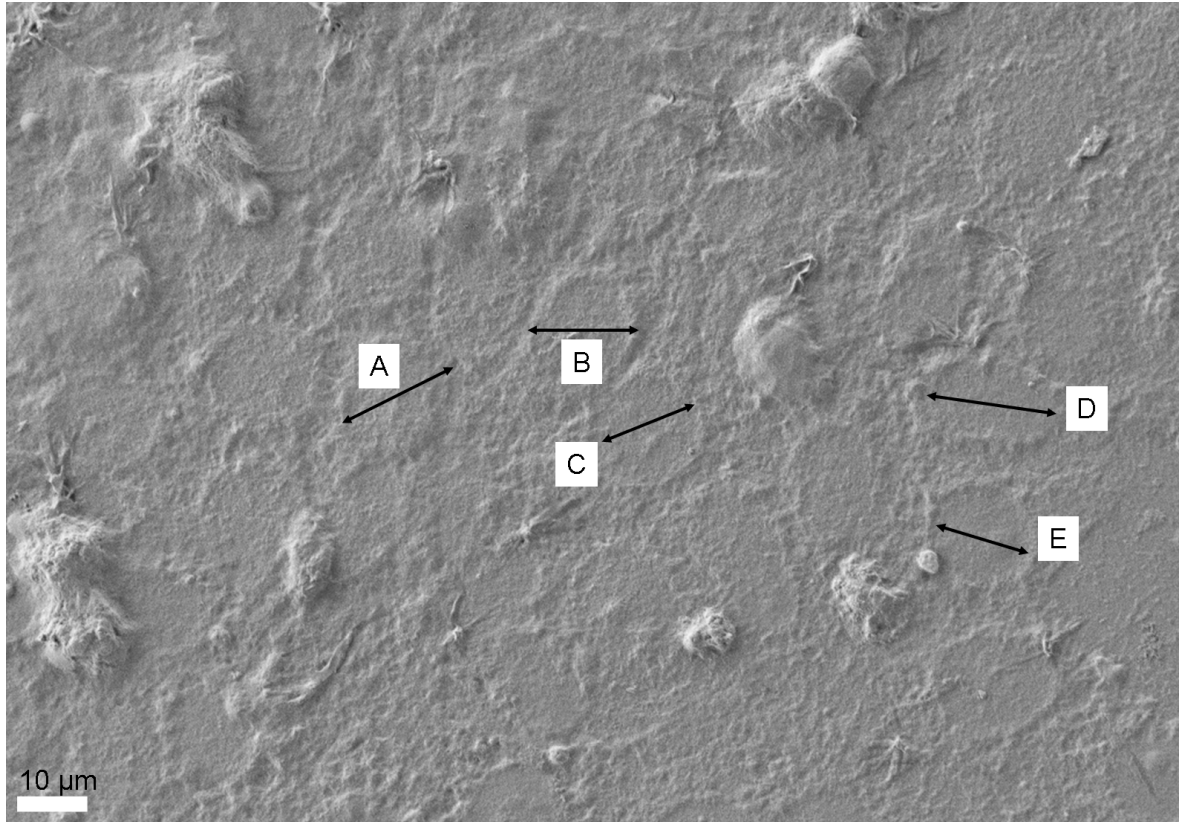
Figure 5.31: SEM image of the Caco-2 cells on the substrate.

The corrugated, rough surface indicates a continuous coating with a biological layer. Several cells on this surface can be recognized. The high vacuum in the scanning electron microscope leads to evaporation of all liquids so that the volume of cells was reduced leaving only the cells. However, the cells' shapes and positions are still visible and indicate a close contact to each other. It was possible to measure the diameter of several cells. The results are presented in table 5.9

Cell	Diameter [μm]
A	18.9
B	16.9
C	15.2
D	19.9
E	14.7

Table 5.9: Diameters of some cells on the specimen.

Although these measurements only present a limited sample of all data measured it can still be

assumed from other samples inspected that the other cells show similar dimensions. Diameters of adherent cells of 15μm to 20μm correspond perfectly to the values reported in literature [Bolsover 04].

The results presented in figures 5.31 and 5.30 deliver valuable information on the growth of Caco-2 cell cultures. Two effects influencing the data displayed in figure 5.30 can be observed by the continuous electrical monitoring:

- Cell growth and proliferation

- Side effects such as exchange of nutrient medium

Both effects were observed to contribute at different ranges of frequencies. They can therefore be differentiated from each other. Cell growth results in effects measurable in a frequency range from 500 Hz to 5 kHz. The standard deviation of the measurement as reported in section 5.2.3 for this range of frequencies lies between 800 mOhm and 7 Ohm. For frequencies larger than 5 kHz the standard deviation is even smaller than 800 mOhm. Cell growth and proliferation start to contribute increasingly to the measured impedance after 5 days post seeding. The impermeability of the Caco-2 cell layer towards charged molecules increases strongly after this period. The cell layer exhibits the highest impermeability after 11 days and 8 hours at a frequency of approximately 700 Hz. Subsequently, the cell layer's ability to inhibit transport of charges decreases abruptly. At all times during cell growth the impedance at larger frequencies is only affected slightly by the cell growth. The dominant factor of the impedance at frequencies higher than 10 kHz is the exchange of RPMI nutrient medium. The this effect is suggested for further investigation, as it is unclear whether the change of impedance related to the exchange of the medium is due to mechanical interference or to metabolic processes of the Caco-2 cell layer.

The results of the Caco-2 cell culture monitoring in the transwell configuration correspond to the results obtained by monitoring of the cells' impedance using a basolateral configuration in previous work [Fischeneder 09]. The measurement of the basolateral impedance showed negligible changes after seeding for several days. This observation could be confirmed in the presented work using a transepithelial electrode configuration. Cell proliferation on 4-pt IDES sensor resulted in an increase of impedance and showed a relative change of impedance by a factor up to 10 (+900%) compared to the impedance immediately after seeding. The trend of this result could be reproduced but increase factors were slightly smaller. It is speculated that the slightly smaller increase is caused by the measurement configuration. For the basolateral measurement a four terminal electrode configuration was used. It is therefore suggested to upgrade the presented transepithelial setup from a two terminal configuration to a four terminal electrode configuration. With the basolateral setup also small changes in the range > 50 kHz could be correlated to RPMI medium exchange: This observation was confirmed in the transepithelial setup. The exchange of RPMI medium caused significant changes of the

impedance in both setups.

The aim of this work was to monitor the transepithelial electrical impedance of Caco-2 mono-layers using microstructured electrode arrays. As reported in this section the setup presented in this work was successfully used to monitor the growth of Caco-2 monolayers noninvasively. It was assumed that characteristic points of the measured impedance spectrum can be correlated to distinct events during the growth and differentiation of the monolayer. This assumption could be confirmed experimentally by the results shown in figure 5.30.

The presented measurement method was proved to be a promising method for future applications to be used in the research of Caco-2 cell monolayers. Further development of the presented method can even lead to a fundamental understanding of the Caco-2 cell line as well as other biological cells and their electrical properties.

Chapter 6

Conclusion

6.1 Summary

The aim of this work was to develop an approach to enable a time resolved measurement of the transepithelial impedance spectroscopy of a Caco-2 cell culture during the complete period of cell growth. A setup to address this task was developed and tested. Electrical properties of Caco-2 cell cultures were analyzed.

The setup was used to measure the impedance spectrum of 8 individual biological cell cultures in eight silicone wells simultaneously. Impedance spectra were recorded by an LCR meter, a passive electrical network analyzer. A specialized multiplexer was developed to enable these measurements. An optimum layout for the microelectrode array was found in an array of 8 sensor fields each with two up to six planar bottom electrodes for each measuring well. These gold electrodes were fabricated using optical lithography and sputter deposition. The approach of microelectronic fabrication proved useful and reproducibly provided electrodes with good conductive properties. The layout can easily be adapted for varying research questions. To perform a transepithelial measurement, top electrodes on a mounting plate were fabricated. The electrical properties of the top electrodes were tested as well and based on figure 5.20 considered as suitable for the measurement. For growth of cells in a fluid environment under standard growth conditions of $95\%CO_2$ atmosphere and $37°$ a specimen holder was developed and used to perform the impedance measurement within the cell incubator. The presented setup as shown in figure 6.1 was tested for its performance in various experiments.
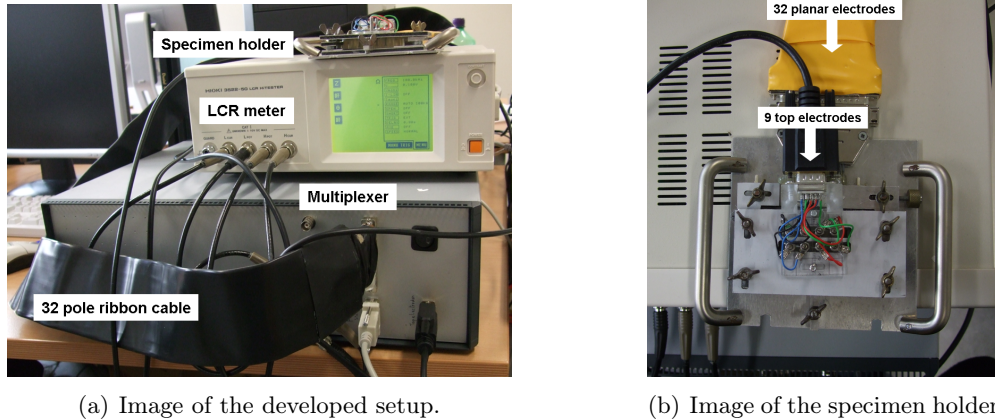
(a) Image of the developed setup.

(b) Image of the specimen holder.

Figure 6.1: Overview of the presented setup.

Full functionality of the setup could be confirmed for operation without electrolytes. In a shorted configuration the parasitic impedance of the entire system was determined to be an ohmic resistance of 200 Ohm. The reproducibility of measurements with electrolytes depended on the measurement frequency and was very high. For a frequency 50 Hz the standard deviation was 3%, wheras for frequencies larger than 893.5 Hz the standard deviation was even smaller than 1%. Concentrations of NaCl in aqueous solution varying from 0.9% to 0.0038% could be correlated to the measured impedance. The measurement of different electrolyte concentrations also revealed that the presented setup shows limitations at lower frequencies. The presented setup measured the impedance in a 2-terminal configuration. This approach experiences parasitic effects in the measured impedance at lower frequencies due to the electrochemical double layer formed at the electrode-electrolyte boundary of the signal conducting electrode.

Starting from these fundamental evaluation experiments and findings, the practically relevant but complex cases for measurements of biological cells were performed. First the effects of RPMI 1640 medium as complex electrolyte containing nutrient, serum and numerous charges species was investigated. Physiological saline, a solution of 0.9% NaCl in distilled water could be identified as an adequate model for the more complex RPMI nutrient medium for the cells. A very important finding was the fact that all construction materials used in the electrode setup were proven to be biocompatible. It is essential for monitoring the Caco-cells' impedance to ascertain that material aspects do not effect the cell growth and differentiation. The presented setup was therefore proven to measure the Caco-2 cells' impedance non-invasively.

Simultaneous monitoring of the transepithelial impedance spectra of eight Caco-2 cultures is a procedure involving several parameters that may be either varied deliberately or kept constant at a certain value. The parameters investigated are frequency, time and the number of monitored cultures. The number of parameters varied simultaneously was systematically in-

creased. A first measurement of a frequency-resolved impedance spectrum immediately after seeding for a single culture showed the high pass character of the cell monolayer when measured in the transepithelial configuration. This fact was expected from previous theoretical considerations and could be verified experimentally. When compared to an impedance spectrum of the same culture after a culturing time of 10 days post seeding a significant change of impedance could be identified. Eventual unrelated effects due to unexpected changes of the measurement setup, that could have emerged within these ten days could be excluded. A simultaneous measurement of a reference solution displayed no changes between the measurement directly after seeding and a measurement 10 days later. In simultaneous test cultures a period of ten days has been shown repeatedly to be sufficient for the Caco-2 cell culture to cover the available sensor area completely. It is therefore concluded, that the observed increase of impedance can be exclusively correlated to the growth of the Caco-2 cells. With a single frequency measured at 12 Hz this behavior is used in pharmaceutical studies to characterize the density of a Caco-2 monolayer. For detailed examination of the temporal change of transepithelial impedance a Caco-2 culture was monitored at a fixed frequency for twelve days. Results indicate that the increase of transepithelial impedance in the frequency range of $500\,Hz$ to $5\,kHz$ display characteristic features already known from measurements using a basolateral impedance measurement [Fischeneder 09]. For the full frequency range from $50\,Hz$ to $100\,kHz$ also the exchange of the cells' nutrient medium could be correlated on the time scale to abrupt increase of the measured impedance. Continuous real time monitoring of all growth displayed a maximum transepithelial impedance after ten days and eight hours. The strong decline after this peak time is suggested to indicate an apparent change of the cell layer's state. For a second Caco- cell culture a relative change of transepithelial impedance by a factor of 3.3 ($\hat{=}\ +230\%$) was found after 11 days. In a final key experiment the transepithelial impedance was monitored for a range of frequencies of eight cell cultures simultaneously. The good correlations observed between several cell cultures underlines the high reproducibility of this method and demonstrates the robustness of this continuous, non-invasive, real time monitoring technique for living cell cultures.

6.2   Outlook

A proof of concept for transwell impedance monitoring was shown by this work. The setup presented in this work delivered valuable informations such as proliferation rate and layer density via the electrical properties of Caco-2 monolayers. These informations provide a fundamental basis for further research on the interface between biological cells and microelectronic devices. Related studies [Fischeneder 09] indicate even stronger signal of cells in frequency bands that are not accessible with the presented two terminal setup. Further studies will therefore measure transepithelial impedance spectroscopy, using a four terminal electrode configuration. Previous work with a four terminal setup has shown the benefits of this configuration with

basolateral impedance spectroscopy of Caco-2 cultures [Fischeneder 09]. A combination of both methods is feasible and is expected to deliver information whether the two configurations - basolateral and transwell - are comparable or do provide complimentary information on the biological system. The measurement electrodes fabricated for this work were built using optical lithography and sputter deposition. The developed fabrication methods can be used for manufacturing electrodes in even smaller dimensions of micrometers. Further works aim to miniaturize the electrode arrays to obtain spatially resolved impedance spectroscopy with resolutions at the order of magnitude for single Caco-2 cells. An other challenge worth to be addressed is the measurement of the transepithelial impedance of Caco-2 cultures grown on permeable membranes. A setup following this approach promises the potential of direct implementation into the pharmaceutical transport studies.
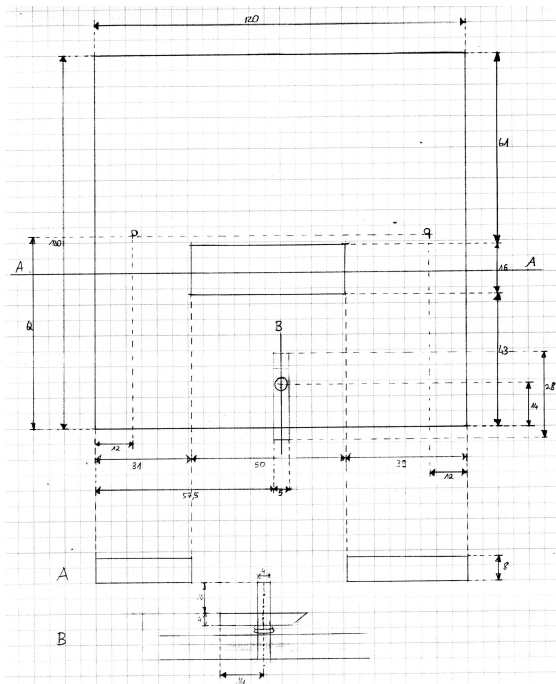
Appendix A

Construction Details

label of wells	number	contact label	area [mm^2]/electrode	area [mm^2] of feed lines
Z		1		6.11
		2		
A	2	3	7.33	3.54
		4	7.33	3.22
B	6	5	1.09	2.49
		6	1.08	2.03
		7	1.09	1.48
		8	1.08	1.29
		9	1.09	1.72
		10	1.08	2.20
C	3	11	4.24	3.29
		16	4.26	3.11
		17	4.32	3.19
D	4	12	2.70	2.20
		13	2.66	1.37
		14	2.66	1.28
		15	2.76	2.26
E	3	18	4.24	3.31
		19	4.26	3.27
		24	4.32	3.26

Table A.1: Table of electrodes A to E and their areas.

label of wells	number	contact label	area [mm^2]/electrode	area [mm^2] of feed lines
F	4	20	2.70	2.42
		21	2.66	1.48
		22	2.66	1.26
		23	2.76	2.16
G	2	31	7.33	3.18
		32	7.33	3.50
H	6	25	1.09	2.32
		26	1.08	1.81
		27	1.09	1.12
		28	1.08	1.26
		29	1.09	1.95
		30	1.08	2.44

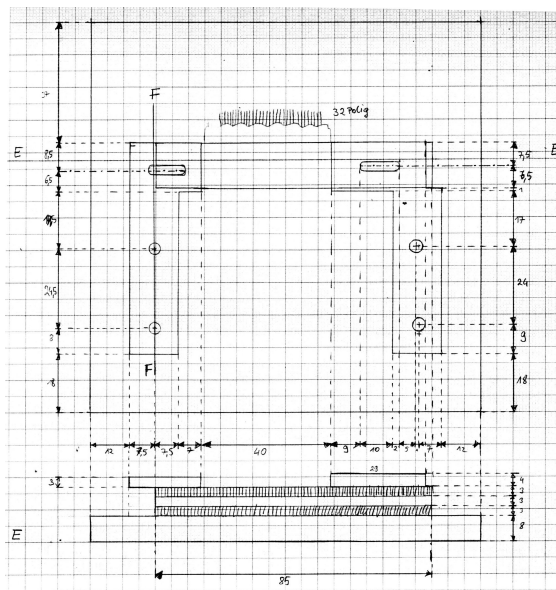Table A.2: Table of electrodes F to H and their areas.

The specimen holder was fabricated from steel - polypropylene composite plates. The figures below give the exact measurements of all components.
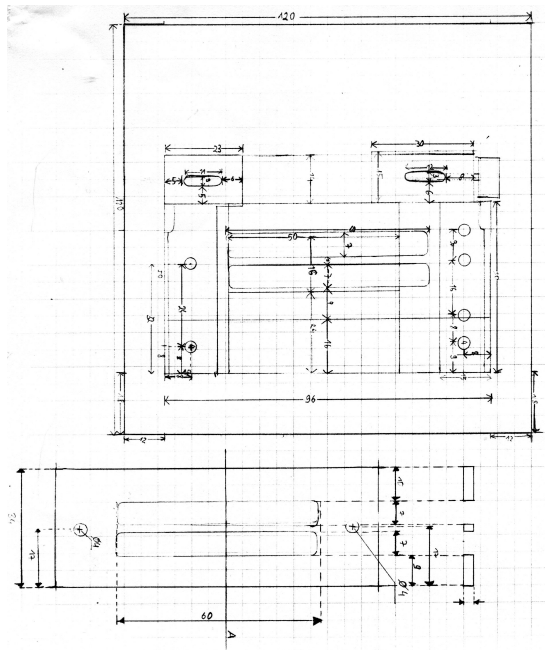

(a) Base of the specimen holder.
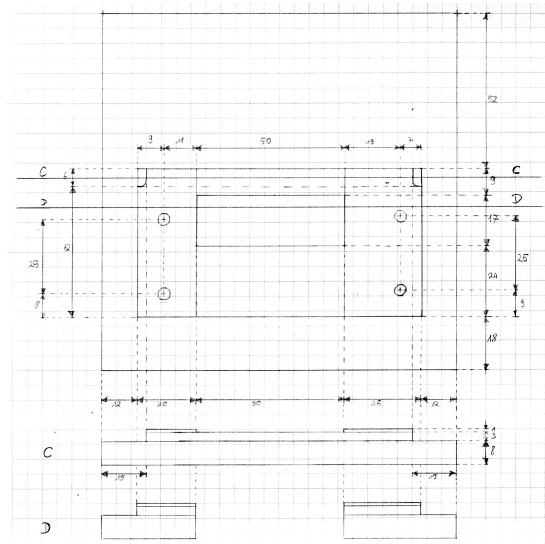
(b) Second layer of the specimen holder.

(c) Third layer of the specimen holder.

(d) Top view of the specimen holder.

Figure A.1: Design of the specimen holder, all lengths given in mm.

Appendix B

Standard Deviation of 9.0%NaCl in H$_2$O

Standard Deviation of the physilogical saline, 0.9%NaCl in H$_2$O. Electrode configuration: Top-Bottom 1/2 well A electrode number 3, maximal voltage 0.1 V
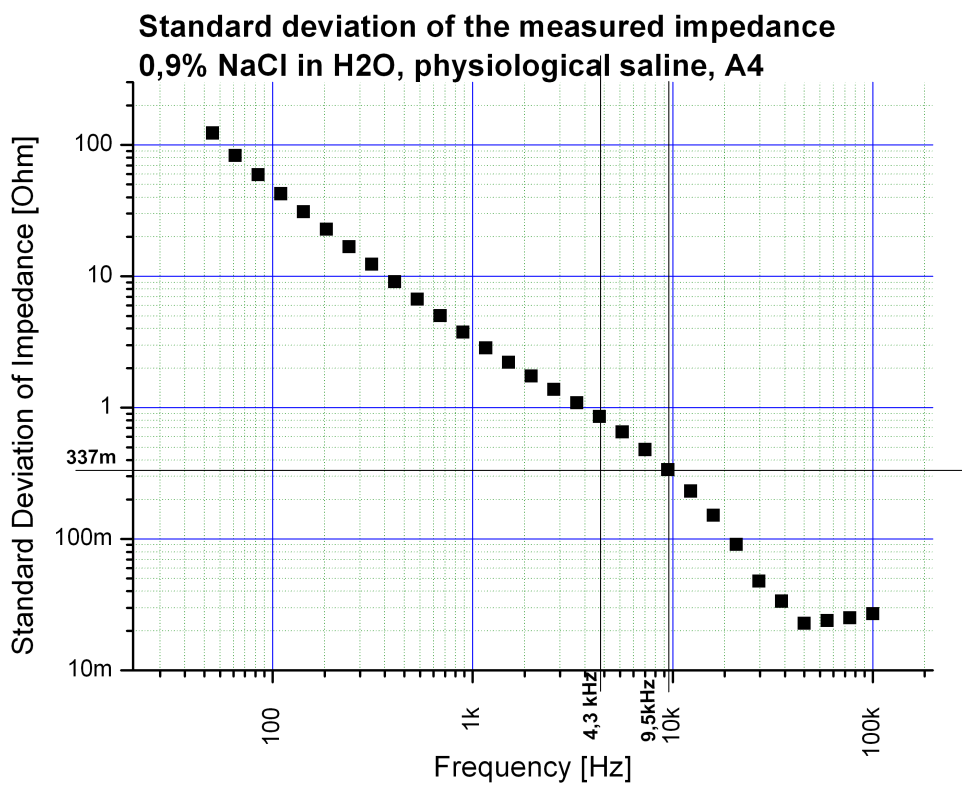

Figure B.1: Standard Deviation of the measured impedance spectrum of a physiological saline.

Literature

[Adam 03] G. Adam, P. Laeuger, G.Stark. Physikalische Chemie und Biophysik. Springer-Verlag Berlin, 2003. p. 193ff.

[Alberts 04] Bruce Alberts, Alexander Johnson, Julian Lewis, Martin Raff, Keith Roberts, Peter Walter. Molekularbiologie der Zelle. L. Jaenicke, 4 Auflage, 2004. p. 53ff.

[Asphahani 07] Fareid Asphahani, Miqin Zhang. Cellular impedance biosensors for drug screening and toxin detection. The Analyst, 132:835–841, 2007.

[AZ 06] AZ. Sicherheitsdatenblatt AZ 726 MIF Developer. AZ Elektronic Materials, 2006.

[Bisquert 98] J. Bisquert, G. Garcia-Belmonte, P. Bueno, E. Longo, L. O. S. Bulhões. Impedance of constant phase element (cpe)-blocked diffusion in film electrodes. Journal of Electroanalytical Chemistry, 452(2):229 – 234, 1998.

[Bogner 06] Elisabeth Bogner. Biokompatibilität von mikroelektronischen Materialien und deren Anwendung in zellbasierten Biosensoren. Dissertation, University of Vienna, 2006.

[Bolsover 04] Stephen R. Bolsover, Jeremy S. Hyams, Elisabeth A. Shephard, Claudia G. Wiedemann. Cell Biology. Wiley-Liss Jersey, 2004. p. 23ff.

[Bouafsoun 08] A. Bouafsoun, A. Othmane, N. Jaffrézic-Renault, A. Kerkeni, O. Thoumire, A. Prigent, L. Ponsonnet. Impedance endothelial cell biosensor for lipopolysaccharide detection. Materials Science and Engineering: C, 28(5-6):653 – 661, 2008.

[Campbell 96] Stephen A. Campbell. The Science and Engineering of Microelectronic Fabrication. Oxford University Press, 1996.

[Clariant] Clariant. AZ 5214 E Image Reversal Photoresist. Clariant GmbH, Germany.

[Con 10] Conrad. 8-Way Relay Board Item No. 19 77 20 User Manual, 09 2010.

[Coster 96] H. Coster, T. Chilcott, A. Coster. Impedance spectroscopy of interfaces, membranes and ultrastructures. Bioelectrochemistry and Bioenergetics, 40(2):79–98, 1996.

[Dean 08] D. Dean, T. Ramanathan, D. Machado, R. Sundararajan. Electrical impedance spectroscopy study of biological tissues. Journal of Electrostatics, 66(3-4):165–177, 2008.

[Demtroeder 99] Wolfgang Demtroeder. Experimentalphysik 2. Springer-Verlag Berlin, 1999.

[Ebbing 90] Ebbing, D. Darrell. General Chemistry. Houghton Mifflin, 3rd Auflage, 1990.

[Fafilek 09] Guenther Fafilek. Bioelectrochemie. Lecture notes. 2010.07.19.

[Fischeneder 09] Martin Fischeneder. In-Situ Impedanzmessung an biologischen Caco-2 Zellen mit IDES-Elektroden. Diplomarbeit, Technische Universität Wien, 2009.

[Fischer 08] Wiebke Fischer, Katrin Praetor, Linda Metzner, Reinhard H.H. Neubert, Matthias Brandsch. Transport of valproate at intestinal epithelial (Caco-2) and brain endothelial (RBE4) cells: Mechanism and substrate specificity. European Journal of Pharmaceutics and Biopharmaceutics, 70(2):486 – 492, 2008.

[Fough 77] J. Fough, J. M. Fough, T. Orfeo. One hundred and twenty-seven cultured human tumor cell lines producing tumors in nude mice. J. Natl. Cancer Inst, 59:221–226, 1977.

[Gockel 08] T. Gockel. Form der wissenschaftlichen Ausarbeitung. Springer-Verlag, Heidelberg, 2008. www.formbuch.de.

[Greiner 04] bio-one Greiner. flexiPERM micro 12, 2004.

[Guo 06] M. Guo, J. Chen, X. Yun, K. Chen, L. Nie, S. Yao. Monitoring of cell growth and assessment of cytotoxicity using electrochemical impedance spectroscopy. Biochimica et Biophysica Acta (BBA) - General Subjects, 1760(3):432 – 439, 2006.

[Hamann 05] Carl H. Hamann, Wolf Vielstich. Elektrochemie. Wiley-VCH GmbH & Co. KGaA, Weinheim, 2005. p.145ff.

[Hidalgo 86] I. J. Hidalgo, T. J. Raub, R. T. Borchardt. Characterization of the human colon carcinoma cell line (Caco-2) as a model system for intestinal epithelial permeability. Gastroenerology, 96:736 – 749, 1986.

[Hio 05] Hioki. LCR HiTESTER 3522-50/3532-50 User Manual, 2005.

[Iliescu 07] C. Iliescu, D.P. Poenar, M. Carp, F.C. Loe. A microfluidic device for impedance spectroscopy analysis of biological samples. Sensors and Actuators B: Chemical, 123(1):168 – 176, 2007.

[Kohlrausch 85] Kohlrausch. Praktische Physik 2. B. G. Teubner Stuttgart, 1985.

[Liu 09] Q. Liu, J. Yu, L. Xiao, J.C.O. Tang, Y. Zhang, P. Wang, M. Yang. Impedance studies of bio-behavior and chemosensitivity of cancer cells by micro-electrode arrays. Biosensors and Bioelectronics, 24(5):1305–1310, 2009.

[Lo 99] C.-M.a Lo, C.R.b Keese, I.b Giaever. Cell-substrate contact: Another factor may influence transepithelial electrical resistance of cell layers cultured on permeable filters. Experimental Cell Research, 250(2):576–580, 1999.

[McRae 99] D.A. McRae, M.A. Esrick, S.C. Mueller. Changes in the noninvasive, in vivo electrical impedance of three xenografts during the necrotic cell-response sequence. Journal of Radiation Oncology, Biology, Physics, 43(4):849 – 857, 1999.

[Mil 09] Millicell® ERS-2 User Guide, 2009.

[Orazem 08] Mark E. Orazem, Bernard Tribollet. Electrochemical Impedance Spectroscopy. John Wiley & Sons, Inc., 2008.

[Press 08] B. Press, D. Di Grandi. Permeability for intestinal absorption: Caco-2 assay and related issues. Current Drug Metabolism, 9(9):893–900, 2008.

[Ranaldi 03] G. Ranaldi, R. Consalvo, Y. Sambuy, M.L. Scarino. Permeability characteristics of parental and clonal human intestinal Caco-2 cell lines differentiated in serum-supplemented and serum-free media. Toxicology in Vitro, 17(5-6):761–767, 2003.

[Renka 84] Robert J. Renka. Algorithm 624. triangulation and interpolation at arbitrarily distributed points in the plane. ACM Transactions on Mathematical Software, 10(4):440–442, 1984. cited By (since 1996) 15.

[Shi 08] Lewis Zhichang Shi, G. Jane Li, Shunzhen Wang, Wei Zheng. Use of Z310 cells as an in vitro blood-cerebrospinal fluid barrier model: Tight junction proteins and transport properties. Toxicology in Vitro, 22(1):190 – 199, 2008.

[Sigma-Aldrich 09] Sigma-Aldrich. Product information on Sigma PRMI-1640 Media. Sigma-Aldrich, 3050 Spruce Street, Saint Lois, Missouri 63103 USA, 2009.

[Thein 10] M. Thein, F. Asphahani, A. Cheng, R. Buckmaster, M. Zhang, J. Xu. Response characteristics of single-cell impedance sensors employed with surface-modified microelectrodes. Biosensors and Bioelectronics, 25:1963–1969, 2010.

[Thews 99] G. Thews, E. Mutschler, P. Vaupel. Anatomie, Physiologie, Pathophysiologie des Menschen. Wissenschaftliche Verlagsgesellschaft mbH, 1999.

[Upreti 05] R.K. Upreti, R. Shrivastava, A. Karman, U.C. Chaturvedi. A comparative study on rat intestinal epithelial cells and resident gut bacteria: (I) effect of hexavalent chromium. Toxicology Mechanisms and Methods, 15(5):331–338, 2005.

[Varshney 09] M. Varshney, Y. Li. Interdigitated array microelectrodes based impedance biosensors for detection of bacterial cells. Biosensors and Bioelectronics, 24(10):2951 – 2960, 2009.

[Virchow 59] Rudolf Virchow. Die Cellularpathologie in ihrer Begründung auf physiologische und pathologische Gewebelehre. Verlage von August hirschwald, Berlin, 1859. Zwanzig Vorlesungen, gehalten während der Monate Februar, März und April 1858 im pathologischen Institute zu Berlin.

[Wanzenboeck 04] H.D.a Wanzenboeck, C.a Almeder, C.a Pacher, E.a Bertagnolli, E.b Bogner, M.b Wirth, F.b Gabor. Cell growth on prestructured microelectronic semiconductor materials. Tagungsband: Materials Research Society Symposium Proceedings, Band EXS, Seiten 369–375, 2004.

[Weissenboeck 04] A. Weissenboeck, E. Bogner, M. Wirth, F. Gabor. Binding and uptake of wheat germ agglutinin-grafted PLGA-nanospheres by Caco-2 monolayers. Pharmaceutical Research, 21(10):1917–1923, 2004.

CURRICULUM VITAE
Maria Hufnagl

Persönliche Daten:

Geburtsdatum	17. November 1982
Geburtsort	Wien

Ausbildung:

2009 - 2010	Diplomarbeit in Kooperation mit der TU Wien:
	"Time Resolved Transepithelial Impedance Spectroscopy Of Caco 2 Monolayers Relying on Lithographically Patterned Basolateral Electrode Cell Arrays"
2001 Oktober	Beginn Studium der Physik an der Universität Wien
1993 - 2001	Neusprachliches Gymnasium; 1150 Wien, Auf der Schmelz
1989 - 1993	Volksschule; 1170 Wien, Halirschgasse

Berufserfahrung:

2009 - 2010	**Projektassistenz TU Wien, Biophysik:** Entwickeln und Testen eines mikroelektronischen Impedanzsensors für adhärente Zellkulturen, Installation und Betreuung des Messaufbaus zur Impedanz Spektroskopie bei den Kooperationspartnern am Institut für Pharmazie der Universität Wien
2007 Sommer	**IAESTE Praktikum University of Novi Sad, Nuclear Physics:** "International Association for the Exchange of Students for Technical Experience" Radongasmessungen (Adsorptionsverfahren), Effizienzbestimmung der Abschirmung eines Gammadetektors
WS 07/08	**Universität Wien** Tutorin der Lehrveranstaltung „Praktikum zu Einführung in die Physik I"
2006 Sommer	**IAESTE Praktikum Queens University Belfast, Medical Imaging:** Entwicklung von Methoden zur Fusion von MRT und SPECT Bildern, Digitale Analyse und Bearbeitung von MRT und CT Bildern,
seit März 2005	**Universität Wien - Zentralbibliothek für Physik:** Beratung zu Fachliteratur, Literaturrecherche,

Publikationen:

- Meet. Abstr. - Electrochem. Soc. 902, 3177 (2009)
  "Microelectronic Impedance Sensor for Adherent Ex Vivo Cell Cultures"
  Maria Hufnagl, Martin Fischeneder, Andreas Hoefer, Slobodan Damnjanovic, Heinz D. Wanzenboeck, Emmerich Bertagnolli, Michael Wirth, and Franz Gabor

- Meet. Abstr. - Electrochem. Soc. 902 1636 (2009)
  "Patterned Microcavity-Arrays for Cell-Trapping in Biomedical Sensor Architectures"
  Slobodan Damnjanovic, Heinz D. Wanzenboeck, Martin Fischeneder, Maria Hufnagl, Emmerich Bertagnolli, Michael Wirth, and Franz Gabor